Modelling and Optimization
of an Industrial Steam Network

J.M.A. Backhausen

TU Delft
Delft
University of
Technology

Modelling and Optimization of an Industrial Steam Network

Case Study at the Royal Dutch Shell Refinery in Pernis

by

J.M.A. Backhausen

to obtain the degree of Master of Science
at the Delft University of Technology,
to be defended publicly on Tuesday July 27, 2020 at 01:00 PM.

TUDelft

Acknowledgements

Summary

This study aims at developing a model which is able to simulate the utility steam network at the Shell refinery in Pernis. Steam is a key component of the utility system as it supplies process units with heat, rotational power and even cooling and soot reduction in the flaring system. Furthermore, steam is used as feed for processes such as cracking and steam reforming of natural gas. The steam network is often seen as just an utility, while it directly influences the operational costs of the refinery and optimization could lead to a significant reduction in these costs and energy usage. Due to the complexity of the refineries steam network and the cost of restructuring a retrofit to increase heat integration is hardly feasible. Existing plants such as Pernis can highly benefit from balancing the power generation, steam production and third party suppliers in real time. However including all the prices and the effects of operating adjustments on the efficiency of the main electricity and steam producers, while providing each process unit with the required steam at the desired conditions, is a complex task. A real time optimisation model could incorporate the market and ambient conditions and help the people working at the refinery to determine the optimal operating mode each and every day.

The main units connected to the steam network are the gas turbines, heat recovery steam generators, steam turbine generators and steam turbine driven compressors. These units among others are reviewed in literature and modelled in greater detail. Correlations are made which are able to model the units under varying ambient conditions and loads. Furthermore, all units connected to the steam network are analysed using the software packages: PI, Seeq and Excel. This information is implemented in the software i-Steam, which resulted in two steam utility models. One is focused on hydraulic calculations and incorporates the steam pipelines, while the other one is focused on optimization and incorporates the main units with ambient, operation and market conditions. The hydraulic model incorporates the pipelines between steam producers and consumers and is able to calculate the pressure and energy losses in each segment. The optimization model is based on multi non-linear integer programming and is focused on the steam and electricity production, while balancing this with the steam intake. Both models are validated with on site measured data and their behaviour is compared to literature.

The hydraulic model is used for a future project to determine how the new unit should be connected to the steam network. These simulations directly locate the bottlenecks of the steam network and the maximum and minimum flowrates through each section. From the results can be concluded that the unit should be connected to the medium pressure network via the pipe LS4413 with a back up connection via the pipe LS980019. The small amount of produced low pressure steam at the end of run during the summer can be exported to the low pressure network via LS980017. However condensation occurs if the flowrate decreases slightly and the economic feasibility of laying a 250 m pipe has to be further researched.

The optimization model is used to optimize 23 cases, based on data measured at those 23 timestamps. The results clearly show when units should be in full operation and when their output should be reduced. Furthermore, the model locates some key aspects which could reduce the operating cost significantly. The result show that the first stage of steam turbine generator 2 should be shut down most of the time. The same is true for gas turbine 1 which is connected to the heat recovery steam generator 1. Another finding of the model is that there is a clear steam overcapacity and more flexibility in the steam intake from power generation plant 2 would give the model more freedom. This would lead to even better results than the average of 1-3 % operating cost reduction which is achieved at the moment.

This research has shown that the Shell Nederland Raffinaderij in Pernis can gain a lot from implementing steam utility models. Not only in operating cost reduction by implementing a real time optimization model, which could calculate the optimal operating point each day. But also with the utilization of a hydraulic model which can simulate new scenarios throughout the network which is far easier, faster and cheaper than performing on site tests.

Contents

Nomenclature

Acronyms

AC   Alternating current

BFW   Boiler feed water

CHP   Combined heat and power

DC   Direct current

EOR   End of run

G   Generator

GT   Gas turbine

HP   High pressure

HRSG   Heat recovery steam generator

IP   Intermediate pressure

KNMI   Koninklijk Nederlands Meteorologisch Instituut

LD   Let down

LHV   Lower heating value

LMTD   Logarithmic mean temperature difference

LP   Low pressure

M   Motor

MINLP   Mixed integer non-linear programming

MIP   Mixed integer programming

MP   Medium pressure

PGP   Power generation plant

SOR   Start of run

ST   Steam turbine

STDC   Steam turbine driven compressor

STG   Steam turbine generator

VHP   Very high pressure

WGSR   Water gas shift reactor

WHB   Waste heat boiler

Symbols

η	Efficiency
T	Temperature
Q	Energy
V	Volume
W	Work
C_p	Heat capacity at constant pressure
U	Energy
A	Area
$\dot{m}$	Mass flow
h	Enthalpy
C	Capacitance
ϵ	Permittivity
d	Distance
ρ	Density
MC_p	Exhaust energy per degree Kelvin
r	Blowdown rate
L_e	Equivalent length
f_d	Friction factor
L	Length
q	Heat flux
λ	Thermal conductivity
α	Heat transfer coefficient
v	Velocity
p	Pressure
R	Ideal gas constant
u	Uncertainty
D	Diameter

List of Figures

List of Tables

<div style="text-align: right;">

1

</div>

Introduction

1.1. Background

This study aims at developing a model which is able to simulate the utility steam network at the Shell refinery in Pernis. Steam is an element of the site wide utility system which provides the units with their demands for electric power, hydrogen, water, air, nitrogen and steam. These are produced by equipment on site such as boilers, gas turbines, condensers and bought form third parties [1]. The system has to be very redundant and flexible to be able to supply the plant with all the required utilities. Steam is a key component of the utility network as it supplies units with heat, rotational power and even cooling and soot reduction in the flaring system [2]. Furthermore, steam is used as feed for processes such as cracking and steam reforming of natural gas [1]. In fig. 1.1 the Pernis refinery is illustrated in a flow scheme, which is applicable to most refineries. The figure shows the import and export of fuel, water and electricity and the on site production of steam, electricity, fuel and condensate. Steam is not only produced in steam generators but also by waste heat boilers which produce steam by cooling down process streams with water. Losses occur during the processes due to flaring of fuel gases, venting of steam and water losses due to leaks.
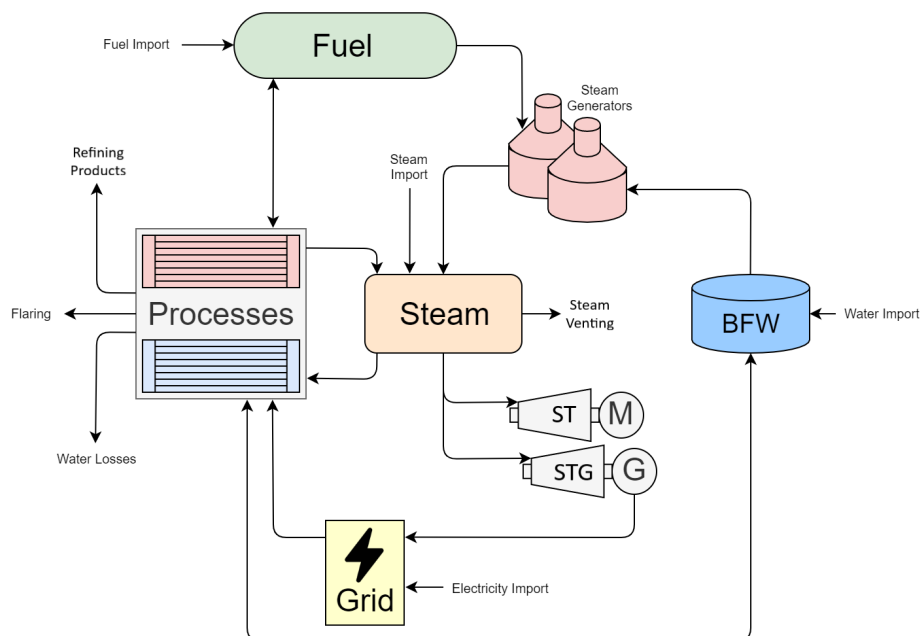
Figure 1.1: Simplified flow scheme of the Pernis refinery, imported utilities are fuel, electricity, water and steam. On site units produce electricity, steam and refining products, during which losses occur due to leakages, flaring and venting. Processes linked to the steam network can either consume or produce steam. Abbreviations are BFW (boiler feed water), ST (steam turbine) and STG (steam turbine generator). Turbine connected to 'M' (motor) is a direct driven turbine connected to an air compressor, the turbine connected to 'G' (generator) produces electricity.

The steam network is often seen as just an utility, while it directly influences the operational costs of the refinery and optimization could lead to a significant reduction in these costs and energy usage [3]. Optimization could be obtained by minimizing the usage of steam, balancing the cost of heat exchanger surface area and utility costs when designing new units [4]. Due to the complexity of the steam network and the costs of restructuring, a retrofit is hardly feasible. However existing plants such as Pernis can have huge benefits from real time optimization by balancing the power generation, steam production and third party suppliers in real time [5, 6]. While balancing the network the energy tax rule has to be kept in mind, which requires a 30 % combined heat and power (CHP) efficiency otherwise tax has to be paid. Furthermore, the rising CO_2 emission penalties will effect the economic feasibility of on site power generation with refinery and/or natural gas. On the other hand a rapid decrease in oil and gas demand dropped the natural gas price by 62% from winter to spring this year due to the global Covid-19 pandemic [7].

1.2. Current State of the Art

In this section the current steam utility network optimization techniques are discussed. The four main techniques used in literature are reviewed to give an overview of how industrial sites can reach their optimal operating point.

Heat Integration

Optimizing the steam utility network by heat integration is a known and widely executed technique. It is based on maximizing the integration of heat between the various process units on site. Often heat integration requires retrofits or alteration of the steam pressure and temperature levels to achieve its optimal point [3, 8]. The selection of integrated process units is made by using pinch analysis, where all heat sources and sinks are analysed to provide the optimal connection between each other [9]. This technique locates the heat surplus and deficit on site, providing a clear overview of the areas where changes in the utility network could result in a better integrated system [10]. Optimizing and retrofitting heat networks and process units have the potential to reduce the overall steam consumption and therefore energy consumption. However analysing all these processes and establishing the economic value is far from straightforward [11]. Except just integrating heat, the utility system can also be optimized by fitting the steam generation perfectly to the varying demand by the process units, minimizing the plants steam overcapacity [6]. Heat integration can also be extended by integrating two or more separate plants to reduce overall energy usage and pollution [12]. Furthermore, it can be implemented during disrupted operation, by determining the heating and/or cooling requirements during start-ups and shut-downs [9]. While most heat integration models are focused on utilizing latent heat, hot liquid reuse can significantly reduce the steam demand and therefore energy consumption [13].

Exergy Analysis

The most common used technique for analysing an energy system is the first law of thermodynamics, as is the case with standard heat integration. Exergy analysis is based on the second law of thermodynamics and provides a tool to locate irreversibly processes inside the refinery. The large contributors to exergy destruction is are processes where a chemical reaction takes place, such as the gas turbines and heat recovery steam generation systems. Measures such as preheating the combustion air decrease the exergy destruction in fired boilers [14].

Mixed Integer Programming

Mixed integer programming (MIP) is an optimization technique which can be implemented for all sorts of processes with linear or non-linear objective functions and constraints. Solving mixed integer non-linear programs (MINLP) requires high computational effort and are therefore not suited for real-time utility optimization [15]. However MINLP simulation models can be designed specifically for optimization by opening the black box and writing the system in terms of energy and mass balances, reducing the solving time significantly [5]. MINLP solution algorithms cannot guarantee robust performance and a global optimum. It is possible to convert these model into linear models by fixing non-linear effects such as the exhaust temperature of the gas turbine. This results in a successive linear model which can incorporate fluctuating market conditions such as: electricity tariffs, fuel price and ambient conditions [16]. Mixed integer programming (MIP) are often used in industry for optimizing utility systems, however discrete decisions such as turning on or off equipment are difficult to resolve [17].

Software Packages

Several software packages are available for the simulation and optimization of utility systems. STAR can be used to optimize the steam network while including the CO_2 emission and emission tax [18]. Aspen Utilities Planner can be used for the simulation and optimization of fuel, steam and power, specially designed to include all business processes related to operating and managing the network [19]. These software packages provide a clear overview of the steam network, while applying mixed integer (non) linear programming as discussed above [18].

1.3. Problem Statement

In this section a short introduction to the refineries operation and the link with the steam networks is given. The requirements of the network are described, which have to be met at all time. Furthermore, the aim of the project is described and how modelling the steam network could help improving its operation.

Refinery Introduction

The Shell Nederland Raffinaderij is one of the largest refineries in Europe with over fifty different process units, which in total process roughly 400,000 barrels of oil per day. To power the refinery the annual consumed energy usage is about 50 PJ which results in CO_2 emission of 4200 kt. The steam network transfers a significant amount of this energy via the grid throughout the three main areas: ABC, DE and KLM. Inside these main areas the steam is distributed via a complex piping network to the over fifty process units which consume and or produce steam.

Requirements

Operating the network is a complex task for the operators working on site. All the constraints listed below have to be met:

- Each unit connected to the steam network has a specific temperature and pressure operating window to ensure the unit runs safe, smooth and reliable.

- The process units follow their throughput targets which are based on the current market trends, which results in a varying steam demand or output.

- For the steam intake from power generation plant 2 (PGP2) a minimum and target flowrate is specified.

- The steam is produced at the highest possible efficiency in order to minimize cost and emissions.

- Process units depend on the steam network, therefore steam production and distribution has to be reliable, even if one of the main steam producers fails to operate.

- Steam and electricity production are directly linked to each other and the electricity grid requires a high reliability as well.

Goal of the Project

The refinery of Pernis started in 1902 and has grown ever since. Step by step evolving of the refinery over the years lead to an extensive and complex steam network which connects all the old and new process units. Creating a good understanding of the network and being able to predict the effects of certain measures is therefore difficult. Simulating the network can help to understand the network and analyse the effects of modifications in operating the network or in steam supply and demand. The simulated network could also solve current operating issues by locating bottlenecks in the the system which are the root for temperature and pressure problems further downstream. Another issue is optimizing the on site steam and electricity production balancing this with the steam intake from the PGP2. Optimizing the network is not only related to increasing efficiency, but also reacting to the current market prices of for example: fuel, CO_2 emission and electricity. However including all the prices and the effects of operating adjustments on the efficiency of the main electricity and steam producers, while providing each process unit with the required steam at the desired conditions, is a complex task. A real time optimisation model could perform all these complex tasks and help the people working at the refinery to determine the optimal operating mode each and every day.

1.4. Methodology

The aim of this work is to create an extensive steam model which is used to discover optimization opportunities as well as investigating the effect of future retrofits. The software used for simulation is i-Steam. This particular software is chosen for its specialisation in steam modelling and the ability to incorporate pipelines. Furthermore, the aim of the project is that the model is used on a daily basis, requiring an uncomplicated and clear interface. The model is split in two: one modelling the main steam and electricity producers and one focused on the hydraulics of the pipelines. The choice of two models is made to achieve a model capable of optimizing steam and electricity production, while the other is capable of modelling the effects of retrofits on the whole steam network. The models will be validated for several scenarios, such as different seasons, loads and operating modes. The optimization model incorporates the cost of fuel, electricity, emissions and the PGP2 steam price. Optimization simulations are run to obtain the optimal operating point in terms of operating cost. The pipeline model is used for the sizing of future projects, locate bottlenecks, test operating modes and implementing retrofits.

Besides the benefits of the the model, there are limitations which are given below:

- No dynamic behaviour
  The system models steady state situations and does not incorporate changes over time (no differential equations). Due to this limitation unit startup and shutdown simulation is impossible due to their dynamic behaviour.

- Limited connection with production
  The model is not capable to calculate the steam requirement or heat duty in process units. These are modelled as black boxes with steam consumption or production characteristics based on measured data.

2

Utility Network

This section describes the utility network in place at the Pernis refinery, focused on the steam and fuel network. The information is gathered from internal documents and discussion with employees of the Shell refinery at Pernis. The refinery is split in three main areas: ABC, DE and KLM, as visible in fig. 2.1. The steam is produced in two CoGen plants: one located in the ABC area and one located in the KLM area. Both plants generate power as well as steam. The facility in the ABC area has production flexibility and can be optimized. This facility is the focus in this study. The CoGen plant in the KLM area provides steam for the refinery of which the quantity has several restrictions which are discussed chapter 6. The working principles of the main units connected to the steam utility network are further discussed in chapters 3 and 5.

Figure 2.1: Approximate overview of the three main areas at the Shell Pernis refinery, called ABC, DE and KLM [20].

2.1. Steam Network
The steam network is built up with six steam pressure levels and a condensate system, of which an overview is illustrated in fig. 2.2. Each level of the steam network is given below with their abbreviations and average operating pressure:

- 90barg saturated

- VHP: very high pressure ≈ 85barg

- HP: high pressure ≈ 70barg

- MP: medium pressure ≈ 18barg

- IP: intermediate pressure ≈ 7barg

- LP: low pressure ≈ 3barg

- Condensate

90barg Saturated

In fig. 2.2 there is a waste heat boiler (WHB) located at the top which produces saturated steam at around 90barg and 305 °C. The unit is located in the ABC area and supplies the 90barg sat. network with a large amount of steam, up to 165 t/h. Saturated steam is perfect for heat transfer when the latent heat is recovered using condensing heatexhangers [21]. However troublesome to transport and not suitable to use in steam turbines due to the risk of the water hammer effect and erosion of the turbine blades [22, 23]. The steam is therefore added to the heat recovery steam generator (HRSG), which are boilers that produce superheated VHP steam from the 90barg sat. inlet together with boiler feed water (BFW) for additional steam production.

Very High Pressure

As mentioned above the superheated VHP steam is produced in the HRSG, which in reality are two gas turbines (GTs) connected to two HRSGs. The VHP network is located at the power generation plant 1 (PGP1) in the ABC area and operates at a temperature of about 525 °C. At the KLM area VHP steam is supplied in relative small amounts, about 10 t/h, by the PGP2. These two sides of the VHP network are in reality not connected.

High Pressure

The HP network is located in the ABC area and only a few units are connected to it. The HP network operates at a temperature of about 370 °C. Between the VHP and HP networks there is a let down valve which reduces the pressure of the steam flow. To reach the required temperature BFW is injected during pressure reduction across the let down valve.

Medium Pressure

The MP network is the largest steam network at the refinery and covers all three production areas. The network operates at a temperature around 320 °C. Most of the units which produce and/or consume steam are connected to the MP network. The largest supplier is the PGP2 located in the KLM area of which the refinery receives about 400 t/h. The PGP2 balances the network depending on the refineries steam production and demand. The second largest supplier is the steam turbine generator (STG) located in the ABC area which consumes around 200 t/h of VHP steam and depressurizes it to the MP network. Furthermore, the third GT HRSG combination is directly connected to the MP network and produces about 100 t/h of MP steam. Three turbines, which are illustrated in fig. 2.2, consume MP steam. On of which is a STG while the other two are steam turbine driven compressors (STDCs) which provide the refinery with compressed air. Besides these main units a lot of smaller producers and consumers are connected to the network.

Intermediate Pressure

There are two IP networks that operate at around 270 °C and both are relatively small. One is located in the ABC area and is supplied by the STDC. The other IP network is located in the DEG area and supplied by a let down valve.

Lower Pressure

The LP network is not interconnected throughout the refinery, it consists of three separate sections. Two located in the KLM area and one in the ABC area. The STG in the ABC area consumes or produces LP steam, which is used to balance the network. Furthermore, LP steam in the ABC area is produced by the STDCs and also by other units in the network. Both of the KLM area LP networks receive LP steam from PGP2 and some of it is produced by units connected to the network as well. A lot of units are connected to the network and LP steam is also the heat supplier for the deaerators located on site.

Condensate

The final stage is the condensed stage, where the water returns in two groups: clean condensate or suspect condensate. Clean condensate can be used directly in the deaerator to remove oxygen and pressurized to be used as BFW. Suspect condensate is water returned from processes where the steam/water is used in heat exchangers where hydrocarbons are heated or cooled. The suspect condensate is cleaned in filters and then added to the deaerator system as well to produce BFW. Not all consumed steam returns as condensate. One of the reasons is that some processes use the steam in chemical reactions such as the strippers and the water gas shift reactor (WGSR).
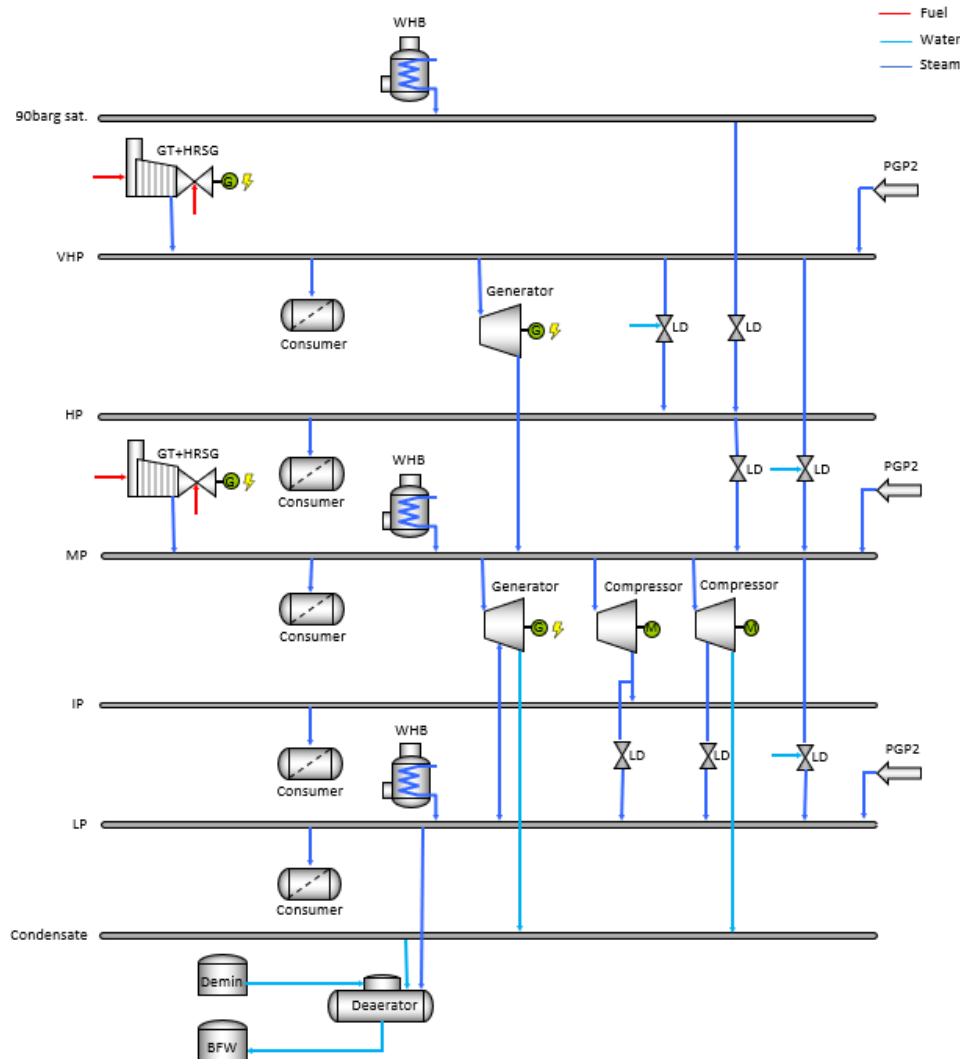
Figure 2.2: Overview of the refineries steam network, units are grouped together to compile the extensive network. The network is built up by six pressure levels and a condensate network, each with their steam/water producers and consumers. Abbreviations are GT (gas turbine), HRSG (heat recovery steam generator), WHB (waste heat boiler), LD (let down valve) and BFW (boiler feed water). Turbines connected to 'G' (generator) produce electricity, while turbines connected to 'M' (motor) are direct driven and connected to an air compressor.

2.2. Fuel Network

The refinery has an extensive fuel network, which is a combination of imported natural gas and fuels which are produced during the refining process. Fuel gas produced on site depends on the crude oil characteristics and on the capacity of the distillation column cooling system. If the cooling systems is less effective due to a high ambient temperature more non-condensables will be formed, which are then used as fuel on site

[19]. The gas consists of lighter petroleum components such as hydrogen, methane, ethane, propane and butane. The non-condensable gases from several distillation columns are mixed together with natural gas to achieve a LHV which is high enough for combustion. Due to environmental regulations the refinery is not allowed to flare excessive fuel gas for economic benefits. Unfortunately the fuel gas cannot be stored, so in case of excessive fuel gas more steam can be produced in the PGP1. The modelled units connected to the fuel network are the GTs and HRSGs, the fuel consumption is illustrated with the red arrows in fig. 2.2.

3

Units

The refineries steam and electricity production is mainly executed by the PGP1 (power generation plant 1). The PGP1 consists of gas turbines, heat recovery steam generators, steam turbine generators, steam turbine direct driven compressors and deaerators. These units form the backbone of the steam and electricity production. Some units on site have their own deaerators, steam direct driven turbines and waste heat boilers. Due to the fact that these systems are driven on product yield instead of steam production the focus in this work is on the main units at the PGP1. The maximum efficiency which can be achieved by the power generation plant can be described with the Carnot efficiency as calculated in eq. (3.1) and illustrated in fig. 3.1 [24]. The Carnot equation can be used to determine the maximum efficiency of the GT HRSG combination and of the BFW pump, HRSG and STG combination. For both the ratio between the hot and the cold temperature determines the maximum achievable efficiency. However for the refineries steam power production this is not a realistic calculation due to the fact that not all produced steam is utilized for power production as will be discussed in this chapter.

$$\eta_{\text{Carnot}} = 1 - \frac{T_{\text{Cold}}}{T_{\text{Hot}}} \tag{3.1}$$
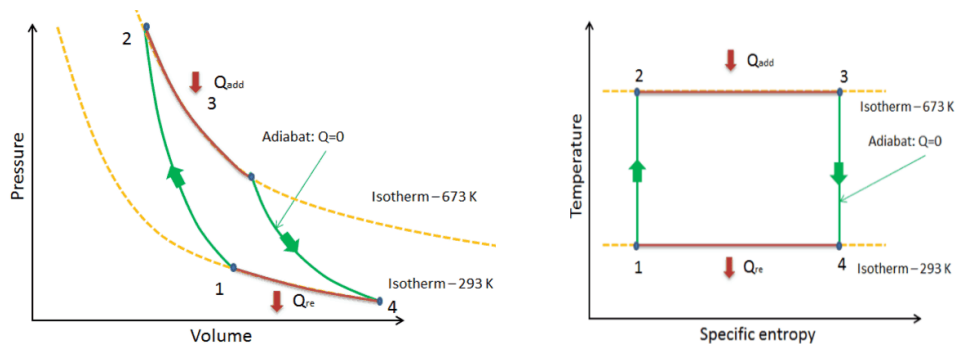
Figure 3.1: Carnot cycle in a PV (pressure vs. volume) and TS (temperature vs. entropy) diagram. Step 1-2 is isentropic compression, step 2-3 isothermal expansion, step 3-4 isentropic expansion and step 4-1 isothermal compression, where Q represents the energy flows [24].

3.1. Gas Turbine

The gas turbines provide the refinery with electric power and with residual heat which will be discussed in section 3.2. This work is focused on the three gas turbines, GT1, GT2 and GT3, at the refinery which are connected to the steam production. GT2 and GT3 are identical General Electric gas turbines and GT1 is roughly similar, the design is pictured in fig. 3.2. GT2 and GT3 can run on either natural gas or a fuel gas mix which is produced during the refinery processes on site as explained in section 2.2. GT1 only uses natural gas to operate.

Figure 3.2: Cross section of the General Electric 6B type gas turbine, similar to GT2 and GT3 [25].

Working Principle

Due to the fact that all three gas turbines are all single-shaft gas turbines the working principles are equal. However GT1 uses natural gas as fuel while GT2 and GT3 run on a mixture of gaseous fuels, with varying lower heating value (LHV). The working principle is visualized in fig. 3.3 and divided in the five main sections:

- Air inlet

- Compressor

- Combustion

- Turbine

- Exhaust

Air enters the gas turbine at ambient conditions after which it is compressed in the axial flow compressor. During compression the air heats up and flows towards the combustion chamber, here gaseous fuels are burned releasing the chemical energy. The hot gases are then converted into mechanical energy. This conversion takes place in two steps, first the hot gas is expanded in the nozzle section converting the thermal energy in kinetic energy. After which the expanded gas flows through the turbine where the kinetic energy is converted to mechanical energy by rotating the gas turbine shaft. The rotating shaft is the driving force for the compression stage, which consumes typically more then 50% of the mechanical energy. The shaft is connected via a gearbox to the generator which converts the rotational energy into electrical energy which can be used on site [26, 27].
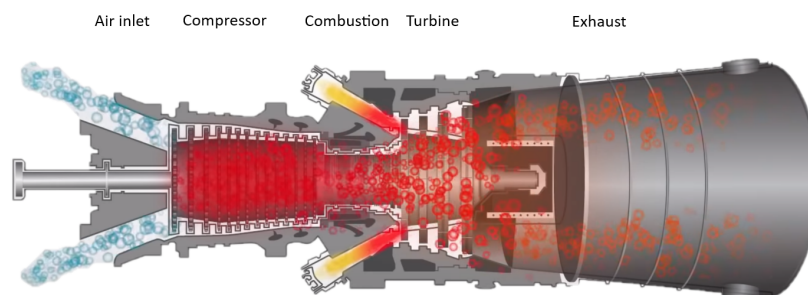
Figure 3.3: Cross section of the gas turbine with the five main sections: air inlet, compressor, combustion, turbine and exhaust [28].

Brayton Cycle

Gas turbines follow the Brayton cycle of which the pressure-volume (PV) and temperature-entropy (TS) diagrams are visible in fig. 3.4. Step 1-2 is the compression stage which ideally is isentropic, however as can be seen in fig. 3.4b there is a small entropy increase. Step 2-3 is the combustion step where pressure is constant and combustion of fuel increases the entropy. Step 3-4 is the decompression stage inside the turbine, ideally isentropic however as can be seen there is a small entropy increase in fig. 3.4b. Step 4-1 is not connected, point 4 is the hot exhaust gases while point 1 is the cold air intake, the decrease in entropy from 4-1 illustrates the non-utilized energy.

(a) Pressure vs. volume

(b) Temperature vs. entropy
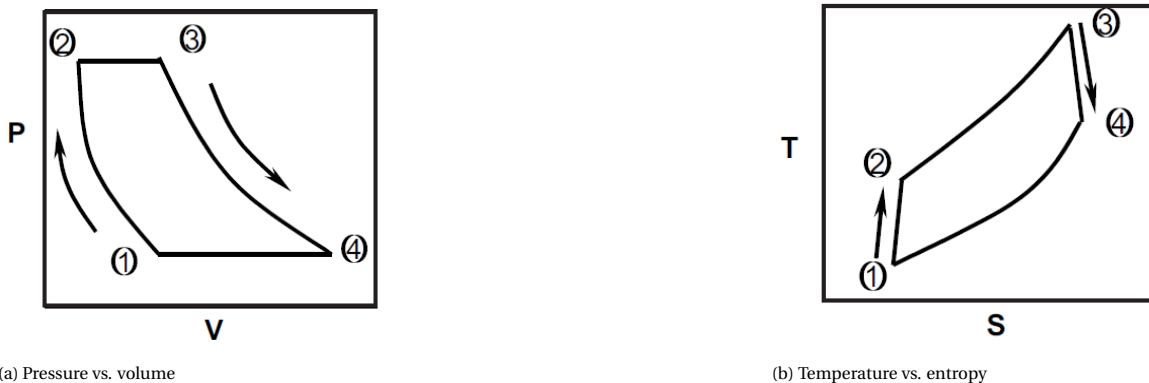
Figure 3.4: Brayton cycle PV (pressure vs. volume) and TS (temperature vs. entropy) diagram. Step 1-2 is compression, 2-3 isobaric combustion, 3-4 decompression and 4-1 isobaric cooling [27].

Performance Factors

There are several factors which effect the performance of the gas turbines and have to be considered when modelling in the i-Steam software. The factors which have the largest effect are listed below [27, 29]:

- Ambient conditions

- Inlet and exhaust losses

- Fuel

- NO_x suppression

- Equipment degradation

- Mechanical and electrical losses

Ambient Conditions

The gas turbine takes in air and therefore ambient conditions such as temperature, pressure and humidity have an influence on the machines performance. International Organisation of Standardisation reference conditions are used in the testing of gas turbines [27]. Site reference altitude is at sea level and 1.013 bar, increasing the sites altitude will reduce the air density due to lower air pressure [27]. This results in an decreased air mass flow through the turbine and therefore a reduced power output of roughly 4% per 30 meters of elevation [29]. While this reduces power output, fuel consumption will decrease proportional and heat rate, calculated with eq. (3.2), is not effected [30].

$$Heat\,Rate = \frac{Q_{\text{Thermal,In}}}{Q_{\text{Electrical,Out}}} \tag{3.2}$$

Ambient temperature also decreases air density and therefore the produced power output as described above. However ambient temperature has an effect on the heat rate, due to the fact that the compressor discharge temperature increases when the air inlet temperature rises. This limits the amount of heat which can be added during combustion due to the maximum firing temperature. The effect can be described with the help of fig. 3.4b, if point 1 increases due to higher ambient temperature point 2, the compressor discharge

temperature, will increase as well if the same pressure ratio is obtained. Point 3 is at the maximum tempera-ture and limits the amount of energy input in step 2-3 [31]. The effects of ambient temperature are illustrated in fig. 3.5, with the heat rate, power output, exhaust flow and heat consumption. Each turbine has its own temperature-effect curve, however the visible trend is similar.
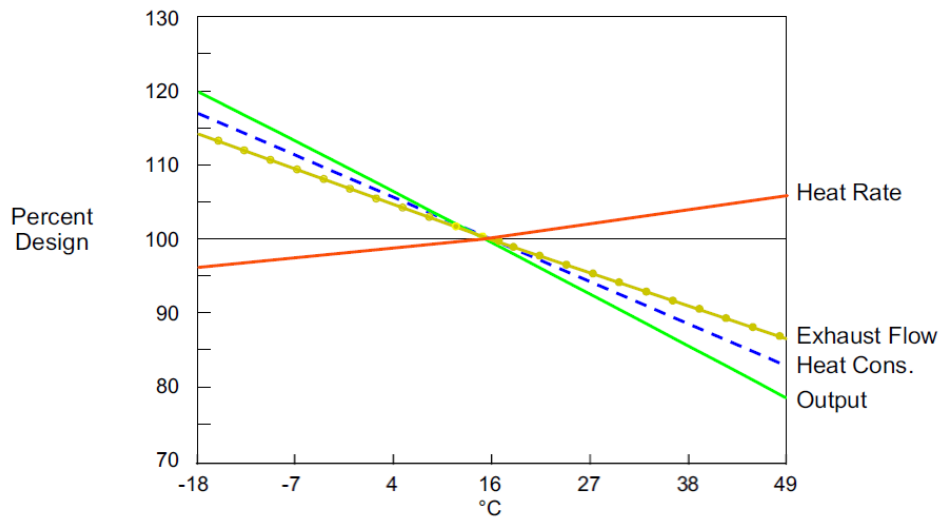
Figure 3.5: Effect of ambient temperature on heat rate, power output, exhaust flow and heat consumption. At 100 percent design the gas turbine operates as it was designed at the ambient temperature of 16 °C. This graph is specific for the gas turbine MS7001 series [27].

Humidity of the air has also an effect on the gas turbine performance, due to the fact that humid air has a lower density than dry air and changes the heat capacity. The reduction in power output is in the 1-2 % range and depend strongly on the gas turbine model, some models show an increase in performance while other show a decrease [31]. Relative humidity at ISO standards is 60%, while for the Rotterdam area the humidity depends on the season and is on average between 76-88% [27, 32]. Due to the missing information of humidity dependency on the GTs at the refinery this is not incorporated in the model.

Inlet and Exhaust Losses
The GT air intake and the exhaust which flows through the HRSG causes pressure losses inside the system [29]. The negative effect of these losses are incorporated in the model because it is based on site measured data. However in reality these losses would increase over time due to fouling and be reduced when mainte-nance is executed.

Fuel
Work delivered by the gas turbine can be calculated in energy per kilogram of mass flow with eq. (3.3), where mass flow is the sum of the air intake and fuel consumption. From the graph it can be concluded that for fuels without oxygen or inert gases power output increases when LHV increases. This is due to the fact that the increasing C_p has a greater effect on the power output than the decreasing mass flow. When adding oxygen or inert gases which decrease the LHV of the fuel the power output increases due the increase of mass flow through the gas turbine. This increase of mass flow due to the low LHV fuel gas has a positive effect on the GT power output, because the fuel gas is not compressed by the GT itself. Increasing the mass flow through the turbine stages results in other issues such as reaching the compressor surge and the turbine power limits. Increasing the mass flow through the fuel network requires larger dimensions and therefore increases the cost of the fuel system [27].

$$W = C_p \cdot \Delta T \qquad (3.3)$$

NO_x Suppression
Gas turbine which require NO_x suppression due to environmental regulations can use steam injection. NO_x formation occurs when high temperatures are reached and steam injection reduces the temperature in the combustion chamber [33]. Therefore when the gas turbines operate on pure natural gas, such as GT1, the
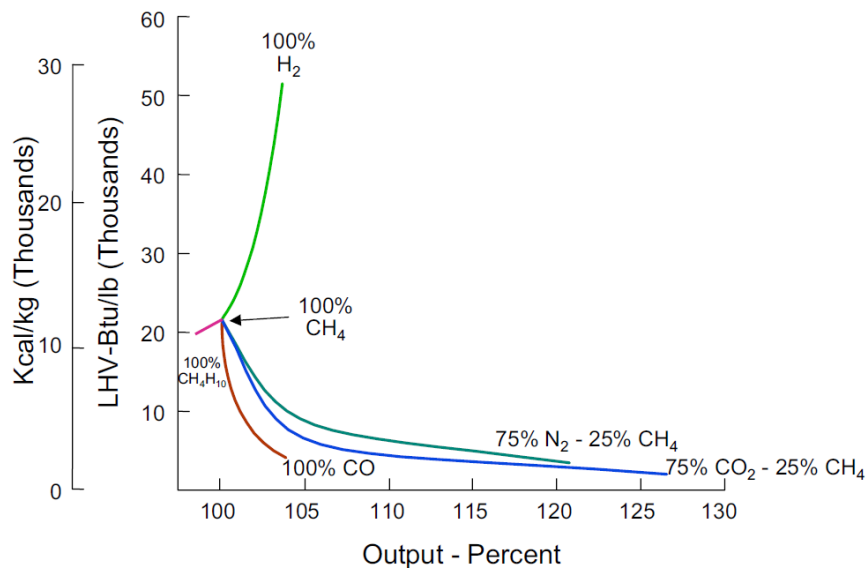
Figure 3.6: Effect of fuel composition on power output percentage. Starting point is 100% CH_4 (methane) towards fuel mixes with higher or lower LHV (lower heating value) due to the addition of inert gases, hydrogen or hydrocarbons [27].

steam injection rate is zero due to the lower combustion temperature. When refinery fuel gas is used, as in GT2 and GT3, the temperature increases due to hydrogen in the fuel and steam is needed to reduce the NO_x formation. The steam injection leads to an increased mass flow through the turbine and therefore an increased power output. Due to the fact that extra fuel is needed to raise the temperature of the steam to the temperature in the combustion chamber, no reduction in heat rate is achieved [27].

Equipment Degradation
During the lifetime of the gas turbine the machine will degrade and decrease in power output and efficiency. The filters at the air inlet clog up over time, increasing the pressure drop over the system and therefore reducing the air intake pressure of the GT. Dust particles which passed through the filtration system cause fouling of the GT compressor blades. Furthermore, combustion byproducts cause fouling of the turbine blades in the GT [29]. These effects are not of direct concern for the model as it is based on measured data which already includes these effect.

Mechanical and Electrical Losses
Mechanical and electrical losses occur when the chemical energy is converted to mechanical energy which powers the generator and creates electrical energy. These losses are very specific for the type of equipment. Again due to the usage of measured data for the model these factor are already included.

3.2. Heat Recovery Steam Generator
Utilization of the residual heat from the gas turbine exhaust can be achieved with heat recovery steam generators (HRSG). At the refinery there are three HRSGs: HRSG1, HRSG2 and HRSG3, which are connected to GT1, GT2 and GT3 respectively. Combining the gas turbine with a HRSG can potentially increase efficiency up to 60% [26]. The combined cycle system utilizes the residual heat in the hot turbine exhaust gases by generating steam. On site there are two types of HRSGs, one produces 85barg superheated steam which is converted into electrical power using STG1 as visualized in fig. 3.7. The other HRSG produces 18barg steam which is directly connected to the MP steam network.

Working Principle
The layout of a single pressure HRSG is shown in fig. 3.8, which is similar to the ones installed at the Pernis refinery. The HRSG systems are dived in three main sections listed below:

- Economizer
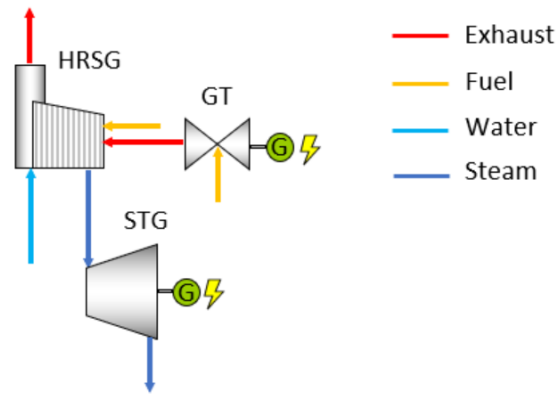
Figure 3.7: Combined cycle of a GT (gas turbine) of which the hot exhaust is utilized for steam production in the HRSG (heat recovery steam generator) with supplementary firing. The steam flows through the STG (steam turbine generator) for the production of electricity.

- Evaporator

- Superheater

The BFW starts in the economizer, where it is heated by the flue gases to nearly saturated conditions. In HRSG2 and HRSG3 the economizer is the final step, from the flue gas viewing point, however HRSG1 has an extra unit called the flue gas cooler which heats water in a closed circuit. That heated water is then used as energy carrier to heat up the demineralized water feed of the deaerators. After reaching nearly saturated conditions in the economizer the water is collected in a steam drum. Water from the steam drum is circulated through the evaporator and flows back to the steam drum. Both HRSG2 and HRSG3 are natural circulation systems, which means that no pump is required to maintain the flow from the steam drum through the evaporator. HRSG1 is an aided circulation system, which uses a pomp to guarantee the circulation of water. Aided systems are often installed when the heat exchanger tubes in the evaporator are placed horizontally as is the case with HRSG1 [34]. The saturated steam leaves the steam drum and enters the superheater, which is closest to the gas turbine and therefore at maximum flue gas temperature. Inside the superheater the saturated steam is heated to the desired temperature and can than be used in the units down the line. At the refinery the HRSG2 and HRSG3 have supplementary firing burners, which would be placed left of the superheater in fig. 3.8, to generate extra heat. The HRSG1 has supplementary firing as well, however the burners are placed more towards the middle of the HRSG and normally not in operation.
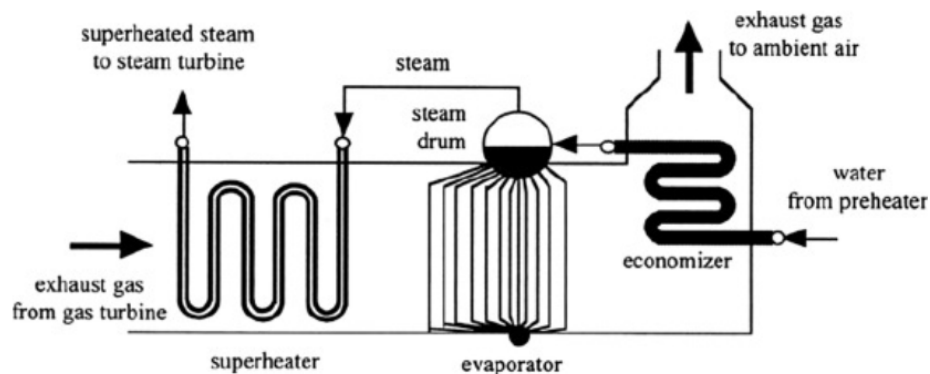
Figure 3.8: Overview of an heat recovery steam generator system which utilizes the hot exhaust gases from a gas turbine to produce superheated steam from preheated water [35].

Minimum Temperature Approach and Pinch Point
The approach and pinch point are at the same location in the HRSG as visible in fig. 3.9 and both depend on the saturated temperature. The approach point is the difference between the water temperature after the

economizer and the saturated temperature. The pinch point is the difference between the flue gas temperature and the saturated temperature. Both the approach and pinch temperature lie normally in the 10-15 °C range [36].
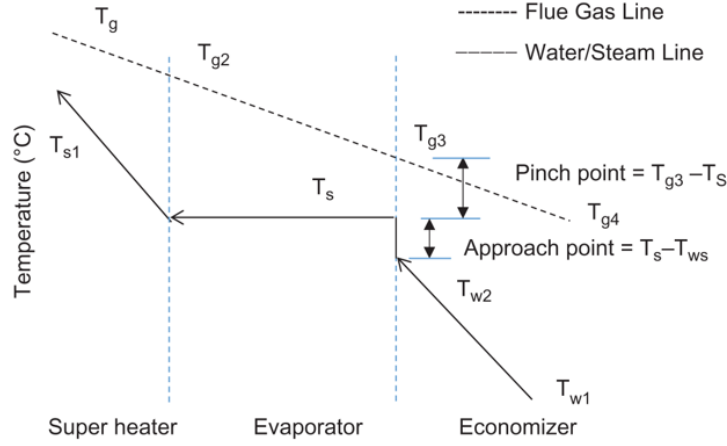
Figure 3.9: Water/steam flow (from right to left) and flue gas flow (from left to right) with corresponding temperature profile inside the heat recovery steam generator. The Location of the pinch and approach point is given at the inlet of the evaporator. Equations for both points are given in the graph as well [36].

The pinch and approach temperatures are selected for a certain steam production rate, conditions of exhaust gas and firing state of the supplementary firing. These points should be selected during the unfired state to prevent steaming in the economizer due to a very low approach point when burners are turned off. The selected pinch and approach temperatures determine the size of the heat exchanger equipment [37].

Heat Balance

The heat equation which calculates the heat transfer for the HRSG is given in eq. (3.4). Where Q is the total heat transferred, U is the overall heat transfer coefficient and LMTD is logarithmic mean temperature difference which is calculated in eq. (3.5) for the superheater using the variables given in fig. 3.9.

$$\sum_i Q_i = \sum_i U_i \cdot A_i \cdot LMTD_i \tag{3.4}$$

$$LMTD = \frac{\left(T_g - T_{s1}\right) - \left(T_{g2} - T_s\right)}{\ln\left(T_g - T_{s1}\right) - \ln\left(T_{g2} - T_s\right)} \tag{3.5}$$

The total heat transferred can also be calculated using the C_p value of the gas which flows through the HRSG as in eq. (3.6) [38]. If supplementary firing is used T_g should be the supplementary firing temperature and C_p should be of the exhaust mixture from the gas turbine and the supplementary burners. As is clear when looking at the heat equation a lower stack temperature results in more heat transfer and will therefore improve the HRSG efficiency. However the stack temperature should be maintained above 100 °C to prevent acid condensation which corrodes the system [39].

$$Q = \dot{m}_g \cdot C_{p,g}\left(T_g - T_{g4}\right) \tag{3.6}$$

Blowdown

Total dissolved solids concentration in the water-steam cycle should be minimized to prevent corrosion and erosion in equipment such as heat exchangers en turbines. To decrease the concentration chemicals are added to the cycle, however this could result in a chemical built up which could cause problems in operation. Blowdown of the steam drum in the HRSG resolves this issue, by constantly draining a portion of the saturated water. Due to the fact that this blowdown occurs after the economizer step the energy in the water is already quite high, resulting in significant losses. The energy losses of HRSG1, HRSG2 and HRSG3 are limited by flashing the blowdown water in a vessel and the produced LP steam is added to the deaerator as in fig. 3.10 [40].
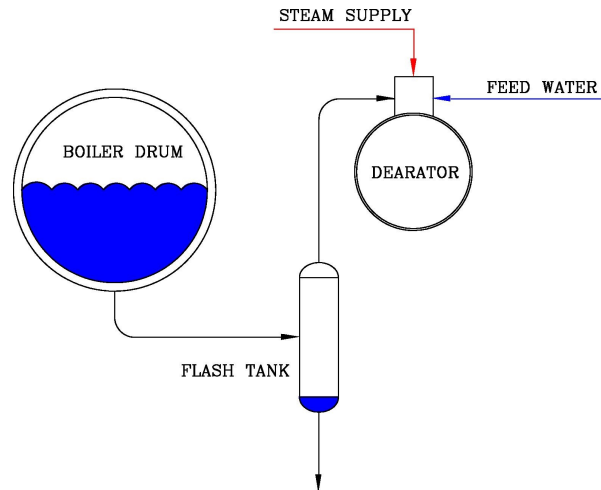
Figure 3.10: Energy recovery of the blowdown stream for the heat recovery steam generator boiler or steam drum. The saturated blow-down stream is flashed to produce LP (low pressure) steam which is the energy source of the deaerator [40].

3.3. Steam Turbine Generator

At the refinery there are two STG units, STG1 and STG2. The STG1 consumes VHP superheated steam from HRSG2 and HRSG3, and has MP steam as an outlet. This is called a back-pressure steam turbine, which is standard in co-generation [41]. The STG2 is a two stage turbine, from MP to LP and from LP to condensate. The energy released by the steam in each stage can be calculated with eq. (3.7). The LP section can be operated to balance the LP steam network, importing steam when there is a surplus in the network or extracting steam when there is a shortage. This first section of the STG2 can be considered a back-pressure steam turbine as well. The second stage is a condensing turbine which consumes LP steam and has a sub atmospheric pressure two phase outlet after which it is condensed in a condenser. The condensing stage is purely for extra electrical power generation when steam is available, the efficiency is much lower than a back-pressure turbine [41].

$$Q = \sum_i \dot{m}_{s,i} \left(h_{in,i} - h_{out,i} \right) \tag{3.7}$$

3.4. Rankine Cycle

The combination of the HRSG and the STG as illustrated in fig. 3.7 can be described with the Rankine cycle [38]. When assuming that the steam and water flowing through the HRSG and condenser are at constant pressure and that the pump and STG are isentropic the process would follow the ideal Rankine cycle as shown in fig. 3.11 [42]. Step 1-2 is the compression stage, where BFW is pumped to the desired pressure. Step 2-3 is the heating, which has 3 sections: the heating of BFW, the two phase evaporation (isothermal) and the superheating of the steam. Step 3-4 is the decompression inside the turbine which generates power. Step 4-1 is the two phase condensation (isothermal). The efficiency for the Rankine cycle can be calculated with eq. (3.8) [34].

$$\eta_{Ra} = 1 - \frac{h_4 - h_1}{h_3 - h_2} \tag{3.8}$$

The cycle illustrated by fig. 3.11 is quite different from the steam/water cycle at the refinery, due to the fact the refineries cycle is not closed. HRSG2 and HRSG3 produce 85barg steam that flows through STG1 of which the output is 18barg steam. This 18barg steam is then consumed by several units and some it flows through STG2. This means that not all the produced steam is used for power generation, but also for heating and other processes.

3.5. Deaerator

Deaerators strip dissolved gases to form boiler feed water (BFW). Dissolved oxygen has to be removed, because it causes rapid localized corrosion in the tubes of the HRSG system. Furthermore dissolved carbon
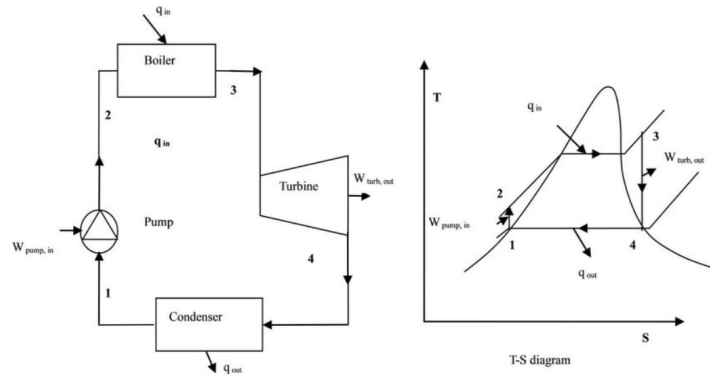
Figure 3.11: Overview of the closed ideal Rankine cycle with on the left the equipment and on the right the corresponding TS (temperature vs. entropy) diagram. Step 1-2 is compression, step 2-3 is heating, step 3-4 is decompression and 4-1 is condensation. W is the work produced or supplied to the cycle and q is the heat added or extracted from the cycle [34].

dioxide lowers the pH level of the BFW and forms carbonic acid. The low pH of the BFW can cause severe acid attacks throughout the BFW, boiler and steam systems. Removing dissolved gases with a deaerator is based on two principles, Henry's law and the relation between gas solubility and temperature. Henry's law dictates that the gas solubility decreases when the partial pressure of the gas above the solution decreases. Based on these two phenomena the deaerator strips the water from dissolved gas by adding low pressure steam which heats up the water to saturation temperature and therefore decreasing the gas solubility. Furthermore the water is sprayed in the deaerator increasing its area and lowering the partial pressure of the gas. The extracted gas is vented at the top of the deaerator [43].

3.6. Measurement Devices

Measuring devices are used on site to determine the flow, temperature and pressure of water and steam. The installed instrumentation with their estimated uncertainty are obtained from internal discussion and documents.

Thermocouples

The most common practice at the refinery is to use thermocouples to determine the temperature of water/steam flows. Thermocouples utilize the phenomenon of voltage production when one junction of two dissimilar metals is heated while the other one is kept cold. This phenomenon is called thermoelectricity or the Seebeck effect as illustrated in fig. 3.12 [44]. On the hot side electron/hole pairs will be formed while absorbing heat and these flow through the N and P side, while on the cold side these pairs are recombined which generates heat and an electrical current [45]. At the refinery the standard thermocouple used for the steam networks is the K-type thermocouple which can operate in the -20 °C to 1000 °C range, where the positive wire is Nickel-Chromium and the negative wire is Nickel-Aluminium [44].
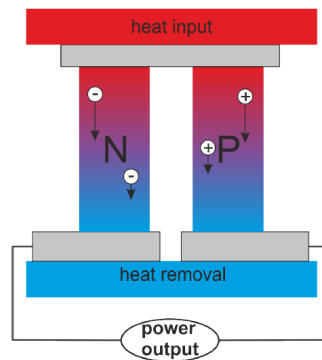
Figure 3.12: Illustration of the Seebeck effect, where an electrical current is generated due to heat flow across the dissimilar metals [45]
.

The voltage produced by the thermocouple is converted in a temperature transmitter to a temperature reading. The combination of the thermocouple and temperature transmitter used for the refineries steam network has an uncertainty of 2-5%.

Pressure Transmitters

The standard approach of measuring the pressure of the steam network is with capacitive pressure transmitters. There are three types of pressure sensors: gauge, absolute and differential. Gauge measures the pressure against atmospheric pressure, absolute against vacuum and differential is the difference between two pressures. Most common ones at the refinery are the gauge sensors for pressures above atmospheric pressure and the absolute sensors for pressures below atmospheric [46]. The capacitive pressure transmitter is illustrated in fig. 3.13, for gauge pressure one side is the measured pressure and the other side is at atmospheric pressure. The pressure difference will move the sensing diagram, which functions as one plate of two capacitors where the other plates are the stationary plates. If the left side has an higher pressure the sensing diagram will move closer to the right capacitor. Using eq. (3.9) it is clear that the capacitance on the lower pressure side will increase and the one on the higher pressure side will decrease [47]. The change in capacitance is measured by the capacitance detector circuit with a high frequency AC signal, which is translated to a DC output which represents a certain pressure.
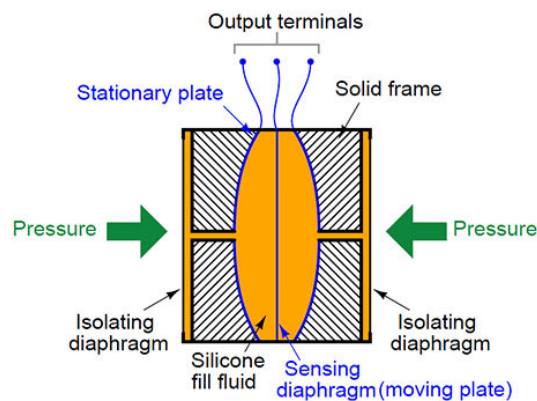
Figure 3.13: Illustration of the pressure capacitor sensor, where an electrical current is generated due to movement of the sensing diaphragm changing the capacitance of the two capacitors [47].

$$C = \frac{A \cdot \epsilon}{d} \tag{3.9}$$

The standard pressure transmitters at the refinery are the Rosemount 3051 and Foxboro 13A. The Rosemount has an estimated uncertainty between 2-5% and the Foxboro has an estimated uncertainty of 5%.

Flowmeters

There are two types of flowmeters which are standard for measurements at the steam network of the refinery. One type is the ultrasonic flowmeter and the other is the differential pressure flowmeter, both are discussed below.

Ultrasonic Flowmeter

Ultrasonic meters are based on the time of flight principle between a pair of transducers as illustrated in fig. 3.14. The transducers can both transmit and detect high frequency sound waves. Going back and forth between the the two transducers of which one is upstream and one is downstream, results in different travelling time. The flow speeds up the sound wave when it travels downstream and slows it down when it travels upstream. This time difference between upstream and downstream is directly proportional to the flowrate. More pairs of transducers and mathematical compensation will reduce the effect of flow distortion on the measurements [48]. The ultrasonic flowmeters used for the steam network of the refinery have an estimated uncertainty of 1-5%.
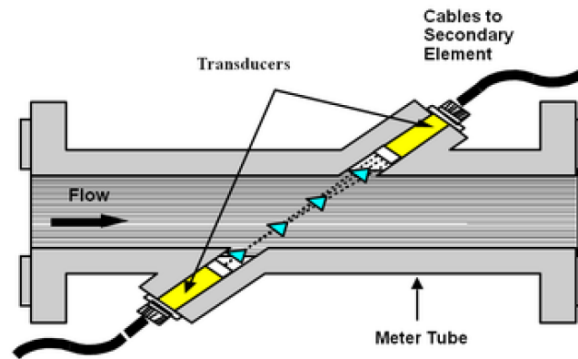
Figure 3.14: Illustration of a single transducer pair ultrasonic flowmeter configuration. The signal goes back and forth between the transducers and the time needed to travel is directly proportion to the flowrate [48].

Differential Pressure Flowmeter

Differential pressure flowmeters are based on the Bernoulli principle and determine the flowrate by obstructing the flow and measuring the pressure before and after the obstruction. The differential pressure can be measured with the capacitor pressure sensor described in section 3.6. The standard obstruction used at the refinery is the square plate orifice, the working principle is illustrated in fig. 3.15. The measured differential pressure, fluid properties and meter geometry are used to calculate the mass flowrate with eq. (3.10) or volumetric flowrate eq. (3.11) [49]. C is the group of flow coefficients and factors which apply to the correction of meter geometry, fluid flow characteristics and compressibility. It is not the focus of this work and therefore it is not discussed in more detail.

$$Q_{\text{Mass}} = C \cdot \sqrt{\rho_F \cdot \Delta P} \tag{3.10}$$

$$Q_{\text{Volume}} = C \cdot \frac{\sqrt{\rho_F \cdot \Delta P}}{\rho_B} \tag{3.11}$$
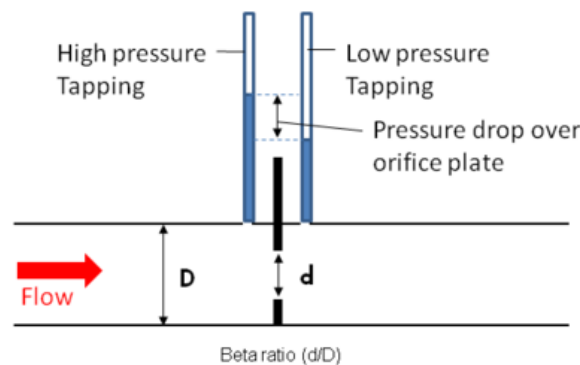
Figure 3.15: Working principle differential pressure flowmeter, flow is obstructed by for example an orifice and the pressure is measured before and after the obstruction. D represents the inner diameter of the pipe while d represents the inner diameter of the obstruction, the given beta ratio is d/D [49].

The equations eq. (3.10) and eq. (3.11) show that the mass and volumetric flowrate are proportional to the square root of the measured differential. This is one of the main limitations of differential pressure flowmeters which can be explained with the following example. If the flowrate is turned down to 70% of the design flowrate, the pressure transmitter will be $(0.7)^2$ which is at 49% of the transmitter span. The uncertainty of the differential pressure meter will increase if it operates further from its design point. The uncertainty of the square orifice plate differential pressure flowmeters installed at the steam network of the refinery have an estimated uncertainty of 5%.

4

Data

The refinery is well equipped with sensors to measure the steam characteristics as well as the power output by the GTs and STGs. The output of these sensors are gathered in the software program PI, where each sensor has its own unique tag which can be used in Excel and Seeq for data analysis. This data is collected of all units and pipelines which are connected to the steam network and used to design and validate the models. The years of which the data is collected are written as year 1 (Y1), year 2 (Y2) and year 3 (Y3).

4.1. Base Case Selection

For the design and validation of the i-Steam models several base cases are selected. The timestamp selection for the pipeline model is discussed in the first section and the selection for the optimization model in the second section.

Pipeline Model

The pipeline model requires production and consumption data of each unit connected to the steam network. The design of the pipeline model is based on four modelled scenarios, the results of these four are then used to validate the model in chapter 7. Using the tags from PI and the data tool Seeq a plot is made of the largest steam production units on site visible in fig. 4.1. The signals in the plot are altered using a low-pass filter to reduce noise in the flow rate output, the low-pass filter has a cut-off period of three hours and a sampling time of ten minutes. The three hour cut-off is chosen to get a clear view of the steam production over a larger period of time, while the ten minutes sample period is necessary to export it to Excel. From fig. 4.1 four cases are selected which are in a stable scenario and all main steam production units are in operation during one or more of the cases. Furthermore the four cases provide a spread of ambient conditions as given in table 4.1. The abbreviations used in figs. 4.1 to 4.5 are explained below:

- WHB1: process unit which exports MP steam

- WHB2: process unit which exports MP steam

- HRSG1: HRSG unit which exports MP steam

- HRSG2: HRSG unit which exports VHP steam

- HRSG3: HRSG unit which exports VHP steam

- WHB3: process unit which exports MP steam

- WHB4: process unit which exports MP steam

- WHB5: process unit which exports 90barg sat. steam

- PGP2: CoGen plant in the KLM area which exports VHP, MP and LP steam to the network
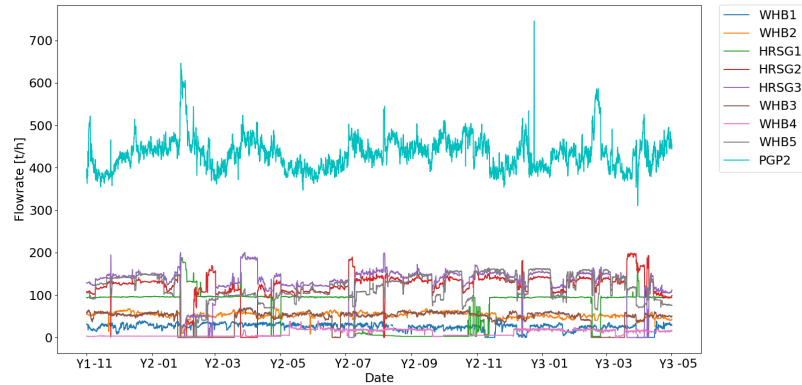
Figure 4.1: Output of the main steam producers for an one and a half year period. The signals are filtered with a low-pass filter using a three hour cut-off period and a ten minute sampling time.

The steam production during the four cases is visible in the figs. 4.2 to 4.5, with a cut-off period of twenty minutes and a sampling time of thirty seconds. Using the graphs the following four days are chosen: 1 January year 2, 17 March year 2, 10 February year 3 and 17 March year 3. These scenarios are selected to test the model in slightly different operational settings and used for validation of flow, temperature and pressure in chapter 7. These scenarios do not just differ from each other in terms of which units are in operation, but also in how the steam flows through the network and through which pipelines.

1 January year 2

The first scenario is 1 January year 2, of which the ambient conditions are given in table 4.1. During this period the WHB4 was out of operation, while all other unit where running stable. This timestamp is the starting point for the design of the pipeline and optimization models. The measured data is averaged over a six hour period, from 12:00pm-18:00pm, to reduce the effect of noise on modelling and validation. This six hour averaging is applied for all four modelling scenarios.
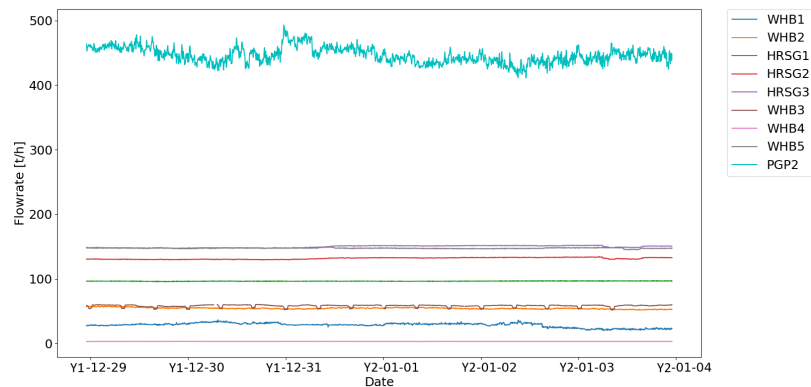
Figure 4.2: Output of the main steam producers from 29 December year 1 to 4 January year 2. The signals are filtered with a low-pass filter using a twenty minute cut-off period and a thirty second sampling time.

17 July year 2

The second scenario is 17 July year 2, of which the ambient conditions are given in table 4.1. As visible in fig. 4.3 HRSG1 was out of operation, which is standard practice during the summer months. In the graph it looks like there is a bit of steam produced by HRSG1, however this is just a measurement error because when in operation this unit normally produces around 100 t/h of MP steam.
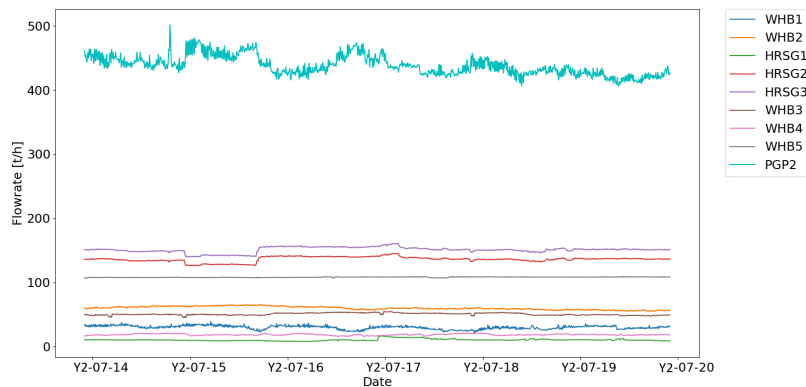
Figure 4.3: Output of the main steam producers from 14 July year 2 to 20 July year 2. The signals are filtered with a low-pass filter using a twenty minute cut-off period and a thirty second sampling time.

10 February year 3

The third scenario is 10 February year 3, of which the ambient conditions are also given in table 4.1. As can be seen in fig. 4.4 all main steam producing units where in stable operation at the time.
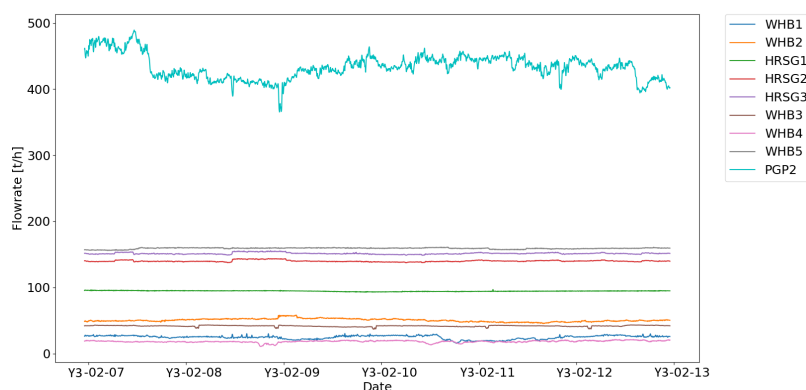
Figure 4.4: Output of the main steam producers from 7 February year 3 to 13 February year 3. The signals are filtered with a low-pass filter using a twenty minute cut-off period and a thirty second sampling time.

17 March year 3

The fourth scenario is 17 March year 3, of which the ambient conditions are also given in table 4.1. During this day the WHB3 and WHB4 where out of operation as visible in fig. 4.5. It seems like the WHB4 is producing a very small amount of steam, however this is a measurement error, when the unit is exporting steam it is around 15 t/h of MP steam.

Ambient Conditions

The weather conditions in Rotterdam, close to the refinery, are collected from the KNMI database and given in table 4.1. To calculate the heat losses during the steam transportation temperature and wind speed are included in the model. The effect of rainfall is not incorporated in the model, therefore four days are chosen with negligible rainfall to exclude the effect on the measured data at the time.

Optimization Model

The optimization model is focused on the steam production by the HRSGs, PGP2 steam import and the electricity generation of the GTs and STGs. The model is designed using the data from 1 January year 2 and
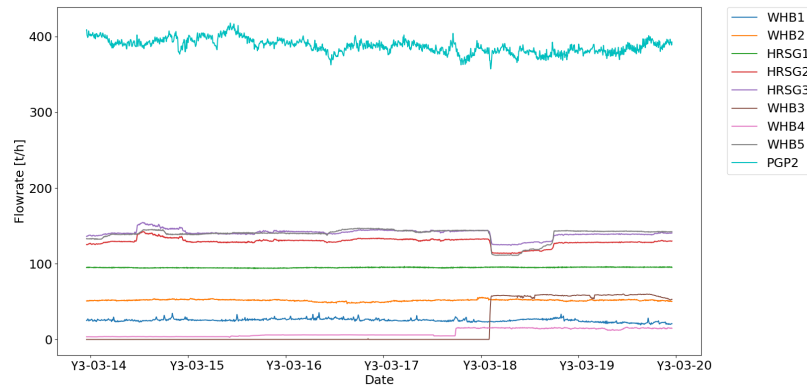
Figure 4.5: Output of the main steam producers from 14 March year 3 to 20 March year 3. The signals are filtered with a low-pass filter using a twenty minute cut-off period and a thirty second sampling time.

Table 4.1: Average weather data for the four base cases based on hourly measurements by the KNMI in Rotterdam [50]

Date	Time	Temperature [°C]	Wind [m/s]	Rainfall [mm]
1 Jan year 2	12-18 p.m.	7.8	6	<0.05
19 Jul year 2	12-18 p.m.	22.0	4	0.0
10 Feb year 3	12-18 p.m.	8.5	12	<0.05
17 Mar year 3	12-18 p.m.	11.7	7	0.0

validated for the first of every month for the years year 1 and year 2. As described above the used data is an average value over six hour period between 12:00pm-18:00pm to reduce the signal noise.

4.2. Data Collection

For each unit the required tags are gathered and the outputs are analysed in the software programs Excel and Seeq. Seeq is used to visualize trends in the signal and to discover if measurement instrumentation is malfunctioning. Excel is used to design a complete flowsheet of the steam network with all the relevant measured values of the current timestamp and the four pipeline model scenarios. Furthermore Excel is used to run the i-Steam software as add-in which has the ability to run multiple scenarios at once, apply input data from PI and gather the results for validation. For simple consumers and producers only steam flow rate, pressure and temperature data is gathered. For the main units, which are the ones that have a large influence on the steam network and will be modelled in further detail, more data is collected such as fuel flow and power output. The main units at the Shell Pernis refinery are the following:

- GTs: GT1, GT2 and GT3

- HRSGs: HRSG1, HRSG2 and HRSG3

- STGs: STG1 and STG2

- STDCs: STDC1 and STDC2

- WHB1

- WHB3

- WHB4

- Deaerators: D1, D2 and D3

The pipeline model contains the length, diameter and the number of bends for all relevant outside battery limit steam pipelines at the refinery. These dimensions are gathered via isometric drawings and Site-SPOT,

which contains a full 3D image of the refinery where the outer battery limit pipes are visible and 3D measurements can be made. The insulation thickness is unknown and determined via validation of the four scenarios in chapter 7. For inside battery limit and for the new project the length of the pipelines are based on estimations via maps of the refinery.

<div align="right">

5

</div>

Pipeline Model

In this section the pipeline model is discussed, with all the main equipment connected to the steam utility network. For each piece of equipment the equations supplied by the i-Steam software company PIL are given. The simplified overview of the refineries steam network is shown in fig. 2.2, the i-Steam pipeline model is added to appendix A.

5.1. Gas Turbine with HRSG

The gas turbine with HRSG combination produces electricity and steam while consuming gaseous fuels for the gas turbine it self and for supplementary firing in the HRSG. First the model for the GT is discussed after which the calculations for the HRSG are reviewed as well.

For the simulation of the gas turbines performance i-Steam provides four different models, which are listed below:

- Fixed performance model

- Regression model (design and retrofit)

- Regression model (operation optimization)

- Sectional model

The pipeline model is aimed at simulating scenarios and calculating the steam properties throughout the network. Due to this scenario modelling it is possible to chose the most basic model, fixed performance model, to simulate the gas turbine. The fixed performance model ensures that the simulation is exactly as in reality, due to the fact that more input data is required for modelling. The required input data is listed below:

- Shaft power

- Gas turbine intake air temperature

- Efficiency

- Exhaust temperature

- Exhaust flowrate

Shaft power, air and exhaust temperature are measured and can directly be used as input for the model. Efficiency is calculated with eq. (5.1), by dividing the GT power output (W_{GT}) by the total fuel energy ($Q_{\text{GT,Fuel}}$). The exhaust flowrate measurements are inaccurate and therefore it has been calculated using the equations supplied by i-Steam in eqs. (5.2) to (5.5). In eq. (5.2) the energy of the GT exhaust is calculated by subtracting the GT power output (W_{GT}) from the fuel energy input ($Q_{\text{GT,Fuel}}$). The $MCp_{\text{GT,Exhaust}}$ is the energy in the exhaust gas per degree Kelvin and calculated in eq. (5.3) by dividing the exhaust energy by the difference between the exhaust temperature and the ambient temperature. With the $MCp_{\text{GT,Exhaust}}$ the required air mass flow through the GT can be calculated in eq. (5.4). The coefficient 'i' is determined by i-Steam at a value

of 1.05 and the fuel consumption ($\dot{m}_{GT,\,Fuel}$) is measured on site. With the calculated air and fuel mass flows the exhaust mass flow ($\dot{m}_{GT,Exhaust}$) is calculated in eq. (5.5).

$$\eta_{GT} = \frac{W_{GT}}{Q_{GT,Fuel}} \tag{5.1}$$

$$Q_{GT,Exhaust} = Q_{GT,Fuel} - W_{GT} \tag{5.2}$$

$$MCp_{GT,Exhaust} = \frac{Q_{GT,Exhaust}}{(T_{GT,Exhaust} - T_{Amb})} \tag{5.3}$$

$$\dot{m}_{GT,Air} = \frac{MCp_{GT,Exhaust} - i \cdot \dot{m}_{GT,\,Fuel}}{i} \tag{5.4}$$

$$\dot{m}_{GT,Exhaust} = \dot{m}_{GT,Air} + \dot{m}_{GT,Fuel} \tag{5.5}$$

The HRSG is connected to the GT's exhaust, which utilizes the exhaust heat and if needed supplementary firing to produce steam. The models used for the evaluation of the HRSG depend on the amount of available information, less information supplied results in assumptions made by the software. The five models which are available in i-Steam for the calculation of the HRSG performance are listed below:

- Supplementary firing duty & Steam flow rate

- Supplementary firing temperature & Steam flow rate

- Supplementary firing duty → Minimum steam flow rate

- Supplementary firing temperature → Minimum steam flow rate

- Steam flow rate → Minimum supplementary firing duty & Supplementary firing temperature

The final three HRSG models, use a limited amount of input data, which results in the required assumptions made by the software. Due to the fact that all input data is available for HRSGs it is best to choose one of the top two models. The first model uses the supplementary firing duty, while the second one uses the supplementary firing temperature. Due to the fact that the geometric of the HRSG are not included in the software it is unknown if the set-up is exactly the same. Therefore it is unclear if the location where the supplementary firing temperature is measured is comparable to the location chosen in the software. Furthermore, radiation can have a large effect on the temperature which is measured with thermocouples inside the HRSG, resulting in a questionable temperature output [51]. The first model is therefore the best fitted to simulate the three HRSGs. The required input data is listed below:

- Percentage of exhaust to HRSG

- Exhaust temperature drop from gas turbine to HRSG 'k'

- Supplementary firing duty

- BFW characteristics

- Steam characteristics

- Blowdown ratio

The equations used for the simulation of the HRSG with the first model are given in eqs. (5.6) to (5.12). First the temperature of the flue gas entering the HRSG system is calculated in eq. (5.6) by subtracting the temperature loss 'k' from the GT exhaust gas. With the flue gas temperature and the $MCp_{GT,Exhaust}$ calculated in eq. (5.3) the flue gas energy is calculated ($Q_{HRSG,GT}$). The total energy entering the HRSG system ($Q_{HRSG,In}$) is calculated by adding the supplementary firing energy ($Q_{HRSG,GT}$) from eq. (5.8) to the flue gas energy in eq. (5.9). The energy needed for steam production is calculated with the known steam production and BFW consumption conditions in eq. (5.11). The blowdown flowrate is unknown and calculated with the blowdown

rate ($r_{\text{HRSG,Blowdown}}$) in eq. (5.10). With the calculated energy needed for steam production and the actual energy input of the HRSG the efficiency is calculated with eq. (5.12).

$$T_{\text{HRSG,GT}} = T_{\text{GT,Exhaust}} - k \tag{5.6}$$

$$Q_{\text{HRSG,GT}} = MCp_{\text{GT,Exhaust}} \cdot \left(T_{\text{HRSG,GT}} - T_{\text{Amb}} \right) \tag{5.7}$$

$$Q_{\text{HRSG,SF}} = \sum LHV_{\text{HRSG,Fuel}} \cdot \dot{m}_{\text{HRSG,Fuel}} \tag{5.8}$$

$$Q_{\text{HRSG,In}} = Q_{\text{HRSG,GT}} + Q_{\text{HRSG,SF}} \tag{5.9}$$

$$\dot{m}_{\text{HRSG,Blowdown}} = r_{\text{HRSG,Blowdown}} \cdot \dot{m}_{\text{HRSG,BFW}} \tag{5.10}$$

$$Q_{\text{HRSG,Prod}} = \dot{m}_{\text{HRSG,Steam}} \cdot h_{\text{HRSG,Steam}} + \dot{m}_{\text{HRSG,Blowdown}} \cdot h_{\text{HRSG,Blowdown}} - \dot{m}_{\text{HRSG,BFW}} \cdot h_{\text{HRSG,BFW}} \tag{5.11}$$

$$\eta_{\text{HRSG}} = \frac{Q_{\text{HRSG,Prod}}}{Q_{\text{HRSG,In}}} \tag{5.12}$$

5.2. Steam Turbine Generator

The refinery has two steam turbine generators: STG1 and STG2. STG1 is a single stage turbine with the inlet at 85barg and the outlet at 18barg. STG2 is a two stage steam turbine which has the inlet at 18barg and a vacuum condenser at the final stage. The turbine balances the 3barg network by producing 3barg steam in its first stage or consuming 3barg steam in its second stage. To model the turbine with a 3barg inlet and outlet STG2 is simulated as two separate single stage turbines. For the simulation of the steam turbine generators i-Steam provides three models which are listed below:

- Fixed isentropic efficiency

- Willan correlation

- L&B correlation

As stated before the fixed isentropic efficiency model is the most simplistic and does not include the changing characteristics of the turbines at part load. The Willan and L&B correlations both use data to calculate certain coefficients to simulate the turbines even at part load. The Willan model calculates the coefficients without taking the steam temperature and pressure into account, it is solely based on power generation and steam flow rate. This model is sufficient if the steam conditions are stable, which is the case for STG1 and STG2. L&B correlations requires more data and after testing both models Willan was more accurate. The equation used to calculate the power generated by the turbine is given in eq. (5.13). The equation calculates the power output at different flow rates with the coefficients n_i and W_{INT} which are calculated using regression over the data from year 2 which is shown in fig. 5.1.

$$W = n_i \cdot \dot{m}_{\text{Out}} - W_{\text{INT}} \tag{5.13}$$

As mentioned above the STG2 is split in two separate turbines to enable the 3barg network balancing. Due to the fact that the power is not known for each independent stage the correlations such as Willan or L&B provided by i-Steam are not an option. Therefore the fixed isentropic efficiency is used to model STG2. The isentropic efficiency of the first stage is calculated with the equation in eq. (5.14) using the installed pressure and temperature sensors. The efficiency can only be calculated if there is a LP outlet, otherwise the measured temperature and pressure are not accurate. The isentropic efficiency is plotted against the flowrate for the first stage of STG2 in fig. 5.2. The linear fit, of which the equation is given in eq. (5.15), is used to determine the isentropic efficiency at various flowrates.
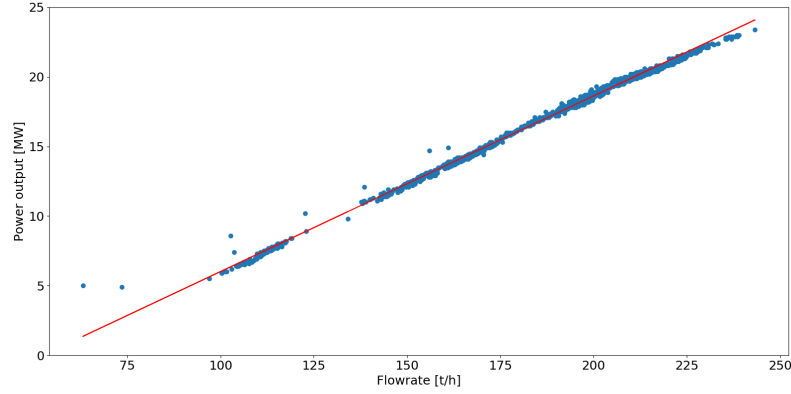
Figure 5.1: Operational data scatter plot with linear fit of the STG1 steam turbine generator power output against the flowrate.
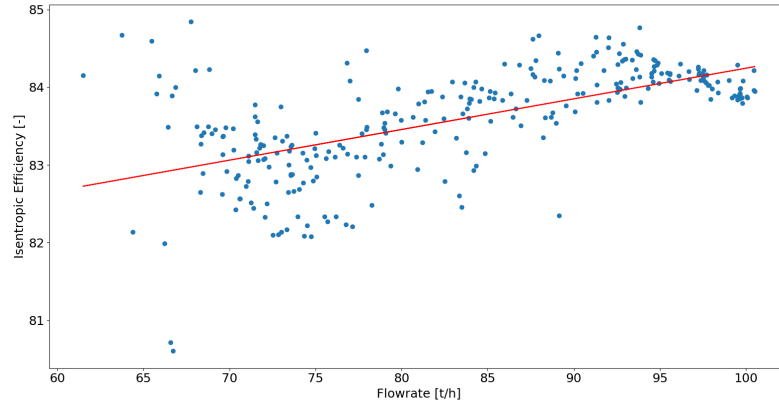
Figure 5.2: Operational data scatter plot with linear fit for the first stage of the STG2 steam turbine generator, showing the isentropic efficiency against the flowrate.

$$\eta_{\text{Isentropic}} = \frac{h_{\text{Out}} - h_{\text{In}}}{h_{\text{Out,Isentropic}} - h_{\text{In}}} \tag{5.14}$$

$$\eta_{\text{Isentropic}} = 0.039 \cdot \dot{m}_{\text{MP}} + 80.30 \tag{5.15}$$

The enthalpy of the second stage outlet cannot be determined with the pressure and temperature sensors, due to its two phase composition. The energy of the MP and LP steam flows are calculated, because LP is an inlet and outlet the energy can be positive or negative. With the calculated energy and the measured power output of the STG2, the enthalpy of the two phase flow outlet is determined using eq. (5.16). The calculated enthalpy and the measured pressure results in the quality of the two phase outlet visible in fig. 5.3. The isentropic efficiency for the second stage is calculated as well with eq. (5.14), resulting in the scatter plot visible in fig. 5.4. The linear fit, of which the equation is given in eq. (5.17), is used to determine the isentropic efficiency at various flowrates.

$$h_{\text{Out}} = \frac{h_{\text{MP}} \cdot \dot{m}_{\text{MP}} - h_{\text{LP}} \cdot \dot{m}_{\text{LP}} - P_{\text{STG2}} \cdot \eta_{\text{Mech}} \cdot \eta_{\text{Elec}}}{\dot{m}_{\text{Out}}} \tag{5.16}$$

$$\eta_{\text{Isentropic}} = 0.73 \cdot \dot{m}_{\text{LP}} + 33.25 \tag{5.17}$$
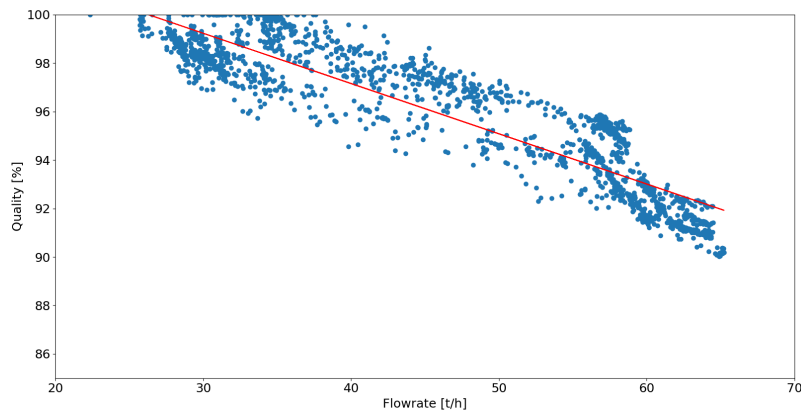
Figure 5.3: Operational data scatter plot with linear fit for the second stage of the STG2 steam turbine generator, showing the steam quality of the two phase outlet against the flowrate.
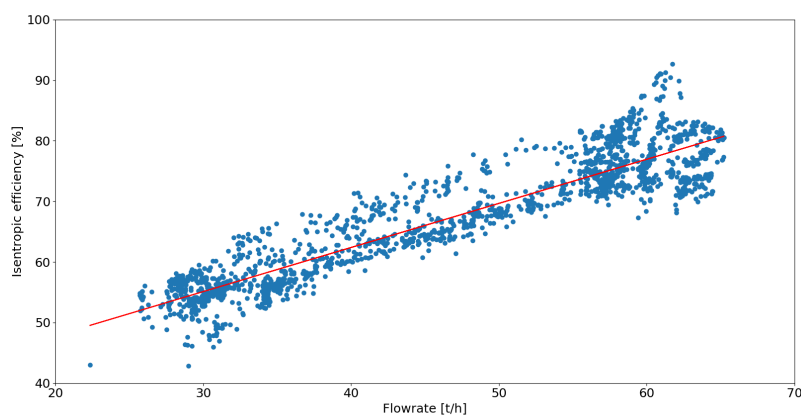
Figure 5.4: Operational data scatter plot with linear fit for the second stage of the STG2 steam turbine generator, showing the isentropic efficiency against the flowrate.

5.3. Steam Turbine Driver

The steam turbine drivers model the turbine driven compressors and pumps located on site. Two large air compressors: STDC1 and STDC2, are the most important steam turbine drivers. Besides these two STDCs there are some smaller drivers to power small pumps and compressors. STDC1 is a single stage turbine which decompresses the steam from 18barg to 7barg. STDC2 is a two stage compressor with a 7barg and a condensed extraction. The software provides the same models as described in section 5.2. However the power output for the drivers is unknown, which prevents the usage of a regression model to determine the coefficients in eq. (5.13). Due to this limitation and the fact that the compressors steam outlet conditions are quite stable the fixed isentropic model is chosen. The known flowrate and required outlet conditions are used to simulate the steam turbine drivers.

5.4. Steam Main

Steam mains are used to model the steam vessels where the output of steam producers is distributed to several smaller pipes which supply the consumers. In contrast to the pipelines discussed in section 5.10, the steam mains operate at a fixed pressure. The operating pressure is lower than or equal to the steam inlets. Inlet streams with a pressure above the operating pressure are depressurized isentropic which results in a small temperature reduction. The steam inside the main is assumed to be perfectly mixed and divided over all the steam outlets. To achieve a balanced steam main 'n-1' flow rates have to be identified, if this results

in higher/lower final flow rate then expected imports and exports as described in section 5.7 can be used to solve mass imbalances.

5.5. Let Down Valves

Let down valves are installed in the network to depressurize steam flows to the desired level. The outlet pressure of the valve is set and the temperature is calculated as described in section 5.4. To prevent high outlet temperatures BFW can be injected to cool down the steam flow. The enthalpy of the outlet stream which leads to the temperature via superheated steam tables can be calculated using eq. (5.18).

$$h_{\text{Out}} = \frac{h_{\text{In}} \cdot \dot{m}_{\text{In}} + h_{\text{BFW}} \cdot \dot{m}_{\text{BFW}}}{\dot{m}_{\text{Out}}} \tag{5.18}$$

5.6. Deaerator

The deaerator input flows are from the condensate producing units and the flash vessels connected to the HRSG2 and HRSG3. The BFW demand is determined by all process units which require BFW. The required LP steam is calculated via an energy balance over the system. The enthalpy of all the streams are known and this results in a required steam flow to heat up the BFW to the set temperature. As mentioned before not all steam returns as condensate and part of the LP steam used in the deaerator is vented, determined by the vent rate ($r_{\text{Vent,Steam}}$). These losses require make-up water, calculated in eq. (5.19). The energy consumption of the BFW pumps to reach the 35barg and 120barg pressure levels is incorporated as well.

$$\dot{m}_{\text{Water,Make-up}} = \dot{m}_{\text{Water,Out}} + \dot{m}_{\text{Steam,In}} \cdot r_{\text{Vent,Steam}} - \dot{m}_{\text{Steam,In}} - \dot{m}_{\text{Water,Recycle}} \tag{5.19}$$

5.7. Import & Export

Import and Export flows can be used for steam which is not generated or consumed by the refinery or to balance the steam network. Balancing of the network is needed when there is a mass imbalance over a section of the steam network. The origin of the mass imbalance is either uncertainty in the flow meters, leakages or venting. When it is clear that leakages or venting are causing the mass imbalance, the effects can be quantified by adding a negative price tag to the export flow rates. If the steam is sold to a third party a positive price tag can be included. For steam intakes which are not modelled in detail, such as the PGP2, it can be modelled as an import with a positive price to calculate the cost of the steam intake.

5.8. Process Loads

The process loads simulate the steam consumers in the network which use steam as heat source or feed stock. Most of the processes that use steam as heat source produce condensate which recycles back to the deaerators as described in section 5.6. When steam is used as feed stock for units such as WGSR or strippers the water cannot be recovered.

5.9. Steam Generators

Besides the HRSGs described in section 5.1 steam is generated in several units by waste heat boilers. The steam generators use BFW at a certain pressure and temperature and the energy needed to provide the required steam is calculated. The calculated energy is a 100% efficiency value, which is acceptable for the model due to the fact that there is no emission or economic value linked to waste heat. The steam generators have a blowdown rate of around 2%.

5.10. Pipelines

The pipelines are used to model the characteristics of the steam flow through the main pipelines on site. The software calculates the pressure drop inside the pipelines with the Darcy-Weisbach equation given in eq. (5.20). In the equation the equivalent length L_{e} is used which is the length of the pipe itself and adds distance for the number of bends. The friction factor (f_{d}) is related to the Reynolds number and the relative roughness of the pipe. The final components of the equation are the density of the fluid (ρ), the velocity (ν) and the inner diameter of the pipe (D). The equation calculates the pressure drop due to friction with the

pipe inner wall. Other losses such as static pressure drop, due to height difference, or acceleration pressure drop, determined by speed flow and density, are not included.

$$\Delta P_f = L_e \cdot f_d \cdot \frac{\rho \cdot v^2}{2 \cdot D} \tag{5.20}$$

Furthermore the heat loss of the steam flow in the cylindrical pipe is calculated by using the equation given in eq. (5.21). The heat flux q calculated in eq. (5.22) where L is the length of the pipe segment. In eq. (5.22) T_0 is the bulk temperature of the steam flow and T_{Amb} is the ambient temperature. D_1 and D_0 are the in and outside diameter of the insulation, respectively. The α_s is the overall heat transfer coefficient at the outer surface of the pipe, calculated with eq. (5.23), where v is the outside wind speed. The λ is the thermal conductivity of the insulation material, which is calculated in eq. (5.24). The coefficients used to calculate λ are related to the insulation material, the equation for microporous calcium silicate which is the used material in the pipeline model is given in eq. (5.25). T_m is the mean temperature and calculated with eq. (5.26), the used surface temperature of the inner pipe T_s is calculated in eq. (5.27) where d_0 is the outside diameter of the pipe. As can be seen λ depends on T_m in eq. (5.24), while T_m depends on eq. (5.24) via eqs. (5.22) and (5.27). To solve this T_m starts at 0 °C and iterations are performed until the values match. Heat losses due to radiation are neglected and the assumption is made that the inner wall temperature of the pipe is equal to the steam temperature.

$$Q = 2\pi \cdot L \cdot q \tag{5.21}$$

$$q = \frac{T_0 - T_{Amb}}{\frac{1}{\lambda} \cdot ln\frac{D_1}{D_0} + \frac{1}{\alpha_s \cdot \frac{D_0}{2}}} \tag{5.22}$$

$$\alpha_s = 11.6 + 7\sqrt{v} \tag{5.23}$$

$$\lambda = a + b \cdot (T_m - c) \tag{5.24}$$

$$\lambda = 0.053 + 0.00011 \cdot (T_m - 0) \tag{5.25}$$

$$T_m = \frac{T_s + T_{Amb}}{2} \tag{5.26}$$

$$T_s = T_a + \frac{q}{\pi \cdot \alpha_s \cdot d_0} \tag{5.27}$$

5.11. Pumps

Besides the pump calculation in the deaerator model, described in section 5.6, separate pumps can be installed when the pressurized water is not used in standard boilers. The four models which are available for pump simulation in i-Steam are listed below:

- Fixed efficiency

- W.K. Jekat formula

- Data in the plate

- Performance curve

Due to fact that there is no information about the shaft power and flow correlation coefficients the third and four models are not an option. The W.K. Jekat equation, given in eq. (5.28), calculates the efficiency based on throughput and density [52]. The characteristics of the pump are neglected and the density used in based on the inlet conditions.

$$\eta = 1 - \frac{0.071}{\left(5 \cdot \frac{\dot{m}_{Pump,Inlet}}{18 \cdot \rho_{Inlet}}\right)^{0.25}} \tag{5.28}$$

Six large pumps are installed to compress the BFW produced by the three deaerators at the PGP1 to 35barg or 120barg. Of these six pumps four are normally in operation, two for the 35barg BFW network and two for the 120barg network. The outlet conditions have no effect on the efficiency, when using the W.K. Jekat equation. The efficiency of the six BFW pumps using the W.K. Jekat equation and increasing BFW flow is plotted in fig. 5.5.
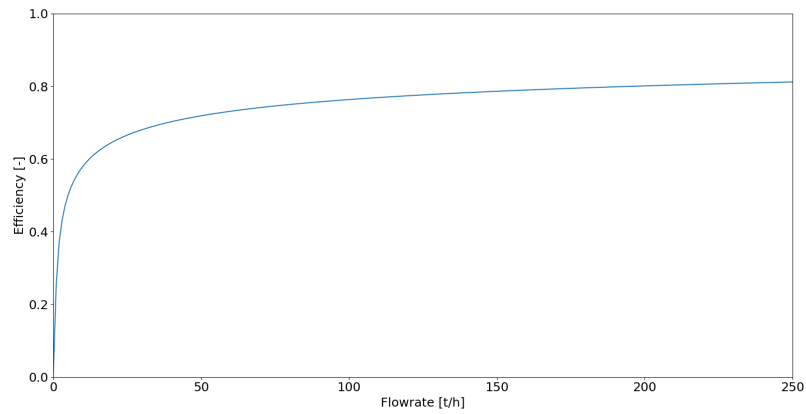
Figure 5.5: Efficiency of the BFW (boiler feed water) pumps under increasing flowrate, efficiency is calculated using the W.K. Jekat equation.

6

Optimization Model

In the following section the optimization model is discussed. Most of the equipment is modelled similar to the pipeline model reviewed in chapter 5. The main difference is that this model is focused on PGP1 and PGP2, all other consumers and producers are grouped and kept constant during optimization. The pipelines are removed to fully focus on steam and electricity production. The monthly average prices for fuel, electricity, CO_2 and steam are incorporated and these form the basis for optimization. The i-Steam optimization model is added to appendix B.

6.1. Gas Turbine with HRSG

As described in section 5.1 the gas turbine has four modelling options in i-Steam. All three gas turbines on site are monitored constantly resulting in available data for regression. There are two types of regression models in the i-Steam software:

- Design and retrofit regression model

- Operational optimization regression model

The design and retrofit regression model requires only four states of operation, two at 15 °C and two at another ambient temperature. The software uses these states to compute a linear regression which is capable to predict the GT's performance under various loads and ambient conditions. The operation optimization regression model uses a set of operational data to predict the GT's performance. After testing both models in i-Steam, the best performing one is selected for each gas turbine. For GT1 the design and retrofit regression model is chosen, due to the fact that it results in a better fit with measured data during simulation. This is probably due to the fact that the GT1 runs quite consistent and shows clear gas turbine efficiency trends over power output and ambient temperature, plotted in fig. 6.1, as described in section 3.1. The equations used by i-Steam are given in eqs. (6.1) to (6.4). The regression of the input data results in eight coefficients (a, b, c, d, e, f, h, j and k). With these coefficients the efficiency and exhaust temperature is calculated for the four states, given in table 6.1.
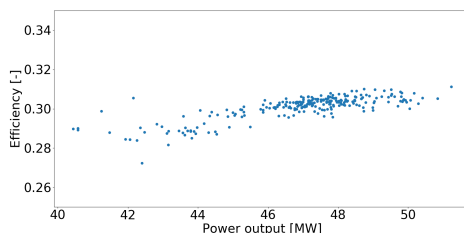
(a) Power output
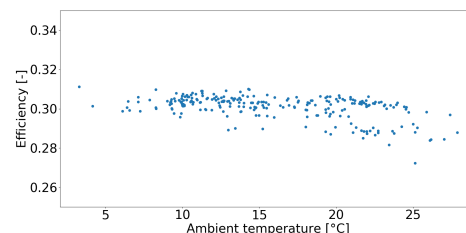
(b) Ambient temperature

Figure 6.1: Operational data scatter plots for GT1 (gas turbine 1) with the calculated efficiency plotted against the power output (left) and ambient temperature (right).

$$Q_{15°C} = a \cdot W_{15°C} + b \qquad (6.1)$$

$$\dot{m}_{Air,\ 15°C} = c \cdot W_{15°C} + d \qquad (6.2)$$

$$\frac{W}{W_{15°C}} = e \cdot T_{Amb} + h \qquad (6.3)$$

$$\frac{F_{Air}}{F_{Air,\ 15°C}} = j \cdot T_{Amb} + k \qquad (6.4)$$

Table 6.1: Input and calculated data with the eight coefficients derived from eqs. (6.1) to (6.4).

T_{Amb} [°C]	Power generation [MW]		Efficiency [-]		Exhaust temperature [°C]	
	Measured	Calculated	Measured	Calculated	Measured	Calculated
15.2	40.44	40.44	0.290	0.290	563.0	560.5
	46.87	46.87	0.302	0.302	541.1	542.2
9.3	50.29	50.29	0.303	0.307	549.4	534.7
	46.76	46.76	0.300	0.301	543.2	543.3

GT2 and GT3 run on a mix of fuel, resulting in less stable operation as visible by the calculated efficiency scatter plots in figs. 6.2 and 6.3. Therefore four states of operation are not sufficient to create a representative model. The operational optimization regression model requires the power generation, ambient temperature, fuel flowrate and fuel LHV to calculate the five coefficients n_1, n_2, W_{Int}, a and b with eq. (6.5). To achieve a trustworthy optimization, data that shows the increasing efficiency trend over increasing power output and decreasing ambient temperature should be selected as discussed in section 3.1. As visible in fig. 6.2 this trend is not that clear for the GT2 in year 2, which resulted in optimization results which are unlikely. The data for GT3 in fig. 6.3 is closer to the expected trend are better suitable for regression. Due to the fact that GT2 and GT3 are identical gas turbines, it is chosen to model the GT2 with the data from GT3. After testing the model this resulted in a trustworthy optimization model for both GT2 and GT3.

$$W_{GT} = n_1 \cdot \dot{m}_{Fuel} \cdot LHV + n_2 \cdot \dot{m}_{Fuel} - W_{Int} \cdot a \cdot T_{Amb} + b \qquad (6.5)$$
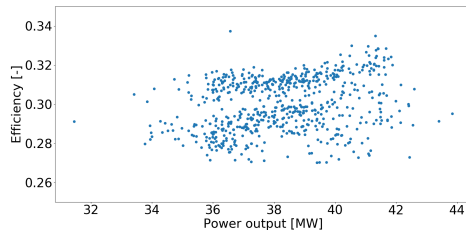
(a) Power output
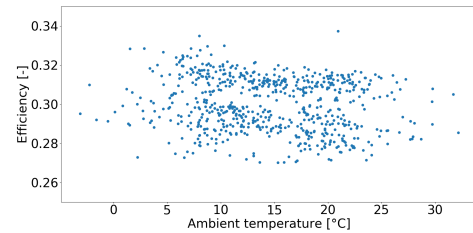
(b) Ambient temperature

Figure 6.2: Operational data scatter plots for GT2 (gas turbine 2) with the calculated efficiency plotted against the power output (left) and ambient temperature (right).

For all three gas turbines a correlation is made between the ambient temperature and maximum fuel flowrate. Due to the fact that the power output of the gas turbine as described in section 3.1 is limited by its throughput, there is a correlation between the air density and maximum fuel inlet based on the ideal gas law in eq. (6.6) [42]. The maximum fuel flowrate can be calculated with the measured ambient temperature in Kelvin using eq. (6.7) and a maximum fuel flowrate with the corresponding temperature. For optimization a reference fuel flowrate is chosen during winter, due to the fact that gas turbines are then operating at their maximum capacity. The minimum power output is determined by analysing the operating data over a five year period. This resulted in the minimum power output of GT1, GT2 and GT3 which is 38, 34 and 35 MW, respectively.

(a) Power output

(b) Ambient temperature
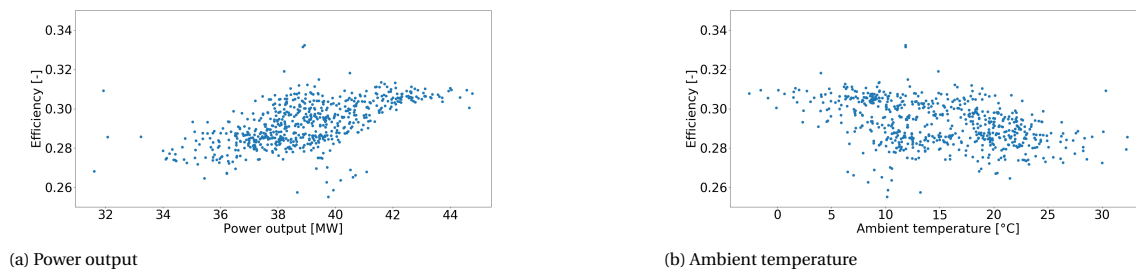
Figure 6.3: Operational data scatter plots for GT3 (gas turbine 3) with the calculated efficiency plotted against the power output (left) and ambient temperature (right).

$$p \cdot V = n \cdot \mathrm{R} \cdot T \tag{6.6}$$

$$\dot{m}_{\mathrm{Fuel,Amb}} = \dot{m}_{\mathrm{Fuel,Ref}} \cdot \frac{T_{\mathrm{Ref}}}{T_{\mathrm{Amb}}} \tag{6.7}$$

The HRSG is modelled as in section 5.1, however there are two options for optimization. During simulation the minimum approach temperature is calculated for that specific scenario, one can choose to keep this constant during optimization or to let this value decrease towards a specified minimum. For optimization is chosen to keep the calculated value constant, because this value has an effect on the efficiency of the HRSG and would therefore affect the whole fuel-steam balance. By keeping the value constant, the HRSG will perform with a similar efficiency and therefore the model will reach a more realistic optimum. The maximum supplementary firing duty is determined by analysing the operating data over a five year period. This resulted in a maximum duty for HRSG1, HRSG2 and HRSG3 of 60, 40 and 40 MW, respectively. The minimum duty for all three HRSGs is set at 0 MW. The same approach is taken to determine the maximum and minimum generated steam. For the HRSG1 the minimum MP steam production is set at 60 t/h and the maximum is at 200 t/h. For HRSG2 and HRSG3 the minimum MP steam production is set at 60 t/h and the maximum at 150 t/h. The final addition to the HRSG in the optimization model is the modified blowdown ratio as calculated in eq. (5.10). Historic trend shows that HRSG3 has a significant higher blowdown ratio then HRSG2, which results in an optimization shift towards HRSG2 steam production. However the blowdown is used for the deaerators and shifting optimization towards a lower blowdown would in reality cause problems for the heat supply of the deaerators. Therefore during optimization the blowdown ratio is set equal for both HRSGs while the resulting blowdown flowrate is equal to the one measured..

6.2. Steam Turbine Generators

The steam turbine generators are modelled similar as in section 5.2. However as discussed above some units have an operating window, which for the STGs is based on steam throughput. Again these are gathered from operating data over a five year period. The maximum VHP inlet for the STG1 is 250 t/h and the minimum 110 t/h. The STG2 has a maximum and minimum for each stage. The MP section has a maximum flowrate of 100 t/h and a minimum of 7 t/h, while the LP section has a maximum of 70 t/h and a minimum of 12.5 t/h. The minimum of the MP section of the STG2 is determined from discussion with Shell employee, however sometimes the flow is below this minimum. If this is the case the minimum MP flowrate boundary for optimization is set at this measured flowrate.

6.3. Steam Main

Steam mains are similarly modelled as described in section 5.4, with the choice of a minimum and maximum operating pressure. Changing the pressure of a steam main could be favorable for the steam turbine generator, allowing a larger pressure drop over turbine resulting in more power output. However most steam mains are connected to units and other steam mains and would therefore increase or decrease the pressure throughout the refinery. These effects require more research, where the impact on every single unit has to be analysed. One steam main which could benefit from a slight pressure increase is the LP steam main at the ABC area. Therefore it is chosen to operate this main with a maximum of 3.5barg. The minimum operating

pressure is chosen as the actual operating pressure, due to the fact that decreasing the pressure could have large effects for the process units connected to the LP network.

6.4. Let Down Valves

During optimization the model can choose to increase or decrease the flow through the valves. In normal operation it is not desired to have a flow through the let down, when it could be utilized by a steam turbine generator. The minimum flowrate on all let downs is set to zero for optimization. When units depend on the let down, such as the HP steam network the required flow through the valve will be maintained by the model.

6.5. Import & Export

In the optimization model exports are used to group all the regular consuming units which do not effect the balance of the PGP1 and the PGP2. These flowrates for the exports are calculated during simulation and then fixed during optimization, ensuring that all those units can run as they should. Some part of the flow in these exports is venting or losses due to leakage, however it is difficult to check whether it is really something which could be solved or just a result of flow meter uncertainty. Keeping these values fixed results in a more trustworthy optimal point. The price of the PGP2 steam intake is determined on a monthly basis and includes the CO_2 emission cost. The optimization model will optimize this input by comparing the PGP2 price to the prices of steam produced by PGP1 and HRSG1. The minimum amount of steam supplied by PGP2 is 380 t/h, while the target is 440 t/h. If the steam network is not able to take in more steam without simply venting it the target is not obligated. However if STG2 is able to increase its throughput, the MP throughput of the first stage should be increased in order to meet the PGP2 target.

6.6. Operating Costs

The optimization model is built to determine the best economic operating point. The prices, retrieved from internal data, are collected for each component for the first of every month during year 1 and year 2. The prices for the following components are included in the model:

- Fuel

- Electricity

- CO_2 emission

- PGP2 MP steam

- Boiler feed water

Fuel

The price for fuel is based on the natural gas price and given in EUR/MWh. In reality the steam utility system is powered by refinery fuel gas as well, however due to the small alterations made by the model these prices can be set equal to the natural gas price. Therefore each fuel price is calculated using the known natural gas (NG) price and the known LHVs of both natural gas and the other fuel eq. (6.8). If the PGP1 yields an energy efficiency above thirty percent no energy tax on the fuel has to be paid. The GT1 HRSG1 is not included in the calculation and has to reach 30% efficiency to avoid the energy tax. GT1 HRSG1 is not connected to a STG so the 30% efficiency has to be reached by the GT1 alone. Normally this is not achieved and therefore the GT1 HRSG1 combination is modelled with the price of fuel including tax. The natural gas price with and without energy tax is plotted in fig. 6.4.

$$Price_{\text{Fuel}} = Price_{\text{NG}} \cdot \frac{LHV_{\text{Fuel}}}{LHV_{\text{NG}}} \tag{6.8}$$

Electricity

The electricity generated in the GTs and STGs reduce the operating cost of the refinery, the price per MWh is given in fig. 6.4. This does not mean that the electricity is sold on the market, but every kWh produced is a kWh less bought from the grid. The balance between the prices of electricity and fuel are one of the main drivers in the optimization model. The ratio of the natural gas price per MWh, energy tax included and
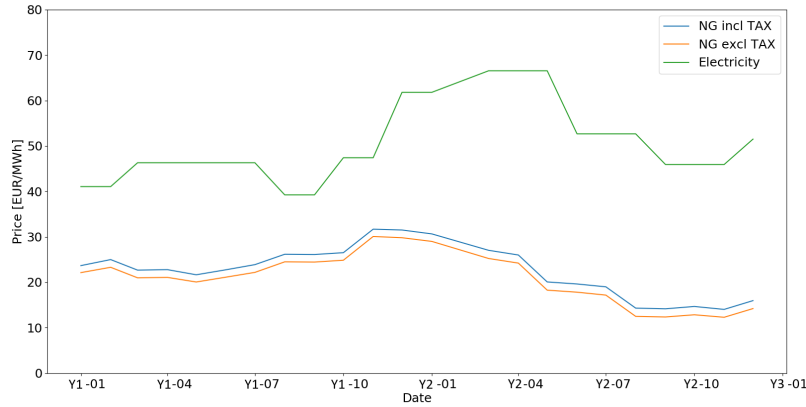
Figure 6.4: Natural gas and electricity price per MWh. Natural gas price is given with and without energy tax. Without energy tax is the price when an energy efficiency of 30% or higher is achieved by the PGP1 and by the GT HRSG1 combination.

excluded, over the electricity price per MWh is plotted in fig. 6.5. This ratio is important because it influences the profitability of the GTs and STGs.
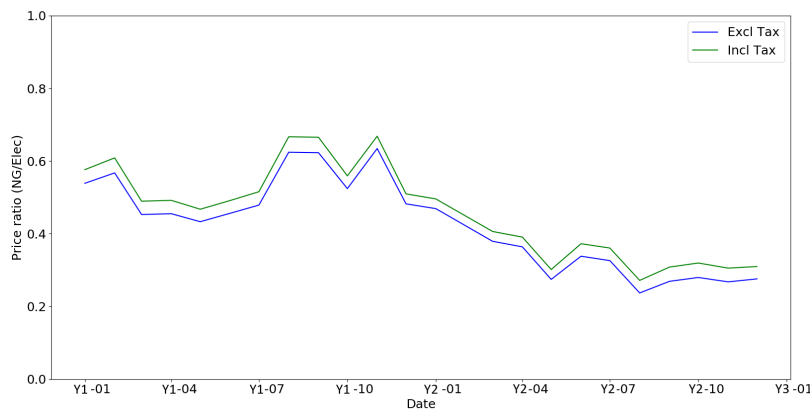
Figure 6.5: Ratio of the natural gas price per MWh over the electricity price per MWh. Ratio is plotted with and without energy tax, energy tax is waived when an energy efficiency of 30% or higher is achieved by the PGP1 and by the GT HRSG1 combination.

Carbon Dioxide Emission

The emission of CO_2 has to be compensated with a price per tonne of emitted gas as given in fig. 6.6. This price is increasing rapidly as can be seen in fig. 6.6 and therefore becoming an important factor of optimizing a system which emits CO_2. The emission of CO_2 per tonne of natural gas is based on the natural gas composition used in i-Steam, given in table 6.2, and the combustion of pure methane in eq. (6.9). As with the fuel price calculation the same is done for the CO_2 emission shown in eq. (6.10). Again due to the small alterations made by the model the CO_2 can be set equal to the natural gas emission. This model is not used to calculate the total CO_2 emission but the CO_2 price is added because it should bring an extra cost to the combustion of fuel.

$$CH_4 + 2O_2 \rightarrow CO_2 + 2H_2O \tag{6.9}$$

$$CO_{2_{\text{Fuel}}} = CO_{2_{\text{NG}}} \cdot \frac{LHV_{\text{Fuel}}}{LHV_{\text{NG}}} \tag{6.10}$$
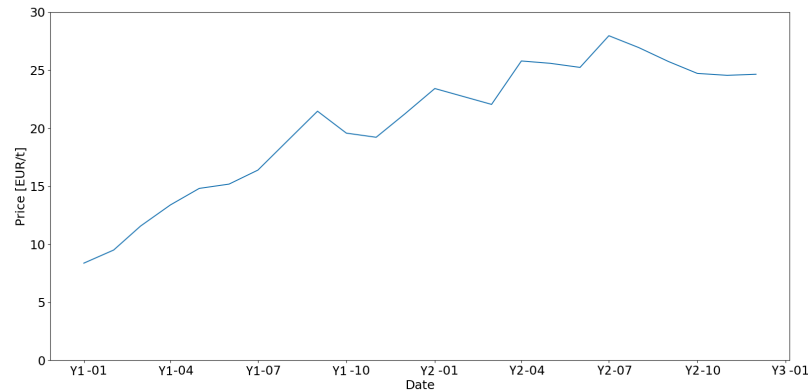
Figure 6.6: Price per tonne of emitted carbon dioxide for year 1 and year 2.

Table 6.2: Natural gas composition with the carbon dioxide emission from 1 t/h of burned natural gas.

Component	Mass fraction [-]	Molar weight [kg/kmol]	Molar flowrate [kmol/h]
Carbon	0.734	16.0	61.2
Hydrogen	0.228	1.01	226
Oxygen	0.008	12.0	0.500
Nitrogen	0.03	14.0	2.14
Carbon dioxide	2.69	44.0	61.2

PGP2 MP Steam

Located on site is the PGP2 which supplies the refinery with steam at three levels as discussed in section 2.1. The LP and VHP levels are not in direct contact with the PGP1 and HRSG1 and therefore not included in the optimization. The PGP2 MP steam price is influenced by the natural gas and electricity price as well, however when comparing the trend in fig. 6.5 and fig. 6.7 one can observe that the the MP steam price is flattened.
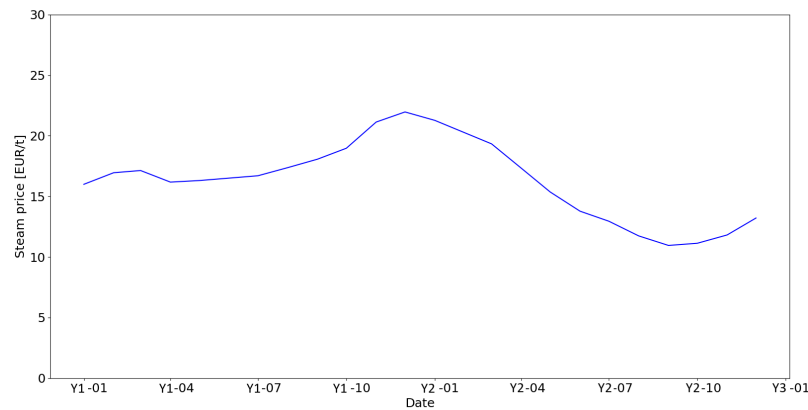
Figure 6.7: Price per tonne of PGP2 medium pressure steam, carbon dioxide emission cost is included in the price.

Boiler Feed Water

The price of BFW is quite constant over time and equal for all three HRSGs which consume BFW. The pressure levels of the BFW for the three HRSGs are not equal, but the effect of compression BFW to 35barg or 120barg on the price is negligible. The price is implemented in the model, because it has a significant effect on the produced steam price and therefore important when balancing own production with the PGP2 steam intake.

7

Validation

In this chapter the validation for the pipeline and optimization model is performed. The pipeline model is validated on several pressure, temperature and flow meters throughout the network to obtain a trustworthy model. The model is used to simulate fixed scenarios and therefore the main equipment is modelled using all data available. In contrary to the optimization model where the main equipment is simulated using regression models to obtain a flexible model which can simulate and optimize the network on a daily basis. The optimization model is validated on power output, temperature and energy consumption. Furthermore the optimization results are compared to the expectations described in chapter 3 to check whether the results are credible. The information related to the uncertainty of the measurement equipment installed at the refinery is obtained from a Shell instrumentation engineer.

7.1. Pipeline Model

As mentioned above the pipeline model is validated on pressure, temperature and flow rates, measured at the inlets and outlets of connected units and in main steam transport lines. For validation 25 units are selected indicated as Val1, Val2, etcetera. Some assumptions are made in the process of designing the model, the assumptions which effect the validation of the model are listed below:

- Steam venting occurs at the end of subsections

- Pressure calculation method as described in section 5.10

- Temperature calculation method as described in section 5.10

- Pipelines are up to the units battery limit, precise location of measurement equipment is uncertain

- Network pressure in sections is determined by lowest pressure input

Temperature Validation

As described in section 4.2 the geometry of the pipes is obtained using isometrics and the software Site-SPOT. However information regarding the insulation such as material, thickness and state of quality in which it occurs is unknown for the majority of the pipes. Therefore all pipes are modelled with the i-Steam standard microporous calcium silicate and the thickness is obtained by comparing the measured temperature with the simulated values of the four different scenarios. The results of the temperature validation are given in table 7.1 with the absolute and percentage error calculated using eqs. (7.1) and (7.2). The errors are not given as absolute values, which results in a clear representation whether the model is under or above the actual measured value. The acceptable uncertainty window is calculated in eq. (7.3) with a 2% measurement uncertainty for modern transmitters using a type K thermocouple [53]. The resulting uncertainty is based on the fact that both the steam producing and consuming measured conditions have a 2% uncertainty. Green values are within the calculated 2.83% window, while red ones are outside the window. The uncertainty window is applicable for modern transmitters, older transmitters have an uncertainty up to 5% which would result in a 7.07% window.

$$\text{Abs}_{\text{error}} = \text{modelled-measured} \tag{7.1}$$

$$\%_{\text{error}} = 100\% \cdot \frac{\text{Abs}_{\text{error}}}{measured} \tag{7.2}$$

$$u^2 = u^2_{\text{production}} + u^2_{\text{consumption}} \tag{7.3}$$

Table 7.1: Temperature validation results in the form of absolute and percentage errors for 25 locations in the network. Green percentage errors lie within the excepted 2.83% uncertainty while red ones exceed the boundary. When the temperature sensor used for validation is out of operation the cells in the table are blanked.

Name	1/1/year 2		19/7/year 2		10/2/year 3		17/3/year 3	
	Abs [°C]	%	Abs [°C]	%	Abs [°C]	%	Abs [°C]	%
Val1 MP	-1.18	-0.36	5.51	1.76	-3.26	-1.01	-3.63	-1.10
Val2 LP	-0.84	-0.42	-1.14	-0.61	1.71	0.85	-2.37	-1.24
Val3 MP	2.01	0.62	7.17	2.27	-3.78	-1.17	-0.79	-0.25
Val4 MP	1.69	0.57	-0.70	-0.23	-6.25	-2.34	-2.12	-0.74
Val5 MP	4.64	1.42	10.62	3.33	-2.26	-0.69	27.78	9.27
Val6 MP	2.24	0.69	-2.16	-0.65	2.25	0.71	7.45	2.32
Val7 MP	-22.63	-8.57	-4.07	-1.81	-14.71	-5.54	-14.87	-5.57
Val8 MP	5.17	1.68	15.01	5.07	11.28	3.75	1.41	0.45
Val9 MP	0.69	0.22	-0.42	-0.13	-1.05	-0.34	-4.32	-1.37
Val10 MP	6.55	2.27	6.82	2.38	-0.04	-0.01	-6.16	-2.05
Val11 MP	7.74	2.43	-1.02	-0.34	1.86	0.57	-1.46	-0.44
Val12 MP	-5.08	-1.67	17.76	6.28	-22.71	-7.81	-10.37	-3.69
Val13 MP					-0.29	-0.10	-1.11	-0.35
Val14 MP	6.21	1.92	-0.97	-0.32	0.93	0.28	-2.10	-0.63
Val15 MP	5.9	1.64	-10.55	-2.82	-1.88	-0.50	-7.72	-1.92
Val16 MP	0.02	0.01	1.98	0.66	-2.94	-0.97	-7.96	-2.55
Val17 LP	0.26	0.11	-4.42	-1.76	-4.67	-1.78	-4.54	-1.69
Val18 MP	9.95	2.81	-0.97	-0.27	5.06	1.40	1.78	0.49
Val19 MP	1.62	0.50	8.35	2.76	-2.58	-0.77	3.43	1.06
Val20 MP	3.89	1.22	2.05	0.64	2.36	0.76	-1.37	-0.44
Val21 MP	2.48	0.76	-2.51	-0.82	-3.23	-0.98	-5.87	-1.78
Val22 MP	-4.01	-1.48	-1.80	-0.56	13.50	5.13	9.29	2.97
Val23 MP	1.30	0.40	-0.19	-0.06	-0.73	-0.23	-4.80	-1.50
Val 24 MP	6.18	1.84	2.13	0.67	0.77	0.22	-1.54	-0.45

In table 7.1 is visible that five validation locations have simulation results outside the 2.83% window. For each unit a possible explanation is given below:

- Val5 MP: Upstream and within 200m of a new unit indicated with Val3 MP, while on 17/3/year 3 the temperature reading for Val5 MP was nearly 20 °C lower compared to the downstream Val3 measurement. Due to the fact that the Val3 unit is new, those measurements are more trustworthy and therefore the base for the validation of this subsection.

- Val7 MP: Separate branch of 110m with a pipe diameter of 350mm, while flowrate is between 0-2 t/h resulting in steam velocities below 1 m/s. The insulation thickness of the pipe in question is equal to the rest of the subsection. It is expected that the consumption flowrate of the unit indicated with Val7 MP should be slightly higher resulting in a higher flow velocity and therefore temperature. This is more likely then increasing the the insulation thickness by 50% to reach the measured inlet temperature.

- Val8 MP: The unit indicated with Val8 MP has high simulated values for pressure and temperature compared to the measured values. Therefore, it is expected that the conditions are not measured directly at the battery limit. The pipe from the subsection to the Val8 MP battery limit is 33m, if conditions are measured further inside the battery limit this would decrease both pressure and temperature slightly.

- Val12 MP: Temperature is highly dependent on the two WHBs located in the subsection. During year 19/7/year 2 the measured temperature is nearly 50 °C lower than the steam produced by the WHB which is unlikely due to the distance of only 600m and a sufficient steam velocity. During 10/2/year 3 and 17/3/year 3 the steam is supplied by the other WHB in the subsection located about 700m from the consumer at Val12 MP. Flow velocities and produced steam conditions are equal for both scenarios, however the measured temperature at Val12 MP differs a lot. From the notes given Val12 MP is probably not a trustworthy temperature and therefore insufficient to use for temperature validation.

- Val22 MP: Temperature measurement seems quite unstable, while the pressure measured at the unit indicated by Val22 MP is stable. The stable pressure and stable steam flowrate through the area with constant steam conditions at the PGP2 should result in stable temperature measurements. Val6 MP is located in the same subsection and has a stable temperature result which is expected because the other conditions of the subsection are stable as well. Val6 MP is therefore selected as the base for the temperature validation of this subsection.

Pressure Validation

The pressure validation is based on the 2.83% uncertainty window as well, applicable for modern pressure transmitter such as the Rosemount 3051. Pressure measurements obtained by the Foxboro 13A or 11GM reach a 5% uncertainty, resulting in the 7.07% window. The results of the pressure validation are given in table 7.2 with the absolute and percentage error calculated using eqs. (7.1) and (7.2).

Table 7.2: Pressure validation results in the form of absolute and percentage errors for 18 locations in the network. Green percentage errors lie within the excepted 2.83% uncertainty while red ones exceed the boundary. When the unit used for validation is out of operation the cells in the table are blanked.

Name	1/1/year 2		19/7/year 2		10/2/year 3		17/3/year 3	
	Abs [bar]	%	Abs [bar]	%	Abs [bar]	%	Abs [bar]	%
Val1 MP	-0.06	-0.33	0.00	-0.02	-0.04	-0.24	-0.12	-0.65
Val2 LP	0.09	2.81	0.05	1.35	-0.07	-2.38	0.21	6.95
Val3 MP	-0.06	-0.31	-0.10	-0.54	-0.11	-0.59	-0.05	-0.27
Val4 MP	-0.17	-0.96	-0.10	-0.51	-0.15	-0.82	-0.16	-0.93
Val5 MP	0.15	0.82	-0.16	-0.87	0.04	0.23	-0.14	-0.73
Val6 MP	0.22	1.14	0.28	1.48	0.20	1.03	0.17	0.90
Val8 MP	0.51	3.02	0.40	2.30	0.40	2.35	0.30	1.85
Val12 MP	0.15	0.88	-0.01	-0.05	0.07	0.39	-0.07	-0.43
Val13 MP					-0.27	-1.47	-0.40	-2.28
Val14 MP	0.36	2.02	-0.08	-0.46	0.04	0.24	0.79	4.71
Val15 MP	-0.14	-0.77	-0.12	-0.62	-0.07	-0.38	-0.06	-0.31
Val19 MP	0.13	0.71	-0.15	-0.85	0.13	0.74	0.15	0.86
Val20 MP	-0.07	-0.40	-0.05	-0.26	-0.12	-0.67	-0.23	-1.33
Val21 MP	0.00	-0.02	-0.18	-0.98	0.16	0.89	0.20	1.17
Val22 MP	0.07	0.41	0.07	0.39	0.04	0.19	0.00	0.00
Val23 MP	-0.05	-0.27	-0.05	-0.27	-0.10	-0.53	-0.22	-1.25
Val24 MP	0.12	0.67	-0.11	-0.58	0.14	0.75	0.13	0.70
Val25 MP	0.33	1.97	-0.03	-0.15	0.05	0.31	-0.04	-0.23

In table 7.2 is visible that three units have simulation results outside the 2.83% window. For each unit a possible explanation is given below:

- Val2 LP: On 17/3/year 3 consumption in the KLM LP section is nearly 50% lower than in the previous three cases. This leads to lower steam velocities in the pipelines and therefore an increased simulated pressure at the inlet, however the measured pressure is not increased.

- Val8 MP: As described in the temperature validation section it is expected that the pressure and temperature sensors of the Val8 location are not directly at the battery limit, due to the fact that the simulated pressure and temperature are above measured conditions for all four cases.

- Val14 MP: Other scenarios have a modelled and measured inlet pressure above 17.5 barg while on 17/3/year 3 the measurement is 16.8 barg. This seems to be an inaccurate measurement, taken into

account that Val24 MP and Val21 which are in the same subsection are simulated within the 2.83% window and around their average pressure.

Flowrate Validation

The flowrate validation is based on the mass imbalances in sections of the steam network given in table 7.3. When the section is mainly supplied by PGP2 an uncertainty of 5.10% is accepted, based on the fact that the PGP2 flowmeter is 1% accurate and the consuming units have a 5% accurate flowmeter. When the section is not connected to PGP2 an uncertainty of 7.07% is accepted, based on both the producing and consuming flowmeter accuracy of 5%. The accuracy of the flowmeters is based on the information supplied in section 3.6. However flowmeters are a bit more difficult to validate, due to the fact that these are all input values for the model. This was not the case with the temperature and pressure validation where they are calculated by the model for the consuming units and not an input value. This leads to the effect that one broken meter can have a huge effect on the steam network section. Because of this effect it is more likely that the red cells in table 7.3 are an indication of a broken meter or open steam vent than of an error is the model.

Table 7.3: Flowrate validation results based on steam imbalances in the selected network areas. The results are in the form of absolute and percentage errors. For areas connected to the power generation plant 2 (PGP2) green percentage errors lie within the excepted 5.10% uncertainty while red ones exceed the boundary. For areas not connected to the PGP2 green percentage errors lie within the excepted 7.07% uncertainty while red ones exceed the boundary.

Name	1/1/year 2		19/7/year 2		10/2/year 3		17/3/year 3	
	Abs [t/h]	%	Abs [t/h]	%	Abs [t/h]	%	Abs [t/h]	%
PGP2 MP	-0.72	-0.19	11.33	3.03	26.11	6.74	8.00	2.24
Rubber C MP	4.69	9.64	5.12	10.44	5.44	9.85	3.49	11.75
KLM LP	2.17	5.90	2.04	7.08	3.48	8.87	1.08	4.69
KLM H&W LP	13.77	53.51	14.15	68.3	12.51	49.68	3.29	15.47
DEG MP	35.62	18.51	41.31	27.05	20.64	12.69	38.10	30.91
UB 13/14 MP	8.62	4.68	2.28	1.73	6.14	4.27	4.01	2.87
UB 6/7 MP	8.51	6.32	-1.85	-4.08	1.87	1.28	1.82	1.36
West/Oost MP	0.66	0.45	7.60	5.14	4.23	2.76	0.13	0.09
N1/N2 MP	7.22	12.90	0.18	0.39	6.90	13.18	3.18	6.17
90barg Sat.	13.86	9.43	7.27	6.70	16.52	10.31	16.27	11.34
HP	8.28	8.64	3.23	3.96	3.58	3.72	2.63	2.83

7.2. Optimization Model

The optimization model is built using regression to simulate the steam and electricity production units. Therefore the validation is focused on efficiency, power output and gas turbine exhaust temperature. The results of the HRSG are not validated, because the values which effect the model, such as energy consumption and steam production, are input parameters. The model uses 23 timestamps for which it simulates the network while using the regression tools to estimate the efficiency of the equipment during each scenario. The timestamps are on the first of every month from year 1-year 3. The first of February in year 2 is removed, due to the fact that almost all equipment for steam and electricity production was shut down at the time.

Gas Turbine Validation

First the efficiency of the gas turbines is plotted in fig. 7.1 to see whether the used regression models are a fitting representation of the reality. An extra validation is executed by plotting the exhaust temperature as well in fig. 7.4, which should follow the trend of efficiency. A relative high gas turbine efficiency should result in a relative low exhaust temperature.

Efficiency

In fig. 7.1a is clear that the GT1 efficiency is well fitted before October year 1 and after August year 2. In between the measured efficiency of the GT1 is quite high, up to 34%, while the exhaust temperature in fig. 7.4a shows no significant change. Using the units data over a period of five years the efficiency of the GT1 is calculated and plotted in fig. 7.2. It is clearly visible that for the period between October year 1 and August year 2 the efficiency is higher then usual. It is expected that the flow meter was inaccurate during the time and

(a) gas turbine 1

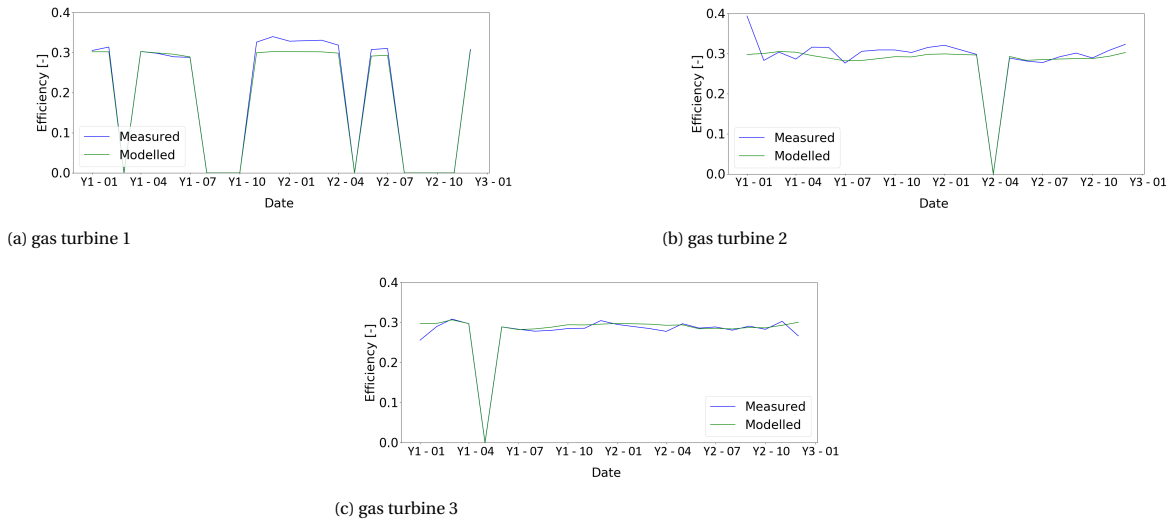(b) gas turbine 2

(c) gas turbine 3

Figure 7.1: Calculated efficiency from operational data and the efficiency modelled by the i-Steam model are plotted for each timestamp. gas turbine 1 (upper left), gas turbine 2 (upper right) and gas turbine 3 (lower center).

that calibration during the summer shut down of year 2 solved the issue and therefore reduced the efficiency. As visible in fig. 7.2 efficiency of the GT1 fluctuates a lot, which is also the case for GT2 and GT3. This results in high peaks such as on the first on January for GT2 in fig. 7.1b, which are not realistic. In section 5.1 is discussed that for roughly the same power output and ambient temperature the calculated efficiency is showing a lot of fluctuations. These fluctuations are not in the model, due to the fact that equal conditions should result in equal efficiency. However the model shows the influence of power output and ambient temperature on the efficiency, visible by the slight dips during the summer months for figs. 7.1b and 7.1c. The ambient temperature for the gas turbines is plotted in fig. 7.3.
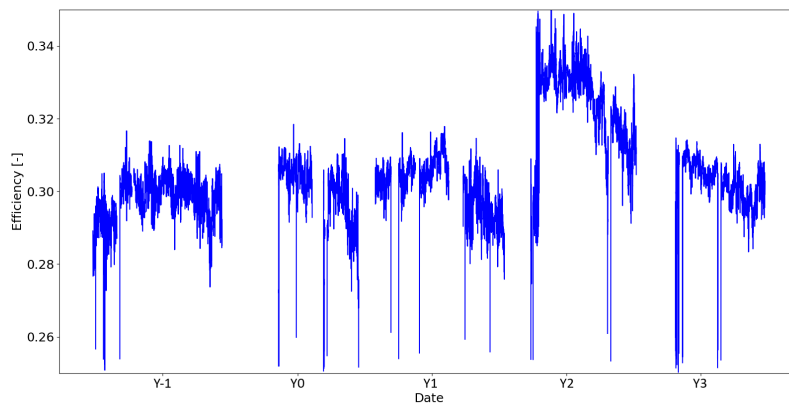
Figure 7.2: Efficiency of GT1 calculated from operational data over a period of five years, filtered to only show relevant values between 0.25 and 0.35.

Exhaust Temperature
The exhaust temperature is validated as well, as it has a large effect on the HRSG which utilizes the residual heat for steam production. In fig. 7.4 the exhaust temperature is plotted for both GT1 and GT3, GT2 is not included due to the fact that the temperature sensor was broken during this period. When the gas turbines are shut down the model gives a zero value output, while as visible in fig. 7.4a the measured value can still read a temperature. The exhaust temperature of GT3 was measured high on March year 1, keeping in mind that the ambient temperature and efficiency where really high at the time. This results in quite a large difference between the modelled value as seen in fig. 7.4b.

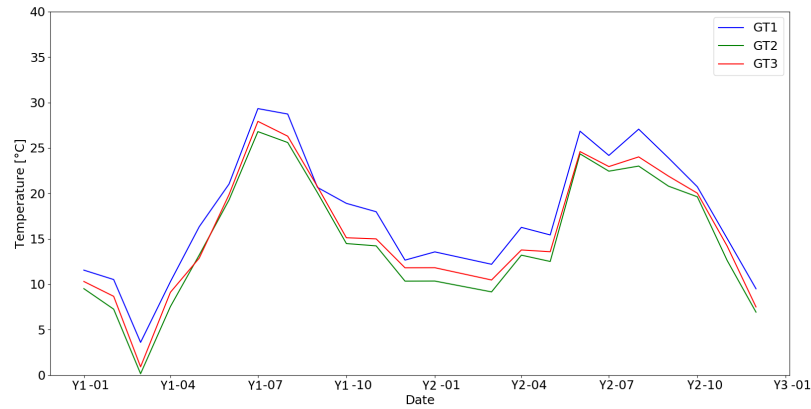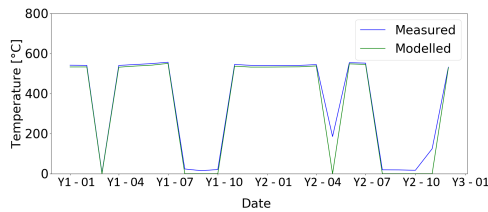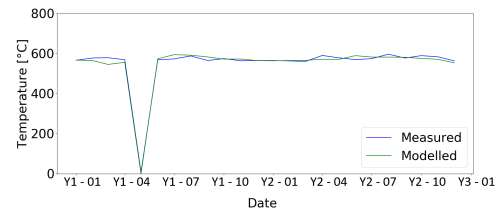Figure 7.3: Measured ambient air temperature in °C for the three gas turbines for each timestamp used in the i-Steam model.

(a) gas turbine 1

(b) gas turbine 3

Figure 7.4: Measured and modelled exhaust temperature in °C during each timestamp for the gas turbines, GT1 (left) and GT3 (right).

Steam Turbine Generator Validation

The validation results for the steam turbine generators STG1 and STG2 are plotted in fig. 7.5. The most noteworthy point is the at November year 2 in fig. 7.5b, at the time the power output meter was broken and therefore a zero value is measured. In reality steam was flowing through the turbine which explains the large difference in power output.
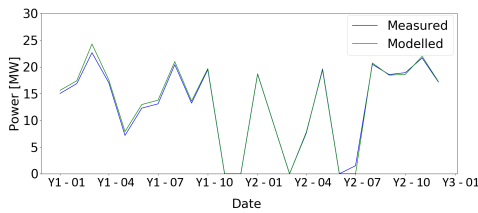
(a) Steam turbine generator STG1
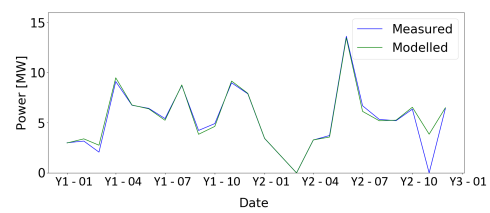
(b) Steam turbine generator STG2

Figure 7.5: Measured and modelled power output in MW during each timestamp for the steam turbine generators STG1 (left) and STG2 (right).

PGP1 Validation

At last the efficiency of the PGP1 is validated, which is a combined result of the separate units validated above. The PGP1 energy efficiency is calculated by dividing the total electrical power output of GT2, GT3, STG1 and STG2 with the total fuel consumption of GT2, GT3, HRSG2 and HRSG3 as shown in eq. (7.4). In November year 2 the model seems a bit of from the measured PGP1 efficiency, however as discussed above the STG2 STG had a bad power output measurement. Removing the simulated STG2 power output for the efficiency calculation brings the modelled PGP1 efficiency back to 32.9 %, while the measured efficiency at the time was 33.0%.

$$\eta_{PGP1} = \frac{P_{GT2,out} + P_{GT3,out} + P_{STG1,out} + P_{STG2,out}}{\dot{Q}_{GT2,in} + \dot{Q}_{GT3,in} + \dot{Q}_{HRSG2,in} + \dot{Q}_{HRSG3,in}} \tag{7.4}$$

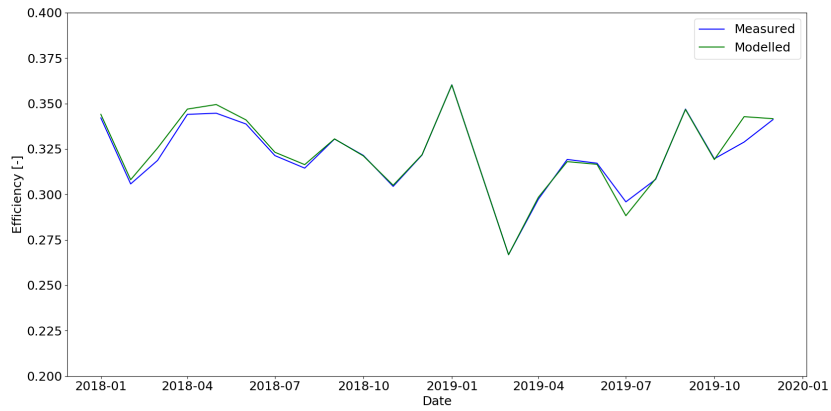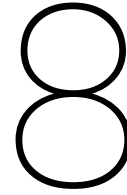Figure 7.6: Measured and modelled efficiency of the power generation plant 1 (PGP1), including the gas turbine heat recovery steam generator (HRSG) combinations, GT2 HRSG2 and GT3 HRSG3, and the steam turbine generators STG1 and STG2. The PGP1 efficiency is calculated by dividing the total electrical power output with the total fuel consumption.

<div style="text-align: right; font-size: 3em;">8</div>

Future Project

In this chapter the model is used to research the possibilities of incorporating a new plant in the existing steam network of the KLM area. Most of the time the plant is a net steam consumer, however at the end of run during winter periods a small amount of steam has to be exported to the network. In the conclusion the advice for the best connection to the existing KLM steam network is presented.

8.1. Background
The new project is planned to be built in the KLM area and has to be connected to the existing steam network. The unit consumes LP and MP steam during most scenarios and produces MP saturated steam at the end of the catalyst lifetime. There are four possible connections to the existing KLM steam network, two for each pressure level. To achieve a redundant system the unit has to be connect to at least two steam transport pipelines. This ensures that the unit can stay in operation while one of the two connections is closed due to maintenance or problems in the pipelines.

8.2. Steam Consumption and Production
The new unit requires MP and LP steam as well as BFW, while it produces saturated MP steam. Research about the expected operation data of the unit has led to three summer and winter scenarios. These scenarios are related to the lifetime of the catalyst. At the start of run (SOR) the unit is a net LP steam consumer while towards the last 20% of the lifetime, at the end of run (EOR), the unit will be a net saturated MP steam producer during the winter. The third scenario is the average consumption and production of steam during the lifetime of the catalyst.The expected steam consumption/production during summer and winter for all three scenarios are given in table table 8.1.

Table 8.1: Expected steam consumption (+) and production (-) of the unit for three scenarios during the winter and summer months.

	Summer			Winter		
	SOR [t/h]	Average [t/h]	EOR [t/h]	SOR [t/h]	Average [t/h]	EOR [t/h]
LP	54.2	59.6	63.3	54.0	57.0	60.1
MP	4.6	4.6	4.6	4.6	4.6	4.6
MP Sat.	-42.0	-52.6	-63.2	-41.3	-52.7	-64.1
HP	0	0	0	0	0	0
Net LP	12.2	7.0	0.2	12.7	4.3	0.0
Net MP Sat.	0	0	0	0	0	-4.0

The net LP consumption is the results of the total LP consumption minus the produced saturated MP steam, which is let down to superheated LP steam. At the EOR during winter the saturated MP production is higher then the LP consumption which results in a net saturated MP output. The saturated MP steam has a pressure of 17 barg which is lower then the required 19 barg at which the KLM MP network operates. The steam production pressure has to be higher than the network pressure to be able to dispatch the steam.

Therefore mixing the saturated MP steam with superheated steam will not solve the issue, because it will lower the pressure of the whole network. The saturated steam can be let down to superheated LP steam and possibly exported to the KLM LP network, which operates at 3barg.

8.3. Modelling Approach

As discussed above there are four locations where the new unit can be connected to the existing KLM steam network. The unit should be connected to two separate pipelines which both can supply the desired steam for redundancy and the possibility of pipeline maintenance. The first and second location is at the inlet of an existing unit connected to the LP and MP steam network. The future unit could be connected to the network via the pipelines LS980017 and LS980019, with a DN (nominal diameter) of 150 mm and 250 mm, respectively. The third location is close to another unit which is connected to the LP steam network via LS1343 with a DN of 200 mm. The fourth and closest location is where an unit is connected to the MP steam network via LS4413 with a DN of 400mm. Up to these points the network is modelled in i-Steam and validated with plant data. The characteristics of the extra needed pipelines to connect the units to the network at the three given locations are based on the existing pipes in material, diameter, insulation and roughness. The lengths are estimated using Site-SPOT, with one expansion loop per 50m pipeline. The characteristics of the added pipelines are given in table 8.2.

Table 8.2: Characteristics of the pipelines which could connect the new units to the existing low and medium pressure steam network in the KLM area.

Pressure level	Pipeline	Diameter [mm]	Length [m]	90° Bends	Insulation [mm]
LP	LS980017	150	250	15	30
LP	LS1343	200	220	15	30
MP	LS980019	250	250	15	30
MP	LS4413	400	150	11	40

The four scenarios discussed in chapter 4 are the base for the modelling of the new project. Consumption and production of existing units are kept constant, while the MP and LP steam import from PGP2 is increased to supply the new units. Furthermore the steam surpluses in the steam network which are vented are kept constant during the simulations. The four connections given in table 8.2 are modelled with increasing consumption flowrate to locate the bottleneck in the steam network. The model calculates velocity, temperature decrease and pressure drop in each of the pipe segments. At the end of the catalyst lifetime the unit transforms to a net saturated MP steam producer, which can be let down to LP superheated steam. The possibilities of exporting the LP steam to the KLM LP steam network are analysed as well.

8.4. Results

In this section the results of the steam model are presented for 1 January year 2. The other three scenarios are simulated as well and the conclusion drawn from these results is discussed briefly. Based on these results an advice is formulated for the best connection to the existing KLM steam network.

Consumption via the KLM LP network

In fig. 8.1a the pressure of the LP steam at the inlet connection is given for the routes LS980017 and LS1343. LS980017 is simulated between 0 and 3 t/h and LS1343 between 0 and 10.8 t/h, these windows are chosen because higher flowrates lead to an unusable steam pressure for the unit. In fig. 8.1b the steam temperature at the inlet connection is given for increasing flowrate through routes LS980017 and LS1343. The flat sections in fig. 8.1b are due to condensation inside the pipelines during low flowrates.

To locate the bottleneck in the system the pressure drop in each pipeline section for both routes is simulated and the results are visible in fig. 8.2a and fig. 8.2b. In both cases is clear that the main pipeline LS12481 which supplies the lower section of the KLM LP steam network is capable of handling higher flowrates. From the large pressure drops can be concluded that both routes are not able to supply the new unit with the maximum LP consumption of 12.7 t/h. Even a combination of both routes is not sufficient.
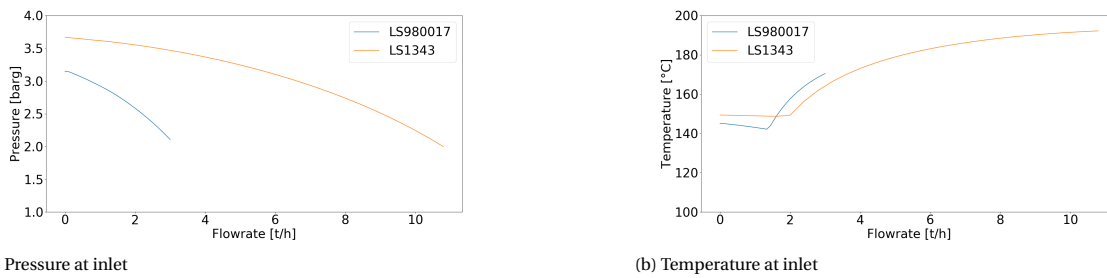
(a) Pressure at inlet

(b) Temperature at inlet

Figure 8.1: Simulated inlet conditions, pressure (left) and temperature (right), for an increasing consumption flowrate via the LS980017 and LS1343 routes through the KLM low pressure steam network.
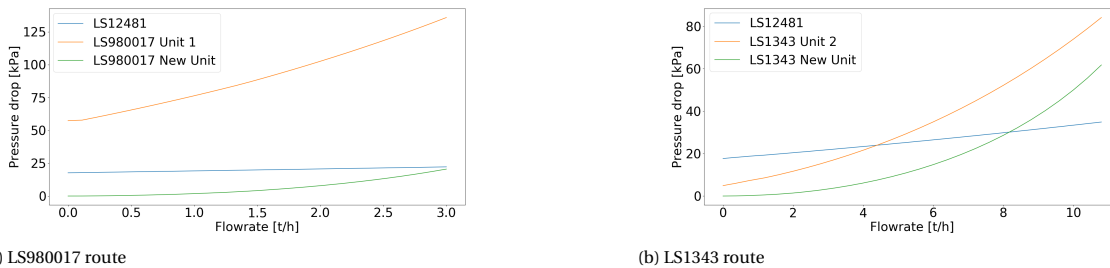

(a) LS980017 route

(b) LS1343 route

Figure 8.2: Simulated pressure decrease in each pipe segment of the LS980017 route (left) and the LS1343 route (right) through the KLM low pressure steam network for an increasing consumption flowrate.

Consumption via the KLM MP network

In fig. 8.3a the pressure of the MP steam at the connection with the new unit is simulated for the routes LS980019 and LS4413. LS980019 is simulated between 0 and 54 t/h and LS4413 between 0 and 81 t/h, these windows are chosen because higher flowrates lead to extremely high velocities and therefore pressure drops. In fig. 8.3b the steam temperature at the inlet connection is given for increasing flowrate through routes LS980019 and LS4413.

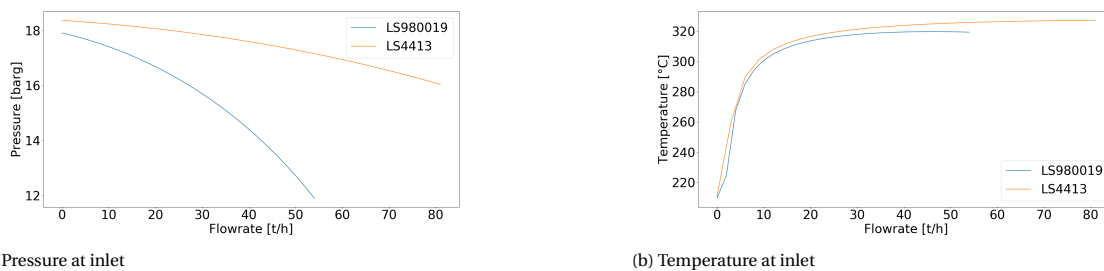(a) Pressure at inlet

(b) Temperature at inlet

Figure 8.3: Simulated inlet conditions, pressure (left) and temperature (right), for an increasing consumption flowrate via the LS980019 and LS4413 routes through the KLM medium pressure steam network.

Again the pressure drop in each pipeline section for both routes is simulated to locate the bottleneck in the MP network and the plots are visible in fig. 8.4a and fig. 8.4b. From the pressure drops can be concluded that both routes are able to supply the new unit with its maximum consumption of LP and MP steam combined, which is 17.3 t/h. The LS4413 route is even capable of supplying the full steam requirement of 67.9 t/h. This scenario could occur during start up or shut down, where the units WHB is not yet in operation but the steam is required.

Production to the KLM LP network

Finally the results for the EOR during winter scenario are presented, where a relative small flow of saturated 17barg steam is let down and supplied to the LP KLM network. The steam is let down to 4barg, which is equal to the PGP2 import pressure, ensuring that the unit is able to export its steam to the network. The pipelines
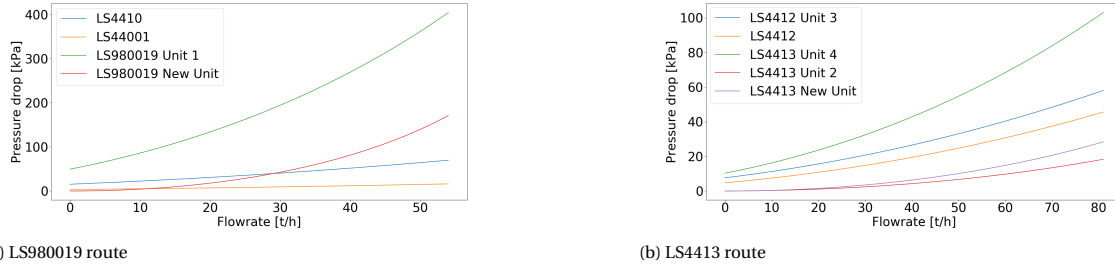
(a) LS980019 route

(b) LS4413 route

Figure 8.4: Simulated pressure decrease in each pipe segment of the LS980019 route (left) and the LS4413 route (right) through the KLM medium pressure steam network for an increasing consumption flowrate.

connecting the new unit to the LP KLM network are identical to the ones presented in table 8.2. In fig. 8.5 the results of the inlet conditions at the first consumer for each route is plotted in the KLM LP network. In fig. 8.5a is clear that LS1343 is condensing inside the pipeline, this is due to the very low consuming rate in the area and the LS1343 has a larger diameter than the LS980017. For the LS980017 route the produced steam in the new unit is directly consumed by the first unit on route. At first most of the consumed steam is supplied by the PGP2 import, resulting in a high temperature. Increasing the export flowrate of the new unit adds steam near condensing temperature and rapidly decreases the mean temperature at the inlet. Both pressure levels plotted in fig. 8.5b are acceptable, because adding steam from the new installed unit decreases the flow rates through the upper part of the network and therefore reducing the pressure loss. The temperature and pressure decrease in the new pipeline sections are plotted in fig. 8.6. In fig. 8.6a is visible that condensation occurs in the pipeline up to 3-4 t/h. The pressure drop in fig. 8.6b is acceptable and results in a pressure high enough for the new unit to be able to export its LP steam to the KLM LP network.

(a) Temperature
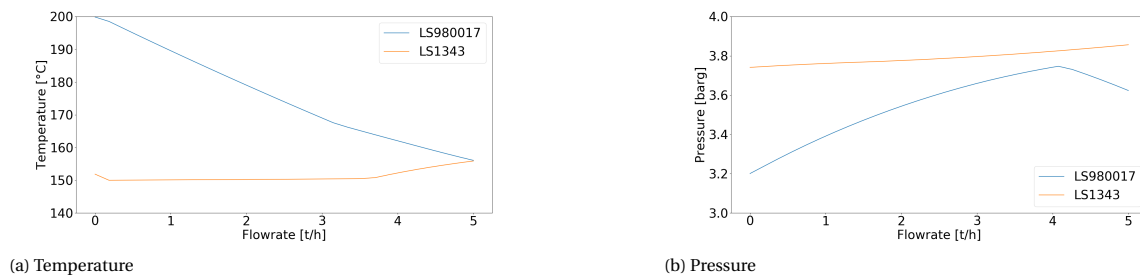
(b) Pressure

Figure 8.5: Simulated conditions at the first consumer on the LS980017 and LS1343 routes. On the left the temperature results are plotted and on the right the pressure results.

(a) Temperature decrease

(b) Pressure drop

Figure 8.6: Temperature and pressure losses in the new pipeline section when the unit produces LP steam from letting down MP saturated steam.

Conclusion

The bottlenecks for each timestamp and route are given in table 8.3. It is clear that all four timestamps have the bottlenecks of the steam system in the same area.

Table 8.3: For all four timestamps and four routes each unit is given where the bottleneck in the steam system occurs.

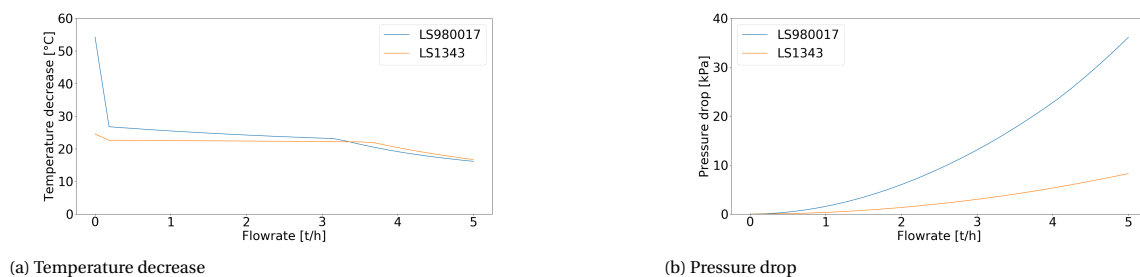| Route \ Date	LP LS980017	LP LS1343	MP LS980019	MP LS4413
1 Jan year 2	Unit 1	Unit 2	Unit 1	Unit 4
19 Jul year 2	Unit 1	Unit 2	Unit 1	Unit 4
10 Feb year 3	Unit 1	Unit 2	Unit 1	Unit 4
17 Mar year 3	Unit 1	Unit 2	Unit 1	Unit 4

These results of the EOR and SOR scenarios combined lead to the most promising connection of the new unit to the KLM steam network. As reviewed above both LP routes are non sufficient to provide the unit when its consuming LP steam. Even when it is producing LP steam the flowrates and temperatures are too low, resulting in condensation in the pipelines. Condensation could be solved by installing smaller diameter pipelines, however this will increase the pressure drop. Furthermore, consumption is not able through these lines so they have to be installed just to export a relative small amount of steam only at the EOR during the winter months. Therefore the most promising connection is to the LS4413 pipelines of the KLM MP grid with an extra connection to LS980019 for redundancy. The units should be connected to at least two pipelines, so maintenance on each pipeline can be executed without limiting the steam consumption of the new unit.

9

Optimization Results

In this chapter the results of the optimization model are discussed. The results are given for the first day of every month during year 1 and year 2. The first of February year 2 is removed, due to the fact that almost all equipment for steam and electricity production was shut down at the time. This resulted in no room for optimization, because GT1 HRSG1 was running on its maximum while the rest of the steam was supplied by the PGP2. Most results are illustrated in graphs with the optimized and modelled values. The modelled values are the results of measured data on site, the optimized values are results from i-Steam when operating cost is minimized.

9.1. Gas Turbines with HRSGs

First the results of the three GT HRSG combinations are discussed. The modelling and optimization approach is explained in section 6.1, with the upper and lower boundaries for GT power output, HRSG supplementary firing and HRSG steam production.

GT1 HRSG1

The results of the natural gas fired GT1 with HRSG1 combination produces MP steam, usually without supplementary firing, are given in fig. 9.1. The modelled and optimized GT1 power output is plotted in fig. 9.1a, the GT1 efficiency in fig. 9.1b, the HRSG1 supplementary firing in fig. 9.1c and the HRSG1 steam production in fig. 9.1d. As can be seen in fig. 9.1a the power output is often reduced to its minimum of 38MW and peaks when the natural gas price is favourable as illustrated in fig. 6.5. Furthermore the peak in May year 1, visible in figs. 9.1a and 9.1d, is due to the shut down of GT3 HRSG3. In fig. 9.1b the efficiency of the modelled and optimized GT1 is plotted, which illustrates the effect of power output on the GT efficiency. As visible the efficiency increases slightly when the power output is increased and decreases slightly when power output is decreased during optimization. As mentioned above the supplementary firing of the HRSG1 is normally not in operation and as visible in fig. 9.1c the firing remains zero during optimization.

GT2 HRSG2

The results of the mixed gas GT2 with HRSG2 combination produces VHP, with supplementary burners normally in operation, are given in fig. 9.2. The modelled and optimized GT2 power output is plotted in fig. 9.2a, the GT2 efficiency in fig. 9.2b, the HRSG2 supplementary firing in fig. 9.2c and the HRSG2 steam production in fig. 9.2d. As can be seen in fig. 9.2a the power output is reduced to its minimum of 34MW from July to December in year 1, this is due to the high ambient temperature in July, illustrated in fig. 7.3, and unfavourable natural gas electricity ratio from August to December as illustrated fig. 6.5. From December year 1 to January year 3 the natural gas price reduces significantly creating a favourable ratio between the natural gas price and electricity price. This effect is clearly visible in the power output of GT2 and the steam production of HRSG2 in figs. 9.2a and 9.2d, where the power output is at its maximum. Comparing the results in figs. 9.2a, 9.2c and 9.2d one can see that when GT2 increases its power output the supplementary can be slightly reduced while maintaining about the same steam flowrate. During the hot summer months the optimized power output is slightly lower than the modelled power output, this is due to the lower efficiency when the ambient
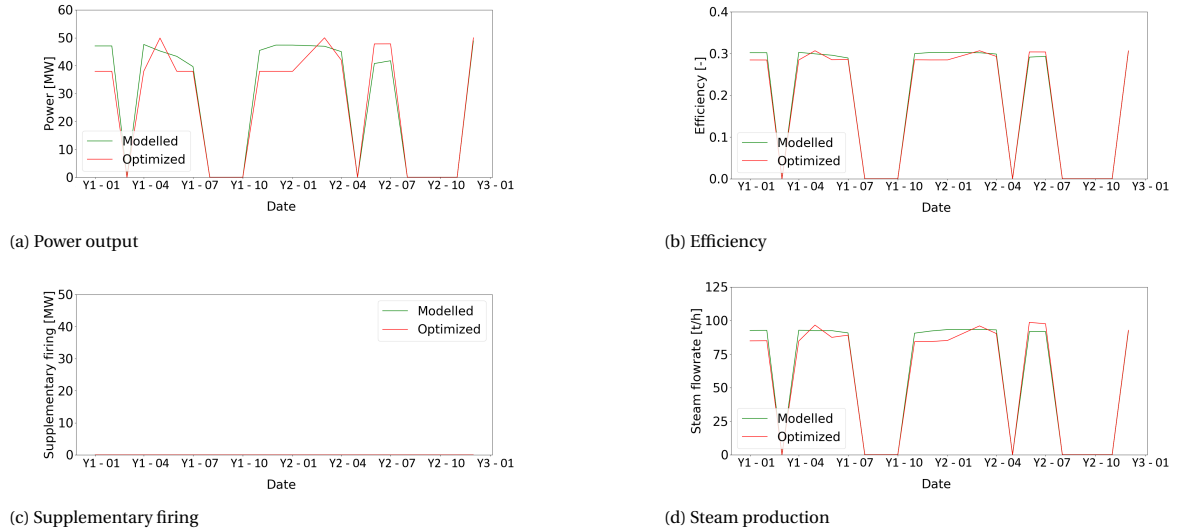
(a) Power output

(b) Efficiency

(c) Supplementary firing

(d) Steam production

Figure 9.1: Optimization results of the gas turbine 1 with heat recovery steam generator HRSG1. Modelled and optimized power output of the gas turbine (upper left), efficiency of the gas turbine (upper right), supplementary firing HRSG1 (lower left) and HRSG1 steam production (lower right).

temperature is high. As with GT1 the efficiency increases slightly when the power output is increased and decreases slightly when power output is decreased during optimization, visible in fig. 9.2b.

(a) Power output

(b) Efficiency

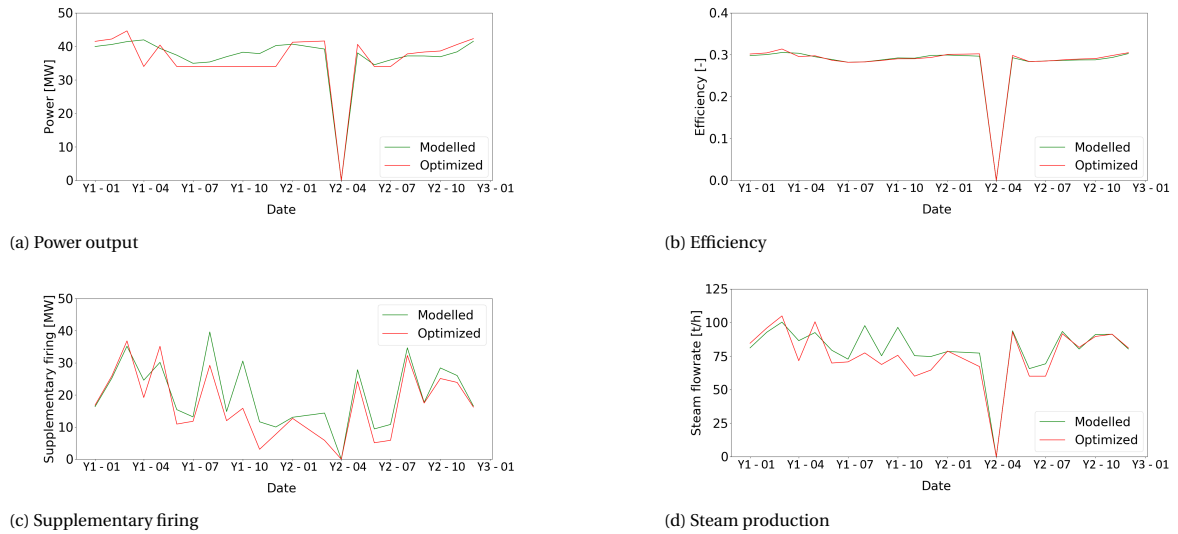(c) Supplementary firing

(d) Steam production

Figure 9.2: Optimization results of the gas turbine 2 with heat recovery steam generator HRSG2. Modelled and optimized power output of the gas turbine (upper left), efficiency of the gas turbine (upper right), supplementary firing HRSG2 (lower left) and HRSG2 steam production (lower right).

GT3 HRSG3

The results of the mixed gas GT3 with HRSG3 combination produces VHP, which has supplementary burners normally in operation, are given in fig. 9.3. The modelled and optimized GT3 power output is plotted in fig. 9.3a, the GT3 efficiency in fig. 9.3b, the HRSG3 supplementary firing in fig. 9.3c and HRSG3 steam production in fig. 9.3d. The GT3 shows the same trend as GT2 which is expected, as they are identical gas turbines. The power output is decreased to its minimum from July to December in year 1, this is due to the high ambient temperature in July, illustrated in fig. 7.3, and unfavourable natural gas electricity ratio from August to December as illustrated fig. 6.5. From December year 1 to January year 3 the natural gas price reduces significantly creating a favourable ratio between the natural gas price and electrify price. This effect is

clearly visible in the power output of GT3 and the steam production of HRSG3 in figs. 9.3a and 9.3d, where the power output is at his maximum. Comparing the results in figs. 9.3a, 9.3c and 9.3d one can see that if GT3 increases its power output the supplementary can be slightly reduced while maintaining about the same steam flowrate. In some scenarios the power of GT3 is reduced and supplementary firing is increased a bit to reach the required steam output. During the hot summer months the optimized power output is slightly lower than the modelled power output, this is due to the lower efficiency when the ambient temperature is high. As with GT1 and GT2 the efficiency increases slightly when the power output is increased and decreases slightly when power output is decreased during optimization, visible in fig. 9.3b.

(a) Power output

(b) Efficiency
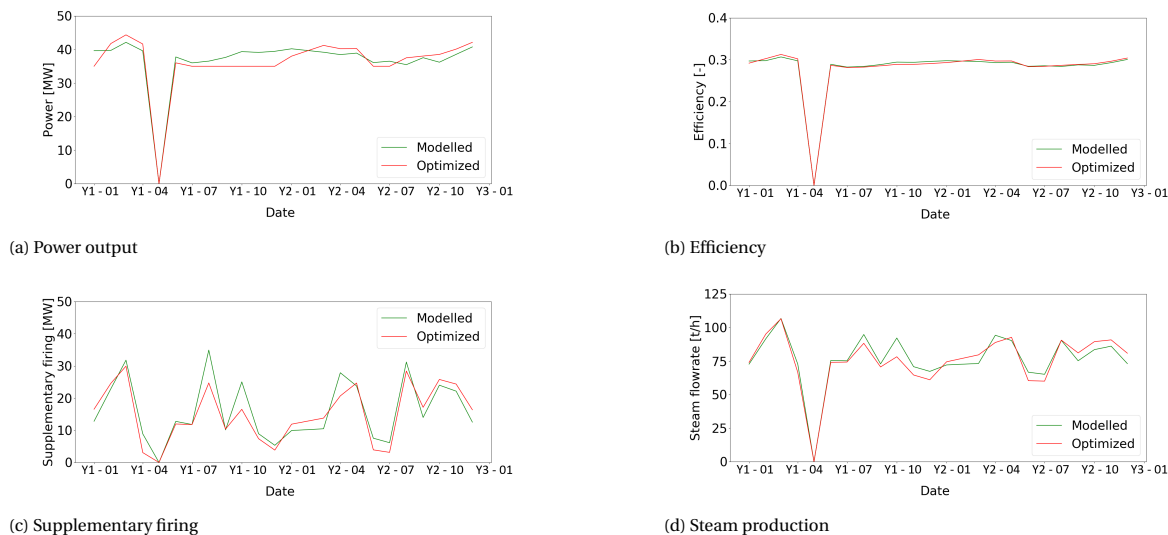
(c) Supplementary firing

(d) Steam production

Figure 9.3: Optimization results of the gas turbine 3 with heat recovery steam generator HRSG3. Modelled and optimized power output of the gas turbine (upper left), efficiency of the gas turbine (upper right), supplementary firing HRSG3 (lower left) and the HRSG steam production (lower right).
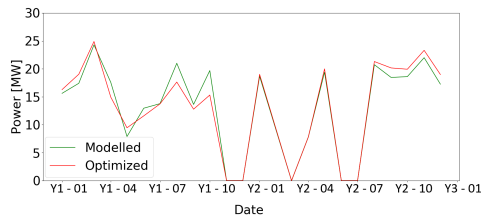
9.2. Steam Turbine Generators

The second set of results is of the STGs: STG1 and STG2. The modelling and optimization approach is explained in section 6.2, with the upper and lower boundaries for steam throughput. The STG1 and STG2 are not influenced by ambient conditions and their efficiency and power output is purely related to the steam conditions and the throughput as discussed in section 5.2.
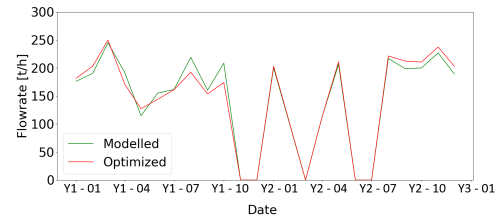
STG1

First the modelled and optimized results for the STG1 are illustrated in fig. 9.4, with the power output in fig. 9.4a and the VHP steam consumption flowrate in fig. 9.4b. As visible in figs. 9.4a and 9.4b the power output is directly related to the steam consumption flowrate. The effect of efficiency is also visible in August year 2 to January year 3, where the increase in power output is relatively higher than the increase in consumption flowrate. This effect is due to the higher efficiency of the turbine at higher flowrates, plotted in fig. 5.1. The pressure of the inlet and outlet are not changed during optimization, because this affects the whole network and all connected units.

STG2

For the STG2 the results of two stages are combined and illustrated in fig. 9.5. The modelled and optimized results for the power output of the complete unit is given in fig. 9.5a, while the results for the MP and LP steam consumption flowrates are shown in fig. 9.5b. As visible in fig. 9.5b the flowrate of the MP stage is reduced to its minimum in the optimization model, even though the isentropic efficiency is around 80%. This reduced flow through the first section also reduces the flow through the second section, due to the fact that there is less LP steam produced.
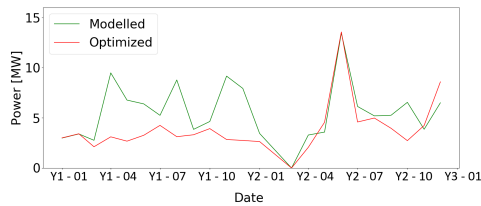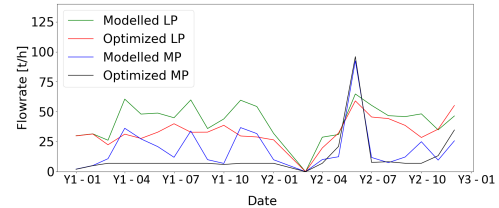
(a) Power output

(b) High pressure steam throughput

Figure 9.4: Optimization results of the high pressure steam turbine generator STG1. Modelled and optimized power output of the STG1 (left) and high pressure steam throughput of the STG1 (right).

(a) Power output

(b) Low and Medium pressure steam throughput

Figure 9.5: Optimization results of the two stage, medium and low pressure, steam turbine generator STG2. Modelled and optimized power output of the STG2 (left) and medium and low pressure steam throughput of the STG2 (right).

Steam Main

As discussed in section 5.4 most of the steam mains, which determine the pressure of each level, have a fixed pressure during optimization. The LP steam main in the ABC area is the only one which has the freedom to increase the pressure during optimization. The optimization results for the LP steam main are illustrated in fig. 9.6. The main driving force of changing the LP pressure is the balance between the first and second stage of the STG2. The first stage has a higher isentropic efficiency, however the flowrate through the second stage is often higher. The balance is clear when the flowrate through the MP stage exceeds the flowrate through the LP stage on 1 May year 2 and 1 June year 2, as visible in fig. 9.5b. This relative high MP flowrate for these two timestamps results in the minimum operating pressure of the LP steam main as visible in fig. 9.6.
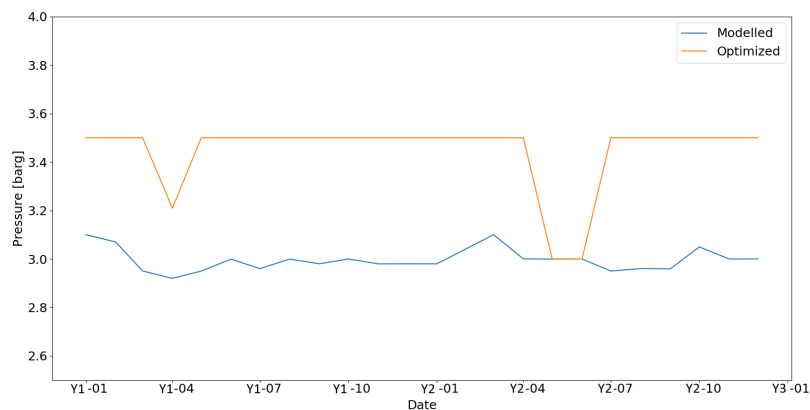

Figure 9.6: Modelled and optimized operating pressure of the low pressure steam main in the ABC area.

9.3. PGP2 MP Steam

The PGP2 optimization results are plotted in fig. 9.7, with the two boundaries as discussed in section 6.5. Visible in the results is that the PGP2 minimum and target flow limit the optimization possibilities. The PGP2

steam flow is reduced for four timestamps, namely: 1 March year 1, 1 May year 1, 1 September year 2 and 1 October year 2. For these moments the supplied steam flow was above the minimum boundary and the STG2 MP stage was not minimized. The price of the PGP2 steam is simply higher than the value of the electricity produced by the STG2. Furthermore, this intake of PGP2 steam is based on the balance between the PGP2 steam price and the produced steam price, which both depend on the natural gas electricity ratio as plotted in fig. 6.5. That is the main reason why extra steam is taken from PGP2 on 1 September year 1 and 1 October year 1, simply because producing steam is more expensive due to the relative high natural gas price.
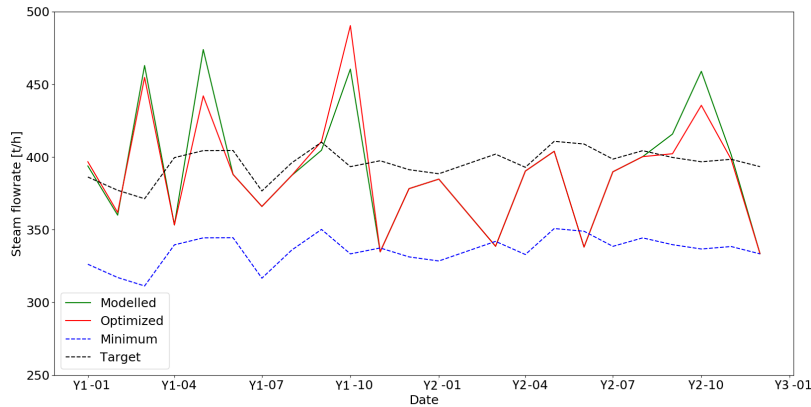

Figure 9.7: Optimization results of the PGP2 medium pressure steam intake. Modelled and optimized results are plotted with the minimum and target PGP2 steam flowrates. The minimum flowrate is the real minimum amount, while flowrates below the target are acceptable if STG2 is running on maximum throughput.

9.4. Energy Tax

The PGP1 efficiency should be monitored due to the energy tax boundary as discussed in section 6.6. In fig. 9.8 the modelled and optimized PGP1 efficiency is plotted, with the yearly averages and the tax boundary at 30% efficiency. It is important to monitor this efficiency, because if the yearly average PGP1 efficiency is below 30% the fuel price will increase as illustrated in fig. 6.4 due to energy tax.
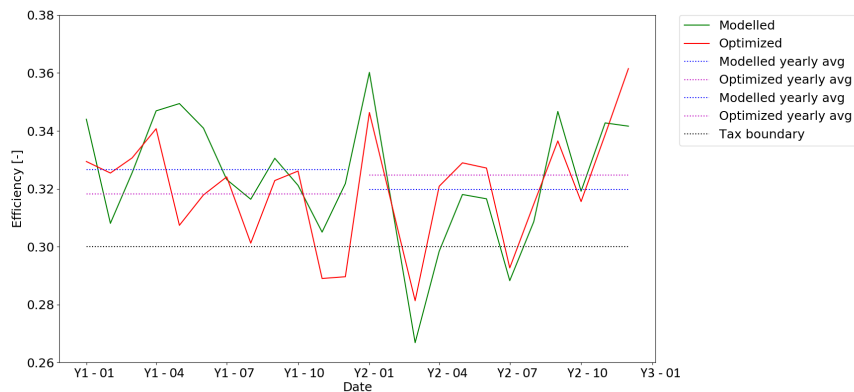
Figure 9.8: Modelled and optimized efficiency of the power generation plant (PGP1), including the gas turbine with heat recovery steam generator combinations GT2 HRSG2 and GT3 HRSG3 and the steam turbine generators STG1 and STG2. The PGP1 efficiency is calculated by dividing the total electrical power output with the total fuel consumption. Above the black efficiency boundary of 0.3, the energy tax on the fuel consumed by the PGP1 is waived.

The GT1 HRSG1 combination is not included in the calculation of the efficiency, due to the fact that this combination normally operates below 30%. However as can be seen from the modelling and optimization results in fig. 9.8 the average PGP1 efficiency for year 1 and year 2 is 31.8 % or higher. In fig. 9.9 the total

efficiency is plotted which includes the GT1 HRSG1 combination. The average over year 1 and year 2 is still above 30%, based on these 23 timestamps. Including GT1 HRSG1 in the efficiency calculation could decrease the fuel price for GT1 and HRSG1 with about 7.6%, calculated with the data from fig. 6.4.
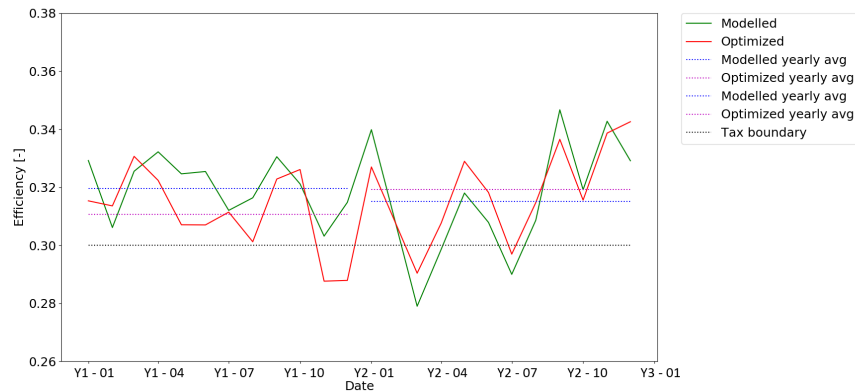

Figure 9.9: Modelled and optimized efficiency of the gas turbine with heat recovery steam generator combinations: GT1 HRSG1, GT2 HRSG2 and GT3 HRSG3 with the steam turbine generators: STG1 and STG2. The total efficiency is calculated by dividing the total electrical power output with the total fuel consumption. Above the black efficiency boundary of 0.3, the energy tax on the fuel consumed by the gas turbines and heat recovery steam generators is waived.

9.5. Carbon Dioxide

The optimization model is not aimed at reducing CO_2 emission. However when optimizing the steam model itself it resulted in a reduction of the CO_2 due to the fact that the sites steam production is reduced as visible in figs. 9.1d, 9.2d and 9.3d. The effect of the optimization model, which reduces operating cost, on the CO_2 emission is given as an absolute value in fig. 9.10a and as a percentage in fig. 9.10b. As discussed in section 6.6 the CO_2 emission calculation is based on a LHV ratio between the fuel used for modelling and natural gas. Therefore the relative reduction in fig. 9.10b is a more realistic approach due to the fact that this is a direct result of the reduced steam and electricity production.
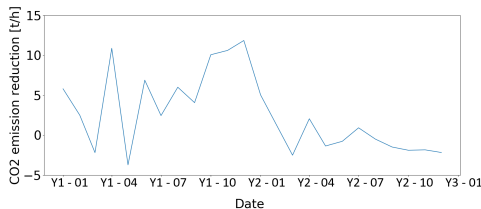
(a) Absolute CO_2 reduction
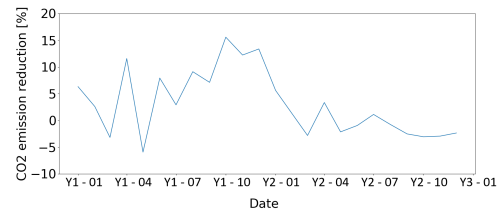
(b) Relative CO_2 reduction

Figure 9.10: Optimization results of the CO_2 reduction as absolute value (left) and relative (right). Negative values indicate an increase in CO_2 emission.

9.6. Operating Costs

The optimization whereof the results are shown in the sections above leads to a reduction in operating cost. This reduction is illustrated as an absolute value in fig. 9.11a and as a percentage in fig. 9.11b. As visible fig. 9.11b the average reduction lies between 1-3%, however there are three clear spikes on 1 August year 1, 1 November year 1 and 1 December year 1. These three moments are during the time that natural gas is relative expensive, while the GTs, except for GT1 on the first of August, where all fully in operation. These large operating cost reductions are achieved by keeping the PGP2 steam intake equal and simply reducing the power output of the GTs. Reducing the power output of the GTs reduces the steam production by the HRSGs and therefore steam consumption by the STGs.
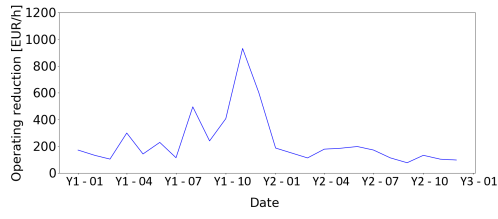
(a) Absolute cost reduction
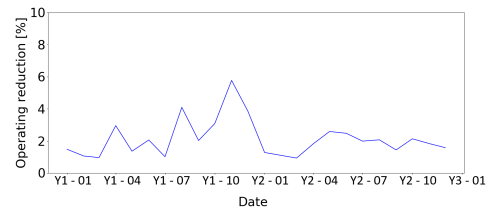
(b) Relative cost reduction

Figure 9.11: Optimization results of the operational cost reduction as absolute value (left) and relative (right).

10

Discussion

In this chapter the results obtained in chapters 7 to 9 are discussed. The discussion is split in two sections: one related to the hydraulic pipeline model and one related to the optimization model.

10.1. Pipeline Model

First the results of the pipeline model are discussed. The discussion of these results is split in two main section: the validation results of the model and the simulation results of the new project.

Validation Results

For the pipeline model the validation results are the most important ones, because it illustrates how close the simulation is to reality during different scenarios. The only changes made to the model over the four scenarios is the input data, which is related to the timestamp and the valve operation of the network. Valve operation determines through which pipelines steam is delivered to and from the process units.

Temperature and Pressure

From the validation results in tables 7.1 and 7.2 can be concluded that the hydraulic calculations of the model are mostly within the uncertainty of 2.83%. This is achieved in four different scenarios, with very different operational modes. These results show that the model is validated on pressure and temperature and can be used to test the effects of modifications or new projects as is executed in chapter 8. Furthermore, this model incorporates the earlier unknown insulation properties of each pipeline segment, which helps in determining whether energy losses are due to thin insulation or low steam flowrates. The same is true for the pressure calculations made by the model. Bottlenecks in the network are easily located with the simulation results. Possible solutions can be tested in the model which is much faster, easier and cheaper than performing tests in the field.

Flowrate

In certain areas of the network a steam overcapacity is present as visible in table 7.3. This overcapacity could be true for small amounts, due to small leaks in the steam network which cannot be modelled. However there are areas where overcapacity is often above 10 t/h. Because most steam vents are not equipped with flow meters it is not clear whether vents are open, which could explain the large surplus of steam. May this be the case large steam clouds would be visible pointing operators directly to the problem of the open vent or large leakage. Therefore one would assume that a consistently large steam excess as is the case for the areas KLM H&W LP, DEG MP and 90barg Sat. are not due to open vents or leakages. Which indicates that the installed flowmeters in these areas might be faulty. For the 90barg Sat. steam area it is known that these meters are not trustworthy, because small droplets in the saturated steam flow disturb the measurement of the flowmeter. For the other regions the steam is mainly supplied by the PGP2, which is due to its use for economic calculations assumed to be very accurate, in the region of 1% uncertainty. The flowmeters inside the transport pipelines do not create a significant mass imbalance over the steam mains, which leaves the flowmeters on the consuming side. These large steam excesses have to be vented somewhere in the model and the choice of location has a huge effect on the steam velocity in certain sections and therefore

the pressure and temperature results of the simulation. This is the reason why these sections are not further validated on temperature and pressure or even modelled in the network. Checking the flowmeters of the consumers in these areas could solve these mass imbalances and create the possibility of modelling and validating these parts of the network.

Future Project

For the analysis of the future project located in the KLM area the model is used to simulate the steam temperature and pressure. This is very useful because it directly locates the bottleneck of a system and is able to test adjustments in the network. Furthermore the model provides an easy approach of determining the minimum and maximum flowrate through each route of which the results can be compared to the characteristics of the unit. The results show that there is a possibility of connecting the new unit to the KLM steam network without modifications except for the new connection pipe. However these results show as well that the only route is via MP steam, while the unit requires LP steam. Letting down MP steam towards LP steam is a non favourable process due to the fact that MP steam has a much higher value. The results can be used to compare the costs of retrofitting the bottlenecks in the LP network with the costs of consuming MP steam instead of LP steam from the PGP2. The results of exporting LP steam show that this leads to a high risk of condensation, which can be prevented by installing a smaller pipe or extra insulation. Installing the smaller pipe will increase the pressure loss through the section. LP export by the new unit is only during EOR in the winter months and therefore it has to be investigated if it is feasible to install a pipe for a relative low flowrate of LP steam and only during that scenario. As discussed in the pipeline validation section there is some steam overcapacity in these sections of the network. The overcapacity is relatively small, around 2.2 t/h for the LS1343 route and 4.7 t/h for the LS4413 route. This overcapacity is fixed during the modelling of the new project, which slightly decreases the acceptable consumption flowrate by the new project. Locating the source of this overcapacity would result in a more reliable analysis for the maximum capacity of these pipeline sections. Furthermore, the length and number of bends of the pipelines connecting the new unit to the existing network are approximated. With more information on where the new unit will be located these pipe characteristics can be changed in the model to achieve a more accurate simulation.

10.2. Optimization Model

In this section the results of the optimization model are discussed. The discussion is split into eight parts, not all results are further reviewed in this section.

GT1 HRSG1

The first results from the optimization model which are discussed are for the GT1 HRSG1 combination. It is shown that GT1 is operating often on its minimum boundary, unless the natural gas electricity ratio is below 0.38. The other two scenarios where GT1 is not operating at its minimum is due to the shut down of one of the other two GTs. Operating the GT1 is not only based on the gas electricity ratio but also on the PGP2 steam price. Normally the GT1 HRSG1 steam production price is higher then the PGP2 price, however at the end of year 2 these prices are competing. HRSG1 operates normally without supplementary firing and the optimization results show that this is the correct approach. When the lower operating boundary of the GT1 HRSG1 combination is removed the model indicates that the combination should be shut down entirely, except for the scenarios described above. Unfortunately the combination is not that flexible that it can start and stop depending on the market conditions. Shutting the GT2 down for a longer period of time would result in another issue, which is related to electrical redundancy. During the summer months the combination is down, however based on statistical calculations by Shell it should be on during the winter months to achieve an acceptable electrical redundancy. An improvement for modelling the HRSG1 would be that the HRSG model is based on historic data to determine a correlation as is used for the GTs and STGs. This will incorporate the effect of increasing or decreasing the steam flow on the efficiency of the HRSG, of which the effect is now neglected.

GT2 HRSG2 & GT3 HRSG3

The results of the GT2 HRSG2 and GT3 HRSG3 are grouped together because the GTs and HRSGs used in both combinations are similar. From the results is visible that the GTs often go towards minimum power output, however significantly less then for the GT1. This result is expected because the VHP steam route with an extra steam turbine generator should in theory be more efficient. During year 2 the systems are often pushed

towards their maximum, again caused by the relatively cheap natural gas price. HRSG2 and HRSG3 normally operate with supplementary firing and the optimization results show that this is indeed necessary to operate the HRSGs. There are moments when the optimization results for both GT HRSG combinations differ, this is due to the modelling of the HRSG. As explained the blowdown ratio is set equal to limit the false preference of HRSG2 over HRSG3 by the model as blowdown is seen as an energy loss, which in reality is not true. However the minimum temperature approach of both HRSGs are calculated based on their steam production and energy usage, so changing the blowdown ratio has an effect on this calculation. The calculated minimum temperature approach is fixed during optimization to provide the most realistic scenario, however due to the average blowdown ratio this minimum temperature approach can be higher or lower than it should. That is why sometimes HRSG2 is favored over HRSG3 and vise versa. This issue is due to the simplified HRSG design i-Steam uses. In reality BFW and 90barg sat. enter the HRSG system and after the economizer a part of the saturated water flows to the deaerators. i-Steam is working on a more complex HRSG model which can replicate the design more accurate. Another improvement would be that the HRSG model is based on historic data to determine a correlation as is used for the GTs and STGs. This will incorporate the effect of increasing or decreasing the steam flow on the efficiency of the HRSG, of which the effect is now neglected. The GT2 and GT3 are modelled based on a natural gas equivalent as fuel with a fixed LHV, while in reality the LHV of the fuel gas used varies a lot. Due to this fluctuating LHV the i-Steam software was not able to obtain a trustworthy correlation, which lead to the choice of using a natural gas equivalent. As discussed in section 3.1 the LHV and composition of the fuel can have an effect on the achieved power output but also on the efficiency. i-Steam is researching the possibilities of designing a correlation model capable of modelling a gas turbine with a mixed fuel LHV which fluctuates between 10.000-50.000 kJ/kg.

STG2
The first stage of the STG2 is nearly always optimized to its minimum boundary for year 1 and year 2. When the natural gas price becomes relatively cheap and steam production increases, the MP inlet of the STG2 is above its lower boundary. When the PGP2 intake is above the 440 t/h boundary, the MP section of the STG2 is directly optimized back to its lower boundary. This is expected because the price of MP steam is higher than the value of the electricity it will produce in the two stages of the STG2. The results for the second stage of the STG2 are as expected, because it is simply there to utilize the final energy in the excess LP steam. Modelling the STG2 can be done more accurate by creating a correlation which can be used in the software i-Steam. At the moment the correlation is in Excel and after optimization the isentropic efficiencies of the two stages are adjusted to the optimized flowrate. With a correlation model based on the power output of the two stages it can be used in i-Steam and play an active role during the optimization. For now the results are acceptable due to the fact that the first stage throughput is lowered most of the time resulting in a lower isentropic efficiency than used in optimization. However if market conditions become so favourable that the STG2 can play an active role the efficiency correlation has to be implemented in the software to achieve a trustworthy result.

Steam Main
The only steam main where the pressure is not fixed during optimization is the LP ABC steam main. The pressure relies on the balance between the two stages of the STG2. It is clear that the first stage of the STG2 has a significant lower flowrate than the second stage of the STG2 for most optimized cases. The three cases where the first stage flowrate is higher the optimized operating pressure is lower than its upper boundary of 3.5barg. Increasing the pressure of the LP ABC main could be very beneficial for the steam network, not only to generate a bit more power in the STG2 but also for the ABC LP network. Currently the pressure in the network is often lower than desired and increasing the LP pressure which enters the network could help solving these issues. The other steam mains might benefit as well from slight alterations in the operational pressure. However these networks contain units which use the steam for other processes than just heating, such as small steam turbines, which require the steam at the provided pressure. An extensive research reviewing all these units could lead to more flexibility in the operational pressure of steam mains.

PGP2 Import
The results of the PGP2 MP steam import show the balance between the imported steam price and the on site produced steam. When the steam price is favourable, on site production is decreased and imported steam is increased as is clearly visible in October year 1. Furthermore, when on site operation is sufficient and steam import lies above the 440 t/h boundary, steam import is reduced. This is expected, because the value created by letting MP steam through the STG2 is less than the value of the steam itself. For the cases

below the 440 t/h boundary it is a difficult agreement area. If steam import is below 440 t/h the STG2 should be operating on maximum load, however this in clearly not the case when comparing the modelling results for steam import and STG2 load. During optimization the steam import lower boundary is set at 440 t/h or when the actual import is lower that will be the boundary. Resulting in a decrease of the throughput of the STG2, while decreasing the steam production by the HRSGs on site. This results in a low throughput of the STG2 and therefore room to take in more steam, adhering to the agreed target steam flow. This questions the optimization results for the scenarios where the import is below 440 t/h. However maximizing the flow through the STG2 if the steam import is below 440 t/h would steer optimization in the wrong direction as it is clear that this is not how the STG2 actually operates.

Energy Tax

The results for the PGP1 efficiency calculations show that during modelling and optimization the efficiency is well above the required 30%. Including GT1 HRSG1, which could reduce its fuel price by 7.3%, lowers the overall efficiency but it is still above the required 30% during modelling and optimization. For year 1 where natural gas was relatively expensive, resulting in a low PGP1 and GT1 efficiency, the average combined efficiency for optimization is decreased to 31.1%. This is based on 23 timestamps, so do not give a complete overview of the effect of including GT1 HRSG1. However the timestamps are chosen throughout the year and during a period with fluctuating gas and electricity prices, therefore it includes low power outputs and efficiencies.

Carbon Dioxide

Carbon dioxide emission is increased and decreased during optimization, because it is not the driving force for optimization. Reduction in operational cost is the goal and when carbon dioxide emission costs increases, as is currently the trend, it has a larger effect on operational costs and therefore on optimization. In the model the carbon dioxide emission is based on the composition of natural gas and scaled according to LHV. In reality only the GT1 runs on pure natural gas, while the other fuel consumers run on a mix of refinery gas and natural gas. For optimization this is acceptable because due to the relative low modifications made in fuel usage and the fact that CO_2 is not yet the driving force of optimization. This leads to results of modelled and optimized CO_2 emissions which can be compared relatively. Absolute emission is not correct due to the broad mix of fuel which is actually used.

Operating Cost

The optimization results are summarized in a significant reduction of 1-6 %, which is comparable to reductions achieved in literature and estimated by the i-Steam software company PIL. This reduction clarifies why steam utility networks should be optimized, especially when there is a steam intake involved such as PGP2 involved. The optimization is achieved by changing the operating approach of the power generation plant and the PGP2 import, without the need of alterations to the network itself.

11
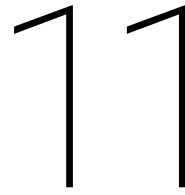
Conclusion

Two i-Steam models have been designed which are able to model and optimize the refineries extensive steam network. One model is focused on hydraulic simulation and incorporates the outside battery limit pipelines, connecting each unit to the steam network. The other model is focused on steam and electricity generation while balancing the network with the PGP2. The conclusion is split in two sections, one for each model.

11.1. Hydraulic Model

The hydraulic model is built based on measured data at the refinery. Each pipeline is incorporated with the correct dimensions and the valve operation is based on discussion with operators. Four scenarios are simulated, each with a different operating mode to test the flexibility of the model. The four scenarios are validated on pressure and temperature with measured steam conditions throughout the network. Mass imbalances are located and partly solved, areas with large mass imbalances are probably due to faulty flowmeters on the consumer side. The hydraulic model can be used to test the effect of retrofits or changes in operation. Furthermore, current operational issues can be located and possible solutions can be simulated which is faster, easier and cheaper than performing real tests as is required at the moment. The model is applied to perform simulations on how to connect a new unit to the existing KLM steam network. Simulations are executed to locate bottlenecks and to determine which is the best route for steam consumption and production. From the results can be concluded that the new unit should be connected to the KLM MP grid via LS4413, with a second connection to LS980019 for redundancy. The LP steam produced by the unit is minimum and only during the EOR winter case, moreover there is a large risk of condensation due to the low flowrate and steam production temperature. Dispatch via the LS980017 pipe to the LP KLM grid seems plausible, however the economic feasibility of laying new pipeline and the accepted steam conditions by unit 1 should be further investigated.

11.2. Optimization Model

The optimization model focuses on the steam and electricity production, without incorporating the extensive pipeline network. The model applies historic data to predict the efficiencies of the GTs and STGs. Correlations are made to model the network under various ambient conditions and operating modes. Twenty three scenarios are modelled throughout a period of two years, ensuring that there is a broad variety of ambient, operating and market conditions. The model is validated by comparing the simulated results with the actual on site measured data in terms of power output, efficiency and temperature. For each simulated scenario optimization is executed which predicts the optimal operating point for the conditions present during that time. The results are analysed and compared to the expected trends described in literature. The optimization results shows that the natural gas over electricity price ratio in combination with the ambient temperature which has a large effect on efficiency are the main drivers during optimization. The CO_2 price is increasing and therefore its role in optimization grows. Furthermore, the results show that the STG2 operation should be minimized. Shutting down the first stage while maintaining the second stage to utilize the excess LP steam is preferred. This is not an option because the STG2 is used to balance the system and to honor the PGP2 agreement. Which shows that the agreement results in a clear overcapacity of the refineries steam network and the intake target should be lowered to gain more flexibility. Another finding of the model is that the LP

ABC steam main should be increased to 3.5barg, which results in more power from the STG2 and probably a higher pressure in the ABC LP network, which is desired. One more finding of the optimizations results is that the GT1 HRSG1 combination should, viewed from an economic standpoint, be turned off in most scenarios. The only moments when GT1 HRSG1 should be in operation is when GT2 HRSG2 or GT3 HRSG is out of operation or when the natural gas over electricity price is below 0.38.

12

Recommendation

In this chapter the recommendations are presented which could improve the models built in this work. The recommendations are not split in two sections, because most recommendations apply for both the hydraulic pipeline model and the optimization model.

Flowmeters

The first recommendation is that the flowmeters which are used to design the models are checked. With a better understanding of which flowmeter is operating correctly and which one needs repairing the model can be made more accurate. As discussed flowmeters are used as an input on the steam production and consumption side of the network and have a huge influence on steam velocities through pipelines and therefore on the simulation results for pressure and temperature. Checking the flowmeters would not only improve the current models but also open the possibility to further validate the model and add the DE area. More accurate flowmeters will also decrease the amount of initial errors when running new scenarios via Excel. At the moment minor errors can occur in the optimization model due to faulty let down valve flowmeters. These errors are very easy and quickly fixed, but still slow the process down of simulating several cases at once.

Excel Interface

The Excel add-in is used to run multiple simulations at once and is able to use the output of measurement equipment as input for the model. Due to the complexity of the pipeline model some minor alterations are needed which determine the flow direction between areas. i-Steam is aware of the issue and when resolved simple statements can be added to the Excel file to change the direction of streams.

HRSG Model

As mentioned the current HRSG model calculates the minimum temperature approach according to the input data at the simulated time. This value is fixed during optimization to prevent misleading results, because the model will simply lower the minimum temperature approach to the set minimum. However changing the produced steam flow has an effect on the minimum temperature approach and that effect should be incorporated in the model by implementing a correlation from historic data as is executed for the GTs and STGs. Another improvement of the HRSG model could be achieved by improving the inlet and outlet streams of the system. The system has BFW and saturated steam as an inlet and superheated steam and saturated water as an outlet. Currently the saturated steam is modelled separately and the saturated water outlet is modelled as blowdown. Incorporating these in the HRSG, results in a model closer to reality and better suitable for optimization.

Daily Prices

Incorporate daily prices or as frequent as possible to benefit from fluctuations in the market. At the moment most prices are on a monthly basis and inserted in the PI database manually. Providing the model with the most recent and accurate data will maximize the potential gain.

Real Time Optimization

For the optimization model it is recommended to include daily prices and automatically run the simulation every day. The daily results can help the operators by providing the market conditions and advise them how to operate the network during the day to create most value under these conditions.

PGP2 Steam Target

It is recommended to investigate the targets of the PGP2 steam intake. When clear boundaries are selected these can be implemented in the model and retained during optimization. Another recommendation is that the steam target of 440 t/h, which determines the minimum steam import, is lowered. This will reduce the steam overcapacity and create more flexibility in operating the steam network.

LP ABC Steam Main

The optimization model increases the operating pressure of the LP ABC steam main to achieve a higher power output of the STG2. This higher pressure can also have a positive effect on the whole ABC LP network, which is currently operating under its desired pressure. Increasing the pressure of the LP ABC steam main, which produces LP steam for the LP network could increase the overall pressure of the network. It is recommended that the effects on the LP network itself and the units which are connected to it are further researched.

Mixed Gas Model

As discussed the GTs and HRSGs, except for GT1, consume a mix of gaseous fuels of which the composition and LHV varies. At the moment GT2 and GT3 are modelled using a natural gas equivalent and the HRSGs use the varying LHV of refinery gas. To improve the model a correlation can be made for GT2 and GT3 which includes the fuel gas mix and is able to incorporate the varying LHV of the fuel. The varying fuel composition can be included to calculate the CO_2 emission of each unit more accurate, this is important when CO_2 emission cost will rise and its roll in optimization grows. Currently the fuel consumption costs is based on the natural gas price, when the refineries fuel network is incorporated with the various fuel mixtures the prices per fuel can be determined and improve the operational cost optimization.

Bibliography

[1] An introduction to all pernis plants. Shell Nederland Raffinaderij B.V., 2010.

[2] T. Farmer. Acceptable operating parameters for steam assisted flares at purge rates. `https://www.zeeco.com/pdfs/AFRC-2011-Flare-Paper.pdf`.

[3] H. Khodaei R. Arghandeh, M. Amidpour. Steam network modeling and simulation in gas refinery by considering pinch technology. `https://ieeexplore.ieee.org/document/5174118`, 2009.

[4] E. Hindmarsch B. Linnhoff. The pinch design method for heat exchanger networks. `https://www.sciencedirect.com/science/article/pii/0009250983801857`, 1983.

[5] D.I. Wilson. J. Currie. The efficient modelling of steam utility systems. `https://pdfs.semanticscholar.org/1de5/b6f73ce7008dfaf7227e869d58a50ee1a205.pdf?_ga=2.104079680.1745271545.1593963946-1954422317.1592568511`, 2012.

[6] Y. Feng X. Dong H. Zhao, G. Rong. Integration optimization of production and utility system for refinery-wide planning. `https://www.sciencedirect.com/science/article/pii/S1474667016431320`, 2014.

[7] R.G. Smead. Oil and gas in the age of covid-19 - where do they go from here? `https://onlinelibrary.wiley.com/doi/10.1002/gas.22181s`, 2020.

[8] R. Subiaco F. Bengtsson S. Harvey S. Marton, E. Svensson. A steam utility network model for the evaluation of heat integration retrofits – a case study of an oil refinery. `https://www.researchgate.net/publication/320431679_A_Steam_Utility_Network_Model_for_the_Evaluation_of_Heat_Integration_Retrofits_-_A_Case_Study_of_an_Oil_Refinery`, 2017.

[9] P.S. Verbanov Z.A. Manan J.J. Klemeš P.Y. Liew, S.R.W. Alwi. Centralised utility system planning for a total site heat integration network. `https://www.sciencedirect.com/science/article/pii/S0098135413000549`, 2013.

[10] K. Raissi S.J. Perry L. Puigjanert J. Klemeš, V.R. Dhole. Targeting and design methodology for reduction of fuel, power an co_2 on total sites. `academia.edu/12941323/Targeting_and_design_methodology_for_reduction_of_fuel_power_and_CO2_on_total_sites`, 1997.

[11] Y. Makwana X.X. Zhu R. Smith P. Varbanov, S. Perry. Top-level analysis of site utility system. `https://www.sciencedirect.com/science/article/pii/S0263876204725538`, 2004.

[12] S.H. Chae S. Park S.H. Kim, S.G. Yoong. Economic and environmental optimization of a multi-site utility network for an industrial complex. `https://pubmed.ncbi.nlm.nih.gov/19880240/`, 2010.

[13] S.G. Beangstrom. Steam system network analysis, synthesis and optimisation. `https://repository.up.ac.za/handle/2263/33340`, 2013.

[14] I.H. Aljundi. Energy and exergy analysis of a steam power plant in jordan. `https://www.sciencedirect.com/science/article/pii/S1359431108001129`, 2009.

[15] H. Arellano-Garcia G. Wozny P. Velasco-Garcia, P.S. Verbanov. Utility systems operation: Optimisation -based decision making. `https://www.sciencedirect.com/science/article/pii/S1359431111003061`, 2011.

[16] R. Smith P.S. Verbanov, S. Doyle. Modelling and optimization of utility systems. `https://www.sciencedirect.com/science/article/pii/S0263876204725289`, 2004.

[17] Y. Natori C.W. Hui. An industrial application using mixed-integer programming technique: a multi-period utility system model. `https://www.sciencedirect.com/science/article/pii/0098135496002682`, 1996.

[18] M. Amidpour M.H.K. Manesh, H. Khodaie. Co_2 reduction through optimization of steam network in petroleum refineries: Evaluation of new scenario. `https://www.researchgate.net/publication/26905459_CO2_Reduction_through_Optimization_of_Steam_Network_in_Petroleum_Refineries_Evaluation_of_New_Scenario`, 2008.

[19] R. Subiaco. Modelling, simulation and optimization perspectives of an industrial steam network. `http://publications.lib.chalmers.se/records/fulltext/235160/235160.pdf`, 2016.

[20] Google maps. `https://www.google.nl/maps/@51.8858292,4.3551943,2760m/data=!3m1!1e3`, 2020.

[21] X. Luo, X. Huang, M.M. El-Halwagi, J.M. Ponce-Ortega, and Y. Cheng. Simultaneous synthesis of utility system and heat exchanger network incorporating steam condensate and boiler feedwater. `https://www.sciencedirect.com/science/article/pii/S036054421731602X`, 2016.

[22] L.X. Sun, Q Zheng, and S.L Liu. 2d-simulation of wet steam in a steam turbine with spontaneous condensation. `https://link.springer.com/article/10.1007/s11804-007-6009-5`, 2007.

[23] R. Wang, Z. Wang, X. Wang, and H. Yang. Pipe burst risk state assessment and classification based on water hammer analysis for water supply networks. `https://ascelibrary.org/doi/10.1061/%28ASCE%29WR.1943-5452.0000404`, 2014.

[24] Nuclear Power. Carnot cycle - carnot heat engine. `https://www.nuclear-power.net/nuclear-engineering/thermodynamics/thermodynamic-cycles/carnot-cycle-carnot-heat-engine/`, 2020.

[25] General Electric. 6b.03 gas turbine (50/60 hz). `https://www.ge.com/power/gas/gas-turbines/6b-03`, 2020.

[26] B. Zohuri and P. McDaniel. Combined cycle driven efficiency for next generation nuclear power plants. `https://www.springer.com/gp/book/9783319155593`, 2018.

[27] F.J. Brooks. Ge gas turbine performance characteristics. `https://www.ge.com/content/dam/gepower-pgdp/global/en_US/documents/technical/ger/ger-3567h-ge-gas-turbine-performance-characteristics.pdf`.

[28] Realpars. What is a gas turbine? `https://realpars.com/gas-turbine/`, 2020.

[29] J. Noordermeer. Understanding gas turbine performance. `http://www.chacanada.com/chacanada/assets/File/GTPerf_0900.pdf`.

[30] U.S. energy information administration. `https://www.eia.gov/tools/glossary/index.php?id=H`, 2020.

[31] R. Kurz. Gas turbine performance. `https://www.researchgate.net/publication/277712286_Gas_Turbine_Performance`, 2005.

[32] Klimaatatlas. `http://www.klimaatatlas.nl/klimaatatlas.php`, 2010.

[33] M.M. Schorr and J. Chalfin. Gas turbine no$_x$ emission approaching zero - is it worth the price? `https://www.ge.com/content/dam/gepower-pgdp/global/en_US/documents/technical/ger/ger-4172-gas-turbine-nox-emissions-approaching-zero-worth-price.pdf`, 1999.

[34] A. Cilindro. Performance analysis and economic effects of maintenance and hot gas path inspection of a combined cycle power plant. `https://www.researchgate.net/publication/285594683_Performance_Analysis_and_Economic_Effects_of_Maintenance_and_Hot_Gas_Path_Inspection_of_a_Combined_Cycle_Power_Plant`, 2015.

[35] A.S.E. Ahmed, M.A. Elhosseini, and H.A. Ali. Modelling and practical studying of heat recovery steam generator (hrsg) drum dynamics and approach point effect on control valves. `https://www.sciencedirect.com/science/article/pii/S2090447918300558`, 2018.

[36] A. Ahmed, K.K Esmaeil, M.A. Irfan, and F.A. Al-Mufadi. Design methodology of heat recovery steam generator in electric utility for waste heat recovery. `https://academic.oup.com/ijlct/article/13/4/369/5095657`, 2018.

[37] V. Ganapathy. Heat-recovery steam generators:understand the basics. `https://pdfs.semanticscholar.org/9183/d4f81b826a68c5412ca7f70a5d07ed2405c7.pdf`, 1996.

[38] J. Miller. The combined cycle and variations that use hrsgs. `https://www.sciencedirect.com/science/article/pii/B9780081019405000026`, 2017.

[39] V. Ganapathy. Industrial boilers and heat recovery steam generators. `https://www.researchgate.net/publication/228887612_Industrial_Boilers_and_Heat_Recovery_Steam_Generators_Design_Applications_and_Calculations`, 2003.

[40] A.M.K. Vandani, M. Bidi, and F. Ahmadi. Exergy analysis and evolutionary optimization of boiler blow-down heat recovery in steam power plants. `https://www.sciencedirect.com/science/article/pii/S0196890415008535`, 2015.

[41] J.D. Kumana. Thermodynamic analysis of steam turbines in industrial applications. `https://www.researchgate.net/publication/318402919_THERMODYNAMIC_ANALYSIS_OF_STEAM_TURBINES_FOR_INDUSTRIAL_APPLICATIONS`, 2017.

[42] M.J. Moran, H.N. Shapiro, D.D. Boettner, and M.B. Bailey. *Principles of Engineering Thermodynamics.* John Wiley and Son, Inc., 7 edition, 2012.

[43] Deaerator working principle and types. `http://www.mechanicalengineeringsite.com/deaerator-working-principle-and-types/`, 2017.

[44] Temperature measurement devices. Shell Global Solutions International B.V., 2017.

[45] S. Wiegand. Introduction to thermal gradient related effects, in functional soft matter. `https://www.researchgate.net/publication/283322686_Introduction_to_thermal_gradient_related_effects_in_Functional_Soft_Matter`, 2015.

[46] Pressure measurement devices. Shell Global Solutions International B.V., 2017.

[47] Capacitance differential pressure transmitter working principle. `https://www.eastsensor.com/blog/capacitance-differential-pressure-transmitter-working-principle/`, 2018.

[48] Linear flowmeters part 1. Shell Global Solutions International B.V., 2017.

[49] Differential pressure flowmeters part 1. Shell Global Solutions International B.V., 2017.

[50] Knmi: Uurgegevens van het weer in nederland. `https://projects.knmi.nl/klimatologie/uurgegevens/selectie.cgi`, 2020.

[51] Y.W. Kim. C.S. Kim, S.D. Hong. Radiaition-corrective gas temperature measurement in a circular channel. `https://www.researchgate.net/publication/271451579_Radiation-corrective_gas_temperature_measurement_in_a_circular_channel`, 2012.

[52] W.K. Jekat. Centrifugal pump theory, first edition of the pump handbook. New York: McGraw-Hill, 1976.

[53] G.O. Lied K.E. Froysa. Uncertainty model for the online uncertainty calculator for gas flow metering stations. `https://nfogm.no/wp-content/uploads/2018/02/Handbook-Online-tool-for-uncertainty-calculations-Fiscal-gas-metering-stations-.pdf`, Norwegian Society for Oil and Gas Measurement.